TAL TECH

DOCTORAL THESIS

Characterisation of Frost-Retted Hemp Fibres for Use as Reinforcement in Biocomposites

Percy Festus Alao

TALLINNA TEHNIKAÜLIKOOL
TALLINN UNIVERSITY OF TECHNOLOGY
TALLINN 2022

TALLINN UNIVERSITY OF TECHNOLOGY
DOCTORAL THESIS
31/2022

Characterisation of Frost-Retted Hemp Fibres for Use as Reinforcement in Biocomposites

PERCY FESTUS ALAO

TAL TECH PRESS

TALLINN UNIVERSITY OF TECHNOLOGY
School of Engineering
Department of Materials and Environmental Technology
This dissertation was accepted for the defence of the degree 06/05/2022

Supervisor: Professor Jaan Kers
School of Engineering
Tallinn University of Technology
Tallinn, Estonia

Co-supervisor: Senior lecturer Triinu Poltimäe
School of Engineering
Tallinn University of Technology
Tallinn, Estonia

Opponents: Associate Prof Dennis Jones
Department of Engineering Sciences and Mathematics
Wood Science and Engineering
Luleå University of Technology

Associate Prof Rünno Lõhmus
Faculty of Science and Technology
Institute of Physics
University of Tartu

Defence of the thesis: 21/06/2022, Tallinn

Declaration:
Hereby I declare that this doctoral thesis, my original investigation and achievement, submitted for the doctoral degree at Tallinn University of Technology has not been submitted for doctoral or equivalent academic degree.

Percy Festus Alao

---
signature

European Union
European Regional
Development Fund

Investing
in your future

ISSN 2585-6898 (publication)
ISBN 978-9949-83-829-5 (publication)
ISSN 2585-6901 (PDF)
ISBN 978-9949-83-830-1 (PDF)
Printed by Auratrükk

TALLINNA TEHNIKAÜLIKOOL
DOKTORITÖÖ
31/2022

Külmligu kanepikiudude karakteriseerimine kasutamiseks sarrusena biokomposiitides

PERCY FESTUS ALAO

TAL TECH KIRJASTUS

Contents

List of Publications

The list of author's publications, based on which the thesis has been prepared:

I Marrot, L.; **Alao, P.F.**; Mikli, V.; Kers, J. (2021). Properties of Frost-Retted Hemp Fibers for the Reinforcement of Composites. Journal of Natural Fibers, 1–12.

II **Alao, P.F**.; Marrot, L.; Burnard, M.D.; Lavrič, G.; Saarna, M.; Kers, J. (2021). Impact of Alkali and Silane Treatment on Hemp/PLA Composites' Performance: From Micro to Macro Scale. Polymers, 13, 851.

III **Alao, P.F**.; Marrot, L.; Kallakas, H.; Just, A.; Poltimäe, T.; Kers, J. (2021). Effect of Hemp Fiber Surface Treatment on the Moisture/Water Resistance and Reaction to Fire of Reinforced PLA Composites. Materials 2021, 14, 4332.

Author's Contribution to the Publications

Contribution to the papers in this thesis are:

I The author prepared the hemp fibres, treated the hemp fibres, fabricated the composite boards, participated in the characterisation of the fibre surface morphology, determined the composite mechanical properties, and participated in the analysis of all the results and was involved writing the major draft of the paper.

II The author prepared the hemp fibres, treated the hemp fibres, participated in the characterisation of the hemp fibre properties at the microscopic level (thermogravimetric analysis and scanning electron microscopy), fabricated the composite specimens, analysed the structural changes observed in the Fourier transform infrared spectroscopy, determined mechanical performance of the composites, analysed the results, and wrote the main draft of the paper.

III The author prepared the hemp fibres, treated the hemp fibres, fabricated the composites, determined the moisture/water resistance properties of the composites, evaluated the reaction to fire properties of the composites, analysed the results, and wrote the main draft of the paper.

Other related publications not included in the thesis:

Alao, P. F.; Kallakas, H.; Poltimäe, T.; Kers, J. (2019). Effect of hemp fibre length on the properties of polypropylene composites. Agronomy Research, 17 (4), 1517−1531.

Kallakas, H.; Liblik, J.; Alao, P. F.; Poltimäe, T.; Just, A.; Kers, J. (2019). Fire and Mechanical Properties of Hemp and Clay Boards for Timber Structures. In: IOP Conference Series: Earth and Environmental Science. IOP Publishing Ltd.

Alao, P.; Tobias, M.; Kallakas, H.; Poltimäe, T.; Kers, J.; Goljandin, D. (2020). Development of hemp hurd particleboards from formaldehyde-free resins. Agronomy Research, 18 (Special Issue 1), 679−688.

Introduction

The increasing growth of the world's population has resulted in a significant consumption of non-renewable resources like petroleum and renewable resources like water, posing severe economic and environmental challenges. Thus, materials derived from natural, renewable resources, such as annual-growth crops, have received much attention (Bourmaud *et al.*, 2018). Policies such as the European Green Deal (EGD), approved in 2020, including European Climate Law (ECL) have been implemented to encourage the efficient use of biodegradable and renewable resources to promote a healthy, circular, and sustainable environment that helps to realise climate neutrality, zero-pollution, and halts biodiversity loss. For instance, the energy consumption for the production of natural fibres is 60% less than that of glass fibre (Bhattacharyya, Subasinghe and Kim, 2015). Consequently, construction, transportation, packaging, and cosmetic sectors are increasingly sorting the application of suitable biobased materials like plant fibres (flax, hemp, jute, and sisal). Interestingly, these plant materials have existed and applied for thousands of years. Hemp, for example, was first discovered in China about 8000 BCE.

Hemp is a flexible and promising plant-based renewable resource that is now receiving attention in the scientific community. Hemp is an annual crop grown from hemp seed that produces strong and woody fibres. Hemp, like other plants, has low input energy to develop and have the potential to capture carbon dioxide (CO_2) from the environment during growth and cleaning the air. Consequently, the environmental carbon footprint decreases. The fibres are harvested from the hemp plant by retting (Nilsson, Svennerstedt and Wretfors, 2005) and they provide an intriguing, specialized performance for the construction of polymer composites. Given that the primary goal of hemp crop grown in most areas of the globe, notably in Europe and Estonia, is to create cannabidiol, the fibre and shives by-products, which are typically dismissed as trash, can become unbelievably valuable if used successfully in composite applications. Though, understanding and defining the fibre characteristics, which determine the intrinsic capabilities and efficacy of the fibre to reinforce polymer composites, it is required to fulfil a variety of applications. Natural fibres offer a wide variety of cell wall composition and strength qualities (Marrot *et al.*, 2013) that are determined primarily by growth, maturity, and retting conditions (Bourmaud *et al.*, 2018). Hydrophilic qualities of natural fibres impair interfacial adhesion with polymer matrices, resulting in voids and inadequate stress transfer, compromising mechanical performance.

As a result, it is critical to comprehend the characteristics and applications of plant fibre. There is a lack of data on the qualities or application of frost-retted hemp fibres (Hungarian species Tisza) in the reinforcement of composites. Therefore, this study seeks to fill this gap. The aim of this research was to augment the contribution to a carbon-neutral environment by applying this underutilised frost-retted hemp fibre as reinforcements in enhancing the technological and physicomechanical properties of sustainable biocomposites. The novelty of current research is based on the characteristics of frost-retted hemp fibres grown in Estonia which is not reported in the literature. Their utilisation will lead to valorisation of local resources. Furthermore, this research applied a uniquely comprehensive approach with double scale analysis, involving the examination of the characteristics of the unmodified and chemically modified hemp fibres on a micro-scale and their influence on a macro-scale (the biocomposite's physicomechanical performance).

For this purpose, the biochemical and strength properties of the hemp fibres were first examined and defined. Surface pre-treatment with water and alkali and combined modification with silane were introduced to fabricate composites with hemp fibre at various wt.%. The impact of the fibre surface modification and content was examined from the mechanical and functional properties of the composites and the most effective treatment for the robust performance of the biocomposite was established. The research provides valuable information on the characteristics of Estonian hemp fibres and their suitability as an alternative composite reinforcing material.

Abbreviations and Symbols

A_f	Alkali pretreated hemp fibre
AH	Alkali pretreated hemp fibre reinforced PLA composites
APTES	3 -Aminopropyl-triethoxysilane
AS_f	Alkali and silane treated hemp fibre
ASH	Combined alkali and silane treated hemp fibre reinforced PLA composites
BCE	Before the Christian Era
CO_2	Carbon dioxide
E	Modulus of elasticity (Young´s modulus) in tension
$EMC_{d.b}$	Equilibrium moisture content (dry bases)
FAO	Food and Agriculture Organization (of the United Nations)
FTIR	Fourier Transform Infrared
HDPE	High density polyethylene
NFC	Natural Fibre Reinforced Composite
M_D	Equilibrium moisture content (EMC)
MOE	Flexural modulus
MOR	Flexural strength
PCL	Polycaprolactone
pH	Potential of hydrogen
PHAs	Polyhydroxyalkanoates
PHB	Polyhydroxybutyrate
PLA	Polylactic acid
RH	Relative humidity
SEM	Scanning Electron Microscopy
T_5	Temperature at 5% mass loss
T_{10}	Temperature at 10% mass loss
TGA	Thermogravimetric Analysis
U_f	Untreated hemp fibre
UH	Untreated hemp fibre reinforced PLA composites
W_f	Water pretreated hemp fibre
WH	Water pretreated hemp fibre reinforced PLA composites
Ws_f	Water and silane treated hemp fibre
WSH	Combined water and silane treated hemp fibre reinforced PLA composites
wt.%	Weight percentage
VIP	Vacuum infusion process
σ	Tensile strength

1 Literature review

1.1 Industrial hemp (*Cannabis sativa*)

In the past, Canada was the largest cultivator of hemp, however the hemp plant is originally native to India and Persia (Manaia, Manaia and Rodriges, 2019). According to 2019 data obtained from (Statista, 2021) shown in Figure 1, approximately 56,196 ha of land area was dedicated to hemp cultivation in Europe. France accounted for 70% of the total land area used for the cultivation, while Lithuania and Estonia make up the second and third largest, respectively. But the recent European Commission report on the cultivation of hemp fibres in Europe puts the Netherlands (10%) and Austria (4%) as the 2nd and 3rd largest producers, respectively, for the same period.

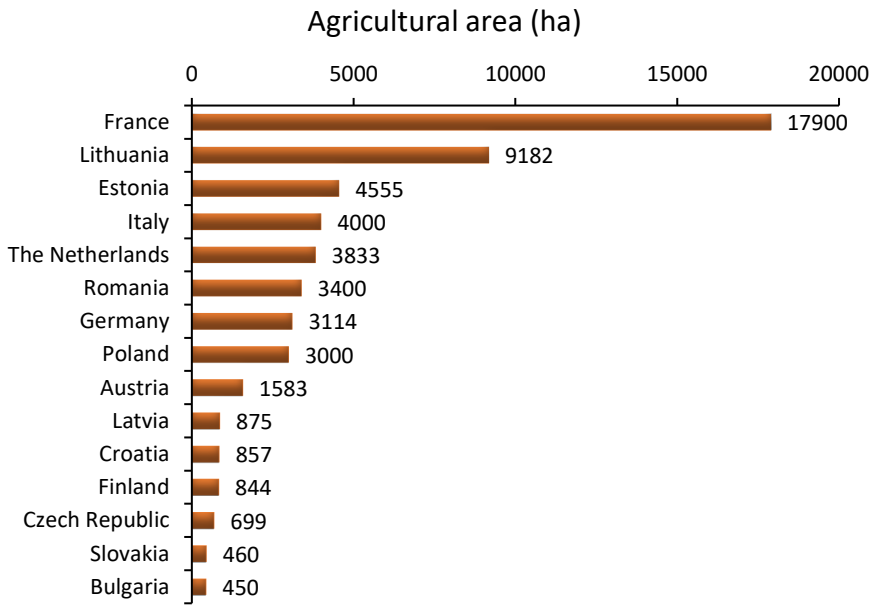

Figure 1. Top 15 hemp cultivators in Europe as of 2019 (Statista 2021).

The market demand for hemp is driven by the growth in the application of cannabidiol (CBD) obtained from the hemp stalk, flowers, and leaves and, the hemp seed used for food and beverages, personal care, and animal feeds. The many benefits of hemp highlighted as important by the member of the board of advisors for the Industrial Hemp Association (EIHA) in the European Commission, Catherine Wilson are listed below:

1. Hemp has a negative carbon footprint. For instance, the cultivation of one hectare of hemp can absorb approximately 15 tonnes of CO_2.
2. Growing hemp minimises environmental pollution as it does not require herbicides, pesticides, or fungicides.
3. Hemp has high growth and shading capacity that is suitable for breaking cycles of disease when used in crop rotation.
4. After the cultivation of hemp, the soil is left in optimum condition which helps prevents soil erosion and can be used for the recovery of land.

5. Additionally, hemp has several good uses, e.g., providing refuge for birds, seeds for animal feed, and because of the differing pollination season (July and September) compared to other crops, it is biodiverse.

Due to these merits, hemp cultivation in Europe is considered one of the means to reaching the European green deal targets. Besides, the land area dedicated to the growth of hemp in Europe has almost doubled. Varieties of industrial hemp include Anka, Uso, Zolotonosha (Canada), Felina, Fedora, Futura, etc (France), Carmagnola (Italy), FIN-314 (Finland, Canada) and Tisza, Kompolti and Fibriko from Hungary. Hemp plants thrive in semi-humid environments with temperatures ranging from 14 to 27 °C. It requires a lot of rain or irrigation (particularly in the first six weeks), roughly 30–40 cm per growing season, and is drought-resistant after that, although the bulk is diminished, and a lack of proper hydration also hastens maturity. Seedlings can tolerate a -5 °C frost, while adult plants can also withstand a -5 °C cold (British Columbia Ministry of Agriculture and Food, 1999).

1.2 Hemp fibre

There is conflicting information about the global production of hemp fibres. According to (Manaia, Manaia and Rodriges, 2019) Russia accounts for the largest global production of hemp fibre with about 33%, but reportedly, China has an output of 93,000 tons/year, which is considered the largest based on FAO data reported by (Dayo *et al.*, 2018). Besides, as of 2020, industrial hemp, hemp products, and end-use items such as paper and textiles were all produced and exported mainly by China (Market Analysis Report, 2021). In Estonia, hemp fibre is obtained as a by-product of cannabidiol (CBD) produced for medicinal purpose. “Estonia is a hidden gem for CBD production since it has a clean environment with good water, organic soil, and no local pests that would induce the use of chemicals for growing hemp” (Stephen J Wyatt, CEO of Hemp Futures).

Hemp fibre is a plant biofibre derived from the bast of industrial hemp (*Cannabis sativa L.*). Ideally, hemp fibres fall in the classification of primary natural fibres like flax, cotton, Kenaf and jute, which are fibres grown for their fibre content (Bhattacharyya, Subasinghe and Kim, 2015). However, most often than not, these agricultural by-products are dumped in the open field or incinerated (Dayo *et al.*, 2018). Hemp and flax are most widely accessible in Europe, and they might be an appealing alternative to glass fibre reinforcement in composites. But hemp fibres suffice as the most desirable of the two plants, owing to their specific mechanical characteristics and a price that has remained lower and more consistent throughout time than flax fibres. Hemp has received less attention by researchers than flax, and its morphology and mechanical behaviour are somewhat understood (Marrot *et al.*, 2013).

1.2.1 Fibre structure

In general, the structure of hemp fibre is quite similar to that of wood. Hemp stems are typically 1.5–2.5 m tall with a diameter of 5–15 mm (Liu, Thygesen, *et al.*, 2017). Figure 2 shows the hemp stem with the arrangement of fibres. Typically, it consists of a pith assembled in layers of xylem, cambium, cortex, epidermis, and cuticle, diameters/thicknesses of which are 1–5 mm, 10–50 µm, 100–300 µm, 20–100 µm, 2–5 µm, respectively (Liu, Thygesen, *et al.*, 2017). Hemp fibres have primary and secondary fibres. The primary fibres range in length from 5 to 100 mm, whereas the secondary fibres, which are missing in the flax fibre, are around 2 mm long (Marrot *et al.*, 2013).

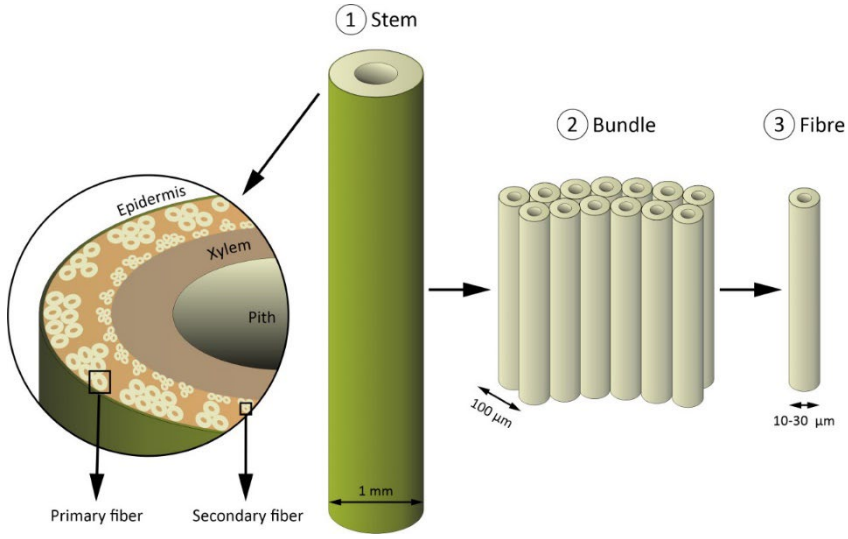

Figure 2. Organisation and morphology of a hemp stem, bundle of fibres and single fibre.

1.2.2 Biochemical composition

Like all plant materials, the hemp fibre features cellulose, hemicelluloses, lignin, pectin, wax, and water-soluble extractives as the cell wall contents. Nevertheless, cellulose, a long-chain polysaccharide formed by units of β-D glucose is the principal cell component of the hemp fibre. The structure of the hemp fibre cell (Figure 3) is categorised into the primary wall, the secondary wall, and the lumen, which is responsible for the transportation of moisture and middle lamella (pectin) that binds the fibre. The primary cell wall deposited in the early growth stage (Pereira *et al.*, 2015) is 70–110 nm thick (Liu, Thygesen, *et al.*, 2017). It consists of disorderly arranged cellulose microfibrils immersed in a matrix of hemicelluloses and lignin. Hemicelluloses are highly concentrated in the primary cell wall, while lignin is an extremely crosslinked amorphous molecular structure that binds the individual fibres.

The secondary cell wall is thicker (3–13 µm) and comprises crystalline cellulose microfibril in three layers: the outer secondary cell wall (S1), the middle cell wall (S2) and the inner cell wall (S3) (Pereira *et al.*, 2015). The composition and structural arrangement of the fibre is influenced by the plant growth conditions, the degree of retting and maturity (Bourmaud *et al.*, 2018). Hence, to effectively apply the hemp fibres, the structural composition must be considered.

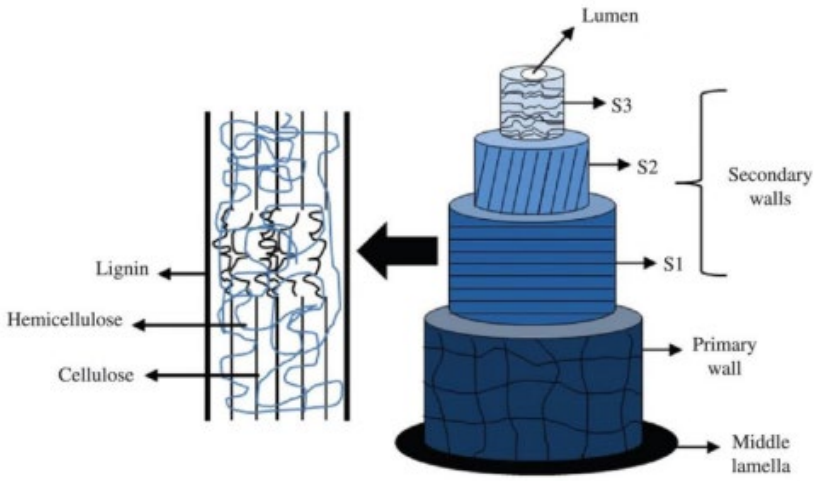

Figure 3. Schematic representation of hemp fibre cell layers (Henrique et al., 2015).

1.2.3 Fibre properties

Table 1 shows that hemp fibres represent one of the strongest and stiffest of the available natural fibres. The high strength of hemp fibre could be attributed to the high cellulosic content and their special function to provide support in the plant stem (Bourmaud *et al.*, 2018). According to (Bhattacharyya, Subasinghe and Kim, 2015), the properties of the hemp fibre depend on the fibre structure, chemical composition, microfibrillar angle, cell dimension, and inherent fibre defects. In other words, the amount and order of cellulose microfibril (microfibril angle) in S2 determines the inherent fibre strength. Additionally, the lignin also determines the fibre rigidity and affects the impact and compression properties (Pereira *et al.*, 2015) whereas fibre retting conditions could influence the morphological and tensile properties of the fibre (Mazian *et al.*, 2018) and affect the adhesion mechanism between the fibre and the polymer (Pereira *et al.*, 2015).

Table 1. Comparison of the mechanical properties of natural and synthetic fibres (Pil et al., 2016).

Properties	E-glass	Carbon (T300-T700)	Flax	Hemp	Bamboo	Jute
Density, g/cm^3	2.55	1.8	1.45	1.48	1.4	1.46
Tensile strength, MPa	2000–2400	3530–4900	800–1500	550–900	750–950	400–800
Stiffness, GPa	70–74	230	55–75	40–65	30–50	10–30
Specific strength, MPa cm^3/g	780–940	1900–2700	550–1030	370–600	535–680	275–550
Specific stiffness, GPa cm^3/g	27–29	128	38–52	27–44	21–36	7–21
Elongation at break, %	3	1.5–2.1	1.5–2	1.6	1.9	1.8

One of the main advantages of hemp fibres over the synthetic alternatives is the low density that results in high specific strength and stiffness (Ku et al., 2011; Manaia, Manaia and Rodriges, 2019). Other benefits include environmental friendliness, non-abrasiveness to processing equipment, cheap cost, renewability, and less processing energy, which results in reduced air pollutants. But, hemp fibres have natural hydrophilic qualities, a high anisotropic nature, limited resistance to microbes, low heat stability, uneven mechanical properties, and inferior mechanical performance, which serve as limitations compared to synthetic fibres (Manaia, Manaia and Rodriges, 2019).

1.3 Retting

Retting is a process that is used to loosen the bast fibres from the stem. This process involves the removal of non-fibrous tissues by the degradation of hemicellulose and pectins (Tavares *et al.*, 2020). During retting, a combination of wet and moderate weather promotes the development of microorganisms (fungi, bacteria) that colonize the plant stem. These microorganisms secrete degrading (or hydrolases) enzymes such as polygalacturonases or xylanases that accelerate the breakdown of the plant's polysaccharides. The enzymes gradually destroy the pectins of the cortical parenchyma's middle lamellae, the epidermis, the xylem, and the bundles of fibres, which then facilitates the mechanical (scutching) or manual detachment of the bundles. There are 5 types of plant retting: (1) dew retting (2) water retting (3) mechanical retting (4) enzymatic retting and (5) chemical retting.

In Europe, the plant stalks are commonly dew (field) retted. This type of fibre retting is subject to weather conditions like rainfall and temperature (Liu, Silva, *et al.*, 2016). Considering the hemp fibre and seed maturity period (mid-August), field retting normally begins in autumn (mid-August or September) in places like Northern France, Belgium, and the Netherlands (Réquilé *et al.*, 2021). However, the autumn period in the Nordic region is often associated with cold and high rainfall (Pasila, 2000), which is unfavourable because of the possibility for high moisture content in the stems, collection difficulty, rotting or in some cases, over-retting, due to the secretion of cellulase that depolymerizes cellulose (Réquilé *et al.*, 2021). Pasila (2000) proposed collecting the hemp straws during spring, which is the driest time of the year, to prevent an increase in moisture content in the plant stem and improve the possibility for mechanical drying. Straws harvested during this period are referred to as frost retted. For frost retting, the fibre separation from the bundle is induced by the daily temperature variation above and below zero. The repeated fluctuation of the springtime temperature causes the freezing and melting of water in the plant stem, creating an enlarging movement which results in the loosening of the fibre from the stalk.

1.4 Fibre modification

The objective of the fibre modification is to treat the fibre surface to remove the wax in natural fats present in the hemp fibre for easy handling or better performance as a reinforcing material (Alix *et al.*, 2009; Väisänen *et al.*, 2018). Chemical and physical methods are commonly used (Manaia, Manaia and Rodriges, 2019) to achieve this. The chemical treatments involve the modification of the fibre surface by any of the following methods: acetylation, peroxide treatment, benzoylation, isocyanate treatment, and using maleated coupling agents (Pereira *et al.*, 2015; Sepe *et al.*, 2018). The objective of chemical treatment is to modify the hydroxyl and carbonyl groups in the fibre and

introduce networking groups that enhance the interfacial bond with the polymeric matrix, because the hydroxyl groups in natural fibres increase hydrophilic properties that limit the interfacial adhesion with the polymer matrices, since these matrices are hydrophobic in nature (Liu, Thygesen, *et al.*, 2017). The poor adhesion between the fibres and matrix causes ineffective stress transfer and induces voids that subsequently impede the mechanical performance of the composites (Islam, Pickering and Foreman, 2010). Hence, the chemical treatment primarily removes non-amorphous fibre contents such as pectin, wax, hemicellulose, and lignin to obtain cellulose rich fibres (Sgriccia, Hawley and Misra, 2008; Liu, Meyer, *et al.*, 2016; Liu, Thygesen, *et al.*, 2017). The physical treatments involve corona, cold plasma, ultraviolet, heat treatment and, electron radiation (Sreekumar *et al.*, 2009). But these treatments can often cause the deterioration of the flexural properties of composites (Sepe *et al.*, 2018; Sood and Dwivedi, 2018).

Nonetheless, of all the listed methods, alkaline treatment with sodium hydroxide (NaOH) has been found to be the utmost applied process (Manaia, Manaia and Rodriges, 2019), because of its' feasibility (Islam, Pickering and Foreman, 2010). The treatment of the fibres with NaOH modifies the fibre surface by removing a certain amount of lignin, hemicelluloses, wax, and oils covering the external surface of natural fibre, revealing more hydroxyl bonding sites and making the fibre surface rough (Demir *et al.*, 2006; Pickering, Efendy and Le, 2016; Dayo *et al.*, 2018; Sepe *et al.*, 2018), thereby causing better interfacial bonding (Islam, Pickering and Foreman, 2010). As a result, alkaline treatment enhances the mechanical behaviour of the natural fibre, particularly fibre strength, and thus the mechanical characteristics of the composite (Fiore, Di Bella and Valenza, 2015). The procedure of the alkali treatment (Kabir *et al.*, 2013a; Sepe *et al.*, 2018) is shown below:

$$\text{Fibre–OH} + \text{NaOH} \rightarrow \text{Fibre–O}^{-}\text{Na}^{+} + \text{H}_2\text{O}$$

Silane treatment has also been used to further improve the composite performance by enhancing the interfacial relationship between the fibre and the polymer matrix. The impregnation process where the hemp fibres are treated with prehydrolyzed silane solution ensures modification of the fibre surface and cell walls (Xie *et al.*, 2010). The silane coupling agents are hydrophilic compounds with a silicon atom attached to separate functional groups, allowing one end to engage with the matrix and the other end to react with the hydrophilic fibre, which acts as a bridge between both (Sepe *et al.*, 2018). However, silane treatment works more efficiently with the presence of more free OH groups. Therefore, it is often combined with alkali treatment. There are four phases to the interaction of silane with the natural fibre: **hydrolysis** phase where the silane monomers are hydrolysed, **condensation** phase that is slowed down using an acidic environment (usually acetic acid) to ensure availability of free silanols that are then **adsorbed** to form siloxane bonds (– Si– O–Si –); consequently, **grafting** on the fibre surface via covalent bonds – Si– O–C – of the silanols. As a result, the hemp fibre becomes less hydrophilic (Cyras *et al.*, 2004), which decreases the water affinity of the reinforced composites. Silanes commonly used for modification of natural fibres/polymer matrices consists of organic functionalities, such as amine, methacrylic, vinylic, azide, alkylic etc. But amino silane such as (3-Aminopropyl) triethoxysilane ($C_9H_{23}NO_3Si$) known as APTES is one of the most versatile because of its ability to treat majority of the commonly used polymer matrices. The processes involved in the siloxane bridges that occur after thermal stimulation (Brochier Salon *et al.*, 2005) are shown:

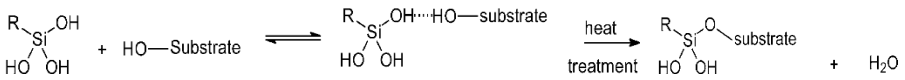

Thermal stimulation occurs when the fibres are oven dried at elevated temperature usually about 120 °C for 1 hour.

1.5 Composite matrices

Thermoplastic and thermosetting matrices are the two types of polymer matrices used in composite production. The parameters of the most widely studied polymer matrices used for hemp fibres are listed in Table 2. The nature of polymers can be thermoset or thermoplastic, depending on the structural and chemical linkages. Thermoplastic polymers contain one- or two-dimensional molecular structures that are flexible under heat or force and may reshape when pressure and heat are reapplied. On the other hand, thermosetting polymers consist of cross-links and form an irreversible chemical connection when pressure and heat are applied. Thermoset polymers cannot be melted or reformed, and they only degrade when heated to a high enough temperature, which is a disadvantage for recyclability. Thus, when chemical and thermal stability are required, thermoset matrices are preferable. Thermoplastic polymers are resistant to damage and can be recycled since they can be heated and reformed. Polymer materials have a low density and a low melting temperature in general. The polymer matrices protect the fibres from environmental degradation, preserve fibre arrangement, transfer stress to the fibres, and influence the form and appearance of the composite. Overall, the polymer matrices govern the composite's optimum service temperature, moisture resistance, chemical resistance, and thermal stability (Manaia, Manaia and Rodriges, 2019). The application, needs, and desired qualities of the composite material being developed, and accessibility in the location where manufacturing is being considered are the factors that influence the matrix selection.

Table 2. Properties of polymer matrices used for hemp fibres (Manaia, Manaia and Rodriges, 2019).

Polymer	Density, g/cm^3	Failure Strain, %	Tensile Strength, MPa	Young's Modulus, GPa	Glass Transition Temperature, °C	Melting Temperature, °C
Synthetic Thermoplastics						
Polypropylene	0.89–0.92	20–400	30–40	1.1–1.6	- 10 to - 23	161–170
Polyethylene - HDPE	0.94–0.96	2–130	14.5–38	0.4–1.5	- 100 to - 60	120–140
Polystyrene	1.04–1.06	1–2.5	25–69	4–5	100	110–135
Polylactic acid (PLA)	1.21–1.25	2.5–6	21–60	0.35–3.5	45–60	150–162
Thermosetting						
Epoxy	1.1–1.4	1–6	35–100	3–6	60 to 170	–
Polyester	1.2–1.5	4–7	40–90	2–4.5	-47 to 120	–

Because of environmental concerns, biopolymers such as polylactic acid (PLA), modified cellulose, soya oil-based epoxy, polycaprolactone (PCL), polyhydroxybutyrate (PHB), lignin, and starch have become more desirable and are studied for many industrial applications. Table 3 presents the properties of some of the known biopolymers. Despite the increased desire for adoptability of these biopolymers, low toughness/commercial availability, processability, prohibitive cost, limited moisture resistance, and low thermal stability are the key drawbacks (Pappu, Pickering and Thakur, 2019). Regardless, PLA is at the fore with regards to utilisation, thanks to a recently developed cost-effective polymerisation process (Sawpan, Pickering and Fernyhough, 2011b; Pappu, Pickering and Thakur, 2019) and good mechanical performance.

Table 3. Bio-based polymers, properties, application (Douglas D. Stokke, Qinglin Wu, Guangping Han, 2013).

Polymer type		Properties	Application
Natural	Starch-based polymers	Short shelf-life, biodegradable and compostable	Films, moulding, extrusion
	Cellulose derivatives	Biodegradable, limited, compostable, good mechanical properties	Films, injection moulding
Derived by bacterial fermentation of sugars or lipids	PHAs	Long shelf-life, varying biodegradability, limited, compostable	Moulding, films
Derived from biobased materials	PLA	Weatherproof, high strength, high modulus	Films, moulding, extrusion, fibres

1.5.1 Polylactic acid (PLA)

PLA polymers are lactic acid polyesters that have lately been used in applications where biodegradability is essential (Oksman, Skrifvars and Selin, 2003). PLA is a bio-based thermoplastic polymer with excellent mechanical characteristics (Hu and Lim, 2007). The polymer fibre is made from the monomer of yearly renewable crops including maize, potato, and cane sugar; it is 100% biodegradable (Oksman, Skrifvars and Selin, 2003; Hu and Lim, 2007), and its life cycle can help to reduce carbon dioxide levels on the planet. It seems to be an obvious alternative to conventional polymers for a product that is both environmentally benign and mechanically sound (Baghaei *et al.*, 2014). Hydrolysis to lactic acid, which is then metabolised by bacteria to water and carbon monoxide, is required for deterioration, which is reported to happen in two weeks, with total absence taking three to four weeks after breakdown. However, according to Hu and Lim, (2007) the degradation process may take several months to two years.

The two polymerisation processes currently employed to make PLA are direct poly-condensation of lactic acid and cyclic intermediate dimer (lactide), which includes a ring-opening process; the latter is favoured owing to its capacity to yield high molecular weight PLA. The polymer is obtained from the monomer of lactic acid (2-hydroxy propionic acid) by the fermentation of dextrose, produced from the enzymatic hydrolysis

of plant starch (Douglas D. Stokke, Qinglin Wu, Guangping Han, 2013). The commercial use of PLA is expected to grow significantly in the future and is already used to make plastic bags for home biowaste, sanitary products and diaper wrappings, planting cups, disposable cups, and plates (Oksman, Skrifvars and Selin, 2003). However, PLA's intrinsic brittleness and poor toughness, as well as its low melt viscosity and excessive cost, may limit its usage as a polymer matrix in composite production (Manaia, Manaia and Rodriges, 2019). Though more research is currently being geared towards improving some of these issues.

1.6 Biocomposites

Composites are the product of a stiff material (the fibre) that reinforces a polymer matrix (thermoplastic or thermosetting). The composite is a biocomposite when at least one of its components is from a natural material (Tavares *et al.*, 2020); hence, composites reinforced with biobased (lignocellulosic) fibres are biocomposites and otherwise known as natural fibre reinforced composites (NFCs). According to Manaia, Manaia and Rodriges (2019), NFCs have a lower environmental impact, reduce the weight and volume of polymeric matrices due to the ability to use higher fibre content for specific performance, and reduce emissions and fuel consumption throughout the life cycle. Because lignocellulosic fibres are employed, NFCs have low health risks and are less expensive than today's most popular synthetic fibre reinforced composites (Merkel *et al.*, 2014). However, in selecting the natural fibre for precise application, it is essential to consider the fibre strength, dimension, structure and the biocomposition (Pereira *et al.*, 2015). According to Liu *et al.* (2017), the fibre and matrix properties, fibre orientation, porosity, fibre length, fibre packing ability, fibre/matrix interface properties and fibre content are the range of parameters influencing the performance of natural fibre reinforced composites.

The application of hemp fibre with the most potential is as reinforcement material in polymeric composites (Pickering, Efendy and Le, 2016; Pappu, Pickering and Thakur, 2019). Considering that hemp growth, in most parts of the world is predominantly for nutritional application i.e., extraction of CBD, the fibre and shives by-products often considered as waste can thus become immensely valuable if effectively utilised for composite application. Some properties of hemp fibre composites published are presented in Table 4. Overall, 30 wt.%. fibrous reinforcement was considered because the fibre reinforcement range of 25 wt.% to 35 wt.% is reported as the most suitable to achieve optimum performance and economic benefit (Pappu, Pickering and Thakur, 2019). Although Islam, Pickering and Foreman (2010) attained a remarkably high mechanical outcome with fibre contents of 65 wt.%, no other study has reported such high values at such fibre content. Additionally, Table 4 shows that the hemp fibre surface was often treated with NaOH solution or by combined a modification using NaOH solution and a coupling agent (silane).

Table 4. An overview of some results previously published for hemp fibre reinforced composites.

Composite description				Mechanical strength	
Fibre content (reference)	Polymer type	Treatment type	Fabrication method	Tensile strength (σ), MPa	Flexural strength (MoR), MPa
30 wt.% Hybrid (15 wt.% hemp + 15 wt.% sisal) (Pappu, Pickering and Thakur, 2019)	PLA	none	Injection moulding	46 ± 7	95 ± 11
Woven hemp fibres (42 ± 1 wt.%) (Sepe *et al.*, 2018)	Epoxy Epoxy	none	VIP	81 ± 3	118 ± 5
		1 wt.% NaOH solution		69 ± 4	114 ± 5
		5% silane		72 ± 1	123 ± 6
65 wt.% (Islam, Pickering and Foreman, 2011)		untreated	Compression moulding	165	180
		2 wt.% Na2SO3 + 5 wt.% NaOH		130 ~	170 ~
30 (2) wt.% (Väisänen *et al.*, 2018)		none		64 ± 14	91 ± 20
		10 wt.% NaOH soln.		41 ± 5	74 ± 9
25 wt.% (Dayo *et al.*, 2018)	Poly benzoxazine	Cyclohexane/ ethanol washing + silane		45 ± 2	114 ± 3
30 wt.% (Baghaei *et al.*, 2014)	PLA	4 wt.% NaOH		77 ± 3	101
45 wt.% (250 wraps/m) (Baghaei, Skrifvars and Berglin, 2013)	PLA yarns	None		59.3	124.2

Composite description				Mechanical strength	
Fibre content (reference)	Polymer type	Treatment type	Fabrication method	Tensile strength (σ), MPa	Flexural strength (MoR), MPa
40 wt.% (Lu, Swan and Ferguson, 2012a)	HDPE	5 wt.% NaOH soln.	Compression moulding	60	44
40 wt.% (Hu and Lim, 2007)	PLA	6 wt.% NaOH		55	113
30 wt.% (Islam, Pickering and Foreman, 2010)		2 wt.% Na2SO3 + 5 wt.% NaOH	Film stacking	83	143

Although using natural fibres as a reinforcement in composites has several advantages, the intrinsic features of the natural fibres cause certain undesirable traits in the composites. Limited mechanical performance, excessive water absorption, poor fire resistance, and concerns linked to manufacturing irregularities and inhomogeneity are the four key challenges that restrict the use of natural fibres in composites (Väisänen *et al.*, 2018). Therefore, it is essential to assess the multifunctional performance of biocomposites to meet a variety of applications (Mohd Ishak and Mat Taib, 2015). As a result, studies have examined the resistance to water in addition to the mechanical performance of biobased composites (Pejic *et al.*, 2008; Sreekumar *et al.*, 2009; Dayo *et al.*, 2018; Thiagamani *et al.*, 2019).

The fire reaction of these composites has also been studied (Naughton, Fan and Bregulla, 2014; Mohd Ishak and Mat Taib, 2015) though in a limited number of publications. Most importantly, a fire resistance test is essential for any construction material to fulfil building standard regulations (Naughton, Fan and Bregulla, 2014). Hence, to classify NFCs as construction materials, there is a need to provide data or improve fire resistance of the biocomposite, which has been achieved through using higher fibre content, an additive such as magnesium hydroxide, or fire retardant treatment (Hapuarachchi *et al.*, 2007).

1.7 Application or potential use of hemp fibres and their biocomposite

The most researched and growing application for hemp and natural fibres, in general, is reinforcement in polymeric composites in automotive applications (Lu, Swan and Ferguson, 2012b; Dayo *et al.*, 2018; Sepe *et al.*, 2018; Alao *et al.*, 2019; Islam and Bhat, 2019) because the automobile sector is continually seeking ecologically friendly materials in its products (Zegaoui *et al.*, 2018). NFCs have been used to make vehicle components such as door panels, glove boxes, hat racks, dashboards, and other components, by the car manufacturers Audi, BMW, Mercedes-Benz, Fiat and Volvo (Manaia, Manaia and Rodriges, 2019). NFCs show prospects for use in the production of parts of musical instrument (Pickering, Efendy and Le, 2016), in sports goods and consumer electronics

(Zegaoui *et al.*, 2018). In particular, hemp fibres have a better vibration dampening ability than synthetic fibres that make them a more suitable alternative. Other applications of NFCs include aircraft interior panelling, toys, packaging, casings for electronic devices like laptops and phones, surfboards, heat insulation materials, fibre reinforced concretes in building construction, and brake pads, which are commonly made of geopolymers reinforced with hemp fibres (Hussain *et al.*, 2019; Manaia, Manaia and Rodriges, 2019; Pappu, Pickering and Thakur, 2019).

Biocomposites made of natural fibres have a wide range of physical and mechanical characteristics, making them difficult to use in structural applications where reliability is critical (Marrot *et al.*, 2013). However, more structural components, such as seat backs and outside underfloor panelling in the automobile, are increasingly being manufactured (Manaia, Manaia and Rodriges, 2019).

1.8 Summary of the literature review and aim of the study

Hemp is regarded as one of the natural resources that can be used to meet environmental sustainability, reduce carbon emissions, and improve population health. Hemp cultivation is mostly for the manufacture of cannabidiol (CBD); the shives and fibres as by-products, acquired after harvesting the plant have received little attention. As demand for CBD oil rises, especially in Estonia, so will the amount of hemp stem waste generated, sparking a need to value this locally created product. An environmentally sound method for retting is required to effectively separate the fibres from the stem. The frost-retting process recommended by (Pasila, 2000) is the most suitable in the Estonian climate to avoid physical fibre damage by moisture and save drying energy.

Amongst natural fibres, hemp fibres show promising mechanical properties for reinforcing biocomposites. However, the performance of the hemp fibre is impacted by the fibres' structural composition of the fibre that is dependent on growth, retting conditions, and further processing. Therefore, it is important to examine the properties of the fibre to determine the most effective processing parameters for durable performance.

Although hemp fibres may be used to reinforce a variety of polymers, the use of PLA matrix creates better environmental impact, because it is a biopolymer obtained from renewable resources that shows comparable strength to the synthetic polymers and is readily available. Due to low surface activity and inherent hydrophilic properties hemp fibres often require surface treatments with chemicals such as NaOH and silane to improve the interfacial bonding for good composite performance with polymer matrices.

Hemp fibre composites can be applied in a broad range of applications but for durable and tailored application, it is essential to understand the compositional and mechanical features of the hemp fibre.

Thus, this research aims to augment the contribution to a carbon-neutral environment by applying underutilised frost-retted hemp fibre as reinforcements in enhancing the technological and physicomechanical properties of sustainable biocomposites. The following objectives were focused on to achieve this aim:

1. To study the fibre properties for determining the biochemical composition and strength features and fabrication of biocomposites from hemp fibres and PLA using various compositions of the fibrous reinforcement to ascertain the strengthening capabilities of the hemp fibre.
2. To obtain the most effective hemp fibre surface treatments (water, alkali, or combined modification with silane) for enhanced mechanical performance of

the biocomposite fabricated from the hemp fibre and PLA composites at various wt.%.

3. To study the influence of the fibre surface treatments and content on the functional qualities of the biocomposites, such as moisture adsorption, water resistance and fire behaviour.
4. To examine the most cost effective and efficient surface treatment for a robust biocomposite performance.

For these objectives, the following activities were carried out:

- Harvested and frost retted hemp stems were manually cleaned to obtain fibres and carded.
- The fibre cell wall composition was determined by using a biochemical composition analysis.
- The strength of the hemp fibre was determined from tensile properties of individual and bundle of fibres.
- The hemp fibre was subjected to a variety of surface pretreatment and treatment procedures.
- The effectiveness of the pretreatment and treatment methods was studied from the structural and morphological properties of the fibres.
- The strength properties of the hemp fibres were subsequently investigated.
- Biocomposites were manufactured with various amounts of fibre contents and PLA.
- Mechanical (tensile and flexural performance), water resistance, and fire reaction capabilities were studied to characterise the biocomposite properties.

2 Experimental

This chapter presents the material parameters, analytical methodologies, composite production process, and testing procedures employed in this study to characterise the frost-retted hemp fibre, treat the fibres, develop the biocomposite and study the properties. Table 5 gives an overview of the materials and methods used in this PhD thesis.

Table 5. Overview of materials and methods.

Materials	Methods	Aim of the study	Paper
Decorticated hemp stem; PLA	SEM observation; Fabrication of biocomposite; Tensile properties	Identify and provide information on Estonian hemp fibre (Tisza variety) and its suitability for biocomposite fabrication using PLA as a matrix.	Paper I
Hemp fibre, PLA, distilled water; chemicals: NaOH, APTES	Fibre surface treatment; Biocomposite fabrication; SEM observation; FTIR analysis; TGA analysis; Mechanical properties: tensile and flexural strength and modulus	Investigate the effects observed at the fibre micro properties, especially the influence of the treatments on the tensile qualities of the fibres, their overall impact at the macroscale (composite properties), and to demonstrate applicability of Estonian hemp fibres in composite reinforcement.	Paper II
Untreated and treated hemp (water, alkali, and combined silane treatment) fibres, PLA	Biocomposite fabrication; SEM observation; Water absorption; Moisture adsorption; Reaction to fire properties	Examine the input of the fibre surface pre-treatment (water; alkali pre-treatment) and silane modification on the moisture adsorption, water absorption and reaction to fire of the biocomposite	Paper III

2.1 Materials

The hemp (*Cannabis sativa: Tisza*) was grown on the Saaremaa Island in Estonia from 10 June 2016 to October 2016. The stems were harvested in May 2017 after standing in the field (shown in Figure 4) for about 6 months. The branches harvested around this period in the Baltic region are referred to as frost retted. Table 6 shows the average monthly temperature and sunlight during growth (June, July, August, September, and October 2016) and the temperature during frost-retting. The biochemical composition of the hemp fibre was examined in **Paper I** (see Table 1 in Paper I).

Figure 4. Hemp stems a) at the seed maturity stage in October 2016; b) during the frost retting period in January 2017.

Table 6. Average monthly temperature and sunlight during growth and temperature during frost-retting.

Parameters during growth			Retting period	
Months	Temperature °C	Sunlight	Months	Temperature °C
June	15	13	November	3
July	18	11.5	December	3
August	17	8.9	January	0
September	15	8.6	February	0
October	7	4.0	March	2
–	–	–	April	4
–	–	–	May	9

In **Paper I**, TREVIRA® 400 PLA fibre was used. In **Paper II** and **III**, biobased polymer (IngeoTM 4043D PLA fibre) from NatureWorks (Minnetonka, MN, USA) was used. The polymer fibre was 60 mm long, with a round cross-section, a finesse of 6.7 dtex (linear density) and a density of 1.24 g/cm^3.

In Paper **II** and **III**, Na granules from Sigma-Aldrich were used to make NaOH solutions for pre-treatment of the hemp fibres. The silane treatment was done using APTES: 3-Aminopropyl-triethoxysilane (98% concentration) produced by Alfa Aesar, ethanol with a concentration of 97%, distilled water and acetic acid produced by Lach-ner s.r.o. (99.8% concentration).

2.2 Methods

2.2.1 Hemp fibre preparation

The decorticated hemp stems (Figure 5a) were hand cleaned to separate the shives and carded (in two runs) using a classic drum carder (300 mm batt width and 72 teeth per inch) shown in Figure 5b. The carded hemp fibres (Figure 5c) were subsequently dried in the oven at 80 °C until uniform weight. By amount of the decorticated hemp stem, approximately 29% and 19% of hemp fibres were obtained after hand cleaning and 2nd carding, respectively. The obtained amount of hemp fibre is similar to the reported total for the fibre content of dry stem matter (approximately 25–35%, depending on variety) (British Columbia Ministry of Agriculture and Food, 1999).

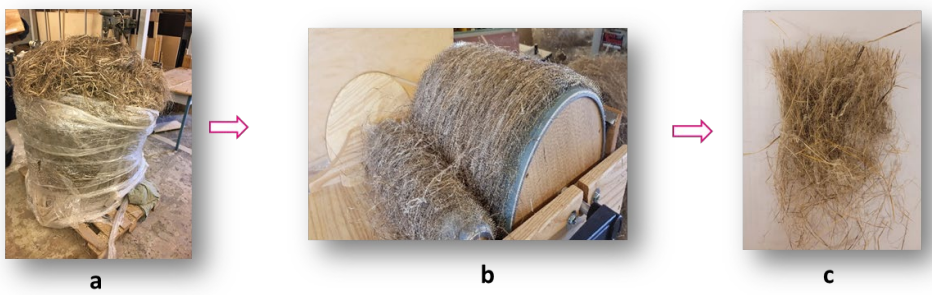

Figure 5. a) Bail of decorticated stem, b) Carding of hemp fibres with a 300 mm batt width; c) hemp fibres.

2.2.2 Fibre surface treatment

First, the hemp fibres were treated using four methods as shown in Figure 6. Water pre-treatment was applied separately to remove water soluble fibre content and to clean the fibre surface while alkali (NaOH) pre-treatment was used to remove pectins, hemicelluloses and lignin content. For both the water and silane pre-treatment, the fibre to water ratio was 1/10. After 4 hours of soaking in the 5 wt.% NaOH solution, the fibres were washed in tap water to remove residual alkali. For the silane treatment, the two variants of pre-treated immersed solutions of 3 wt.% APTES were stirred in ethanol, and water. The ethanol/water volume ratio was 80/20. The solution pH was controlled to 5 with acetic acid and pre-hydrolysed by stirring for 2 h at 23 °C.

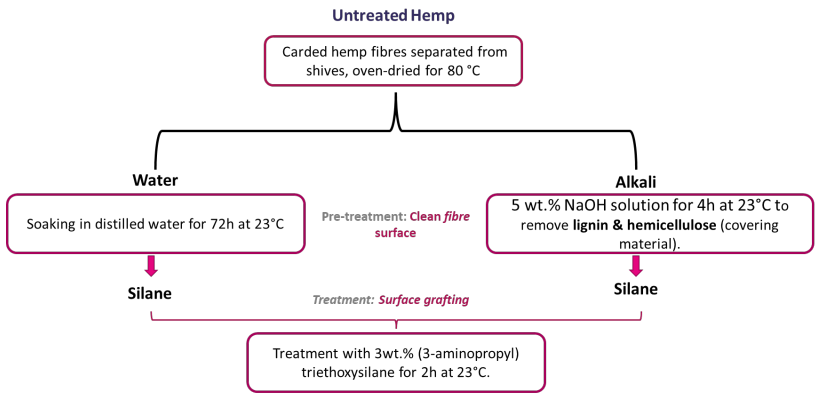

Figure 6. Hemp fibre surface modification with water, NaOH solution and silane presented in Paper II & III.

2.2.3 Determination of fibre mass loss

In Paper III, the reduction in fibre weight (W_{loss}) after the surface modification was estimated from the equation (1).

$$W_{loss} = \frac{w_0 - w_1}{w_0}, \ (1)$$

where W_0 is the weight of the fibre before any treatment, and W_1 is the weight of the fibre after pre-treatment/treatment.

2.2.4 Biocomposite fabrication

The biocomposites were fabricated by thermocompression using a hot press at a temperature of 180 °C and pressure of 3 MPa for 10 minutes. The blend of hemp and PLA fibres was dried for 4 hours at 80 °C before hot pressing. Figure 7(a) shows a blend of 50 wt.% hemp and PLA fibres while Figure 7(b) shows the biocomposites reinforced with the hemp fibres. The biocomposite density was measured using a Mettler Toledo AX balance by EN ISO 1183-1. The samples were conditioned following ISO 291.

(a)

(b)

Figure 7. (a) Hemp (50 wt.%) and PLA fibre blend; (b) fabricated biocomposite.

In **Paper I**, composites were fabricated from untreated hemp and PLA fibres at two hemp/PLA ratios (30 and 50 wt.% based on hemp fibre weight) with a metal frame of 300 x 300 x 4 mm. The mixtures were weighed using a Mettler Toledo PL202-s and combined with a drum carder (15 mm batt width). The test samples were machine cut using a saw blade.

In **Papers II** and **III**, a metal frame of 450 x 450 x 2 mm was used to produce the four variants: untreated, water pre-treated, alkali pre-treated, water with silane treated and alkali with silane treated) of the biocomposites using hemp fibre reinforcements of 30 and 50 wt.%. The blends were combined using a classic drum carder (300 mm batt width, 72 teeth per inch (tpi) and 100 g capacity). The composites of the resulting fibre variants were labelled UH, WH, AH, WSH and ASH.

2.2.5 Compositional and structural characterisation of the hemp fibre and composite

1 **Scanning Electron Microscopy (SEM).** The hemp fibre surface and composite cross sections were examined using a Zeiss Ultra 55 scanning Electron Microscope to a depth of 100 nm at energy between 4 to 20 kV and resolution of 50000. All the examined specimens (fibre and composites) were carbon glued to the stud and vacuum coated with Au/Pt before observation.

In **Paper I**, the SEM observation was only carried out on the frost retted, untreated hemp fibres to examine the fibre separation and nature of the composition. In **Paper II**, the morphology of the fibres and the composite cross section were examined. In **Paper III**, the composite cross sections were thoroughly observed.

2 **Fourier Transform Infrared (FTIR).** The FTIR spectroscopy was done to qualitatively identify the constituents of the fibre before and after surface/FR treatments. Before the sample scanning processes, a background scan of a clean Zn–Se diamond crystal was performed. All spectra were taken at a spectrum resolution of 4 cm^{-1}. In **Paper II**, the analysis was performed on twisted bundles of hemp fibres using a Nicolet™ iS50 FTIR spectrometer after conditioning in the spectrometer room for two weeks. 22 scans were collected on each specimen and from 10 replicas per batch.

3 **Thermogravimetric Analysis (TGA).** The TGA was performed in a nitrogen atmosphere (20 mL/min) on the untreated and modified hemp fibres using a NETZSCH STA 449F3. Three (3) replicates of 6 mg of the granulated fibre were measured from 40 to 600 °C at the rate of 2 °C/min, after an isothermal segment at 40 °C for 1 min. The specimens were conditioned in the testing room with relative humidity of (43 ± 10)% and temperature of 22 ± 1 °C for at least one week before the test. All samples were held in an aluminium pan (Al_2O_3) during the test. TGA analysis was applied in **Paper II**.

2.2.6 Determination of the mechanical properties of the fibre

In **Paper I** tensile tests were carried out on single hemp fibres on a Zwick Roell Z010 universal test machine equipped with a 20 N load cell (Class 0.5, ISO 7500-1) at a speed of 1 mm/min and gauge length of 10 mm. At least 50 samples were tested. The mean diameter of each fibre was measured before testing (average of 3 points). In **Paper II**, the test was carried out on the treated batches and compared to the untreated hemp fibre.

2.2.7 Determination of the mechanical properties of the biocomposite

1. **Tensile and Flexural test.** The tensile and flexural properties of the composite specimens were examined by EN ISO 527 (type 2) and EN ISO 14125 (Class II), respectively. All tests were carried out at a test speed of 2 mm/min. The specimens were conditioned at room conditions for seven days prior to the test.

   In **Paper I** only the tensile properties of the biocomposite were examined. Five replicas were used, and all specimens were machine cut with a circular saw. The test was performed on an Instron 5688 universal test machine. In **Paper II**, both tensile and flexural properties were characterised. Test specimens were cut with a circular saw. The test was conducted on 5 replicates per batch using an Instron 8516 universal test machine with a load cell of 10 kN (Figure 8).

Figure 8. Rectangular tensile test specimen being tested with extensometer.

2.2.8 Determination of moisture behaviour of the biocomposite

1. **Water adsorption (hygroscopic properties).** In **Paper III**, the water adsorption test was performed on the ten batches (five variants at 30 and 50 wt.%) of biocomposites by EN ISO 12571:2013 at relative humidity (RH) levels of 30, 50, 75 and 95% and constant temperature (23 ± 0.5 °C) using an Ecocell conditioning chamber. The dimension of the specimens was 100 mm x 100 mm. Four (4) replicates were tested per batch. The samples were dried in the oven according to EN ISO 12570:2000 until constant weight to ≤ 0.1% before the test. The $EMC_{d.b}$ was determined using the following equation (2).

$$EMC_{d.b}(\%) = \frac{m - m_0}{m_0} \times 100, \textit{(2)}$$

where m_0 is the mass of the oven dried samples; m is the mass of the specimens at any given RH.

The moisture adsorption curve was also fitted using the modified Oswin model shown in equation *(2).*

$$M_D = \frac{(A+BT)}{(H_R-1)^{\frac{1}{C}}}, (3)$$

where M_D is equilibrium moisture content, d.b %; H_R is the relative humidity in decimal; T is the temperature, °C; A, B and C are the modified Oswin model constants.

Nonlinear regression analysis was used to find the parameters of the equation. Constants *A*, *B*, and *C* were assumed values in this case, and the model (M_D) was then calculated at the observed temperature and specified RH. For each RH, the sum of squares was calculated using the differences between the observed equilibrium moisture contents ($EMC_{d.b}$) and the predicted equilibrium moisture contents (M_D). The sum of squares was then used in a non-linear regression to re-obtain the values of the constants *A*, *B*, and *C*, which were then employed in model fitting.

2. **Long-term water behaviour**. In **Paper III**, the long-term (28-day) immersion of the composite in water was used to determine the composite water absorption (WA) and thickness swelling (TS) by EN ISO 16535 and EN 325, respectively. WA was obtained by measuring the mass change of the specimen following the 28 days immersion in water, using five replicas that were initially conditioned at 23 ± 2 °C and 50% RH for 24 hours. For the TS, the specimens' original thickness was measured with an accuracy of 0.01 mm using a digital micrometre screw gauge (Hans Schmidt). Before the test, all specimens were conditioned in the climatic chamber at a temperature of (20 ± 2) °C and a RH of (65 ± 5) %.

2.2.9 Fire reaction test

The reaction to fire was determined by the cone calorimeter method, according to EN 5660-1:2015. The dimension of the specimens was 100 x 100 mm. The test was administered with a heat flux of 50 kW/m^2. The specimens were conditioned for at least seven (7) days prior to the test at a temperature of 23 °C and RH of 50%. To record the temperature during the test, a 0.25 mm diameter type K thermocouple (Pentronic AB, Sweden) was connected to the midpoint (50 mm) of the surface directly exposed to the cone heater and to the surface of the composite placed on the timber block. Figure 9(a) shows the prepared samples with the attached thermocouple, while Figure 9(b) shows the testing in progress.

(a) (b)

Figure 9. (a) PLA samples with thermocouples; (b) fire testing with a cone calorimeter.

3 Results and discussion

3.1 Characterisation of the fibre properties following surface treatment

3.1.1 SEM analysis

In **Paper I**, the limited data on the Tisza variety of hemp fibres that have undergone frost-retting inspired the authors to investigate morphological (see Figure 1A and 1B in Paper I) and biochemical features (see Table 1 in Paper I). The SEM observation of the frost retted hemp fibres presented a morphology consisting of unitary and large amount of unindividualized fibres (with diameters up 300 µm). This substantial presence of bundles of fibres is attributed to the high amount of soluble content (approximately 13%) identified by the biochemical analysis. The high pectin content and the agglomeration of the hemp fibre led the author to further study by applying fibre surface treatment (with water, alkali, and silane) to clean the hemp fibre and enhance the fibre separation in **Paper II**.

Figure 10 (same as Figure 6 in Paper II) shows that there was no major removal of a large quantity of cortical residues by the water pre-treatment (W_f) as the fibre morphology is similar to the untreated fibres (U_f). However, combining the pre-treatment with silane modification led to a slightly cleaner surface (WS_f) implying that silane treatment may have caused an additional removal of the fibre constituents. When the surface pre-treatment was done for 4 hours with 5 wt.% NaOH solution, a much cleaner, clearer fibre surface was observed (A_f) compared to U_f, W_f and WS_f. which is reportedly due to the extraction of substantial amounts of hemicelluloses, lignin, and soluble contents (Sawpan, Pickering and Fernyhough, 2011a; Kabir *et al.*, 2013a; Liu, Thygesen, *et al.*, 2017; Väisänen *et al.*, 2018). With subsequent silane treatment of the alkali pretreated hemp fibres (AS_f), a slightly smoother surface was observed, which is due to the formation of a siloxane layer (Sepe *et al.*, 2018).

These observations are further supported by the mass loss result published in **Paper III** (see Table 2 in Paper III). The fibre surface pre-treatment with water for 72 hours led to 4 % fibre mass loss, which was meaningfully lower than the total non-cellulosic fibre contents. On the other hand, the 4-hour pre-treatment with 5 wt.% NaOH solution caused the substantial removal of the non-cellulosic fibre content (14%). Besides, the mass loss result of the combined water and silane treatment showed that an additional 3% mass loss had occurred. Conversely, the fibre weight remained almost unchanged for the combined alkali and silane modification. This was explained as the ability of silane treatment to extract non-cellulosic contents in the event where there is still a substantial amount; in this regard, at 14% majority of the water solubles contents together with other amorphous components were reduced to the extent that the silane treatment of alkali pre-treated hemp fibres showed no further weight loss.

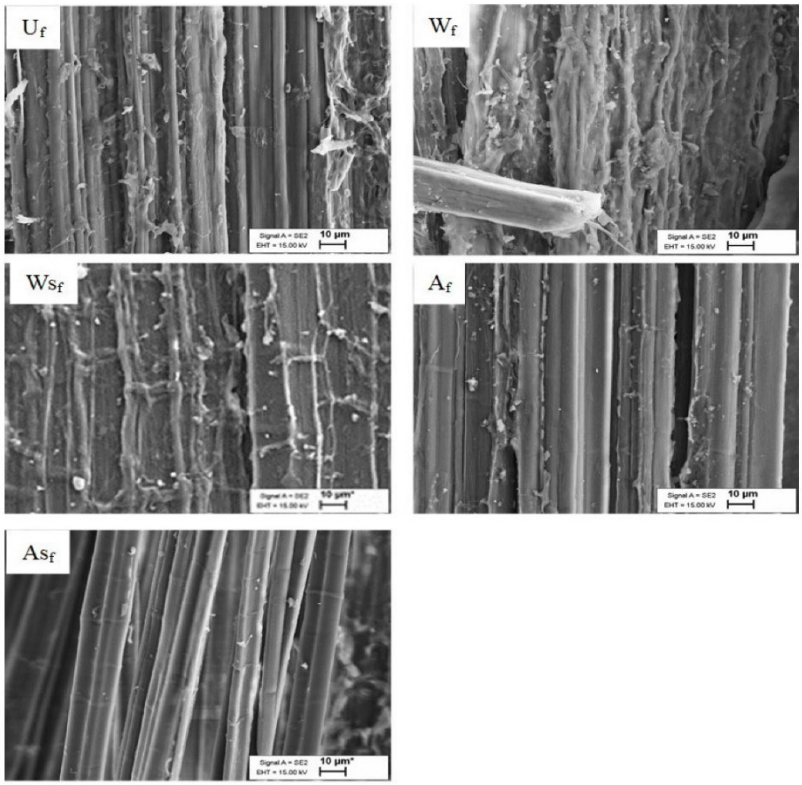

Figure 10. SEM images of (U_f) untreated, (W_f) water-treated, (Ws_f) water + 3% silane-treated, (A_f) 5% alkali-treated, and (As_f) 5% alkali + 3% silane-treated hemp fibre surfaces (Paper II).

3.1.2 FTIR analysis

The FTIR spectra of the hemp fibres are shown in Figure 11a and b (See Figures 3a and 3b in Paper II). The untreated (U_f) and waterpre-treated (W_f) hemp fibre spectra look similar, but a slightly higher absorbance is observed at the wavelengths between 3000–3600 cm^{-1} for W_f compared to U_f which indicates that the water pre-treatment may have caused an increase in the OH functional groups. According to Dayo *et al.* (2018), this increase in functional groups leads to a decrease in hydrophilic properties and is due to the removal of non-cellulosic polysaccharides from the fibre surface (Bourmaud, Morvan and Baley, 2010). However, the alkali pre-treated hemp fibre spectrum was much different compared to that of U_f with peak absence or attenuation at 1735 cm^{-1}, 1235 cm^{-1} 1635 cm^{-1} and 2850 cm^{-1}, 2918 cm^{-1}. These peaks are associated with carboxylic ester groups of hemicellulose or wax (1735 cm^{-1}), non-aromatic compounds of cellulose and hemicelluloses contents (2850 cm^{-1}) and acetyl groups (1235 cm^{-1}), conjugated carbonyl (1635 cm^{-1}), aromatic hydrocarbon, methoxyl, and methylene groups of lignin (2918 cm^{-1}) (Dayo *et al.*, 2018; Panaitescu *et al.*, 2020; Viscusi *et al.*, 2020). The alterations in these peaks following alkali pre-treatment are evidence of the significant reduction in the amount of the non-cellulosic components of the fibre.

Minor changes were observed in the spectra of the silane modified samples Ws_f and As_f compared to W_f and As_f (see Figure 4a and 4b in Paper II). A peak shift (1635 cm^{-1} to 1624 cm^{-1}) was observed and reduction at about 1539 cm^{-1}, 1369 cm^{-1}, and 1248 cm^{-1} are seen in the spectra of Ws_f compared to W_f. Kabir *et al.* (2013); Panaitescu *et al.* (2015);

Dayo *et al.* (2018), who attributed such a peak shift to the extraction of some hemicellulose, wax, and lignin fibre contents, which supports the estimated decrease in the fibre weight. Compared to A_f, the spectra of As_f revealed new peaks between 1500–1680 cm^{-1} that could be due NH_2 bending vibrations in amino silane (see Figure 4b in Paper II). Overall, the FTIR result agrees with the findings of the SEM observation and fibre mass loss and presents the level of effectiveness of the types of fibre modification processes examined.

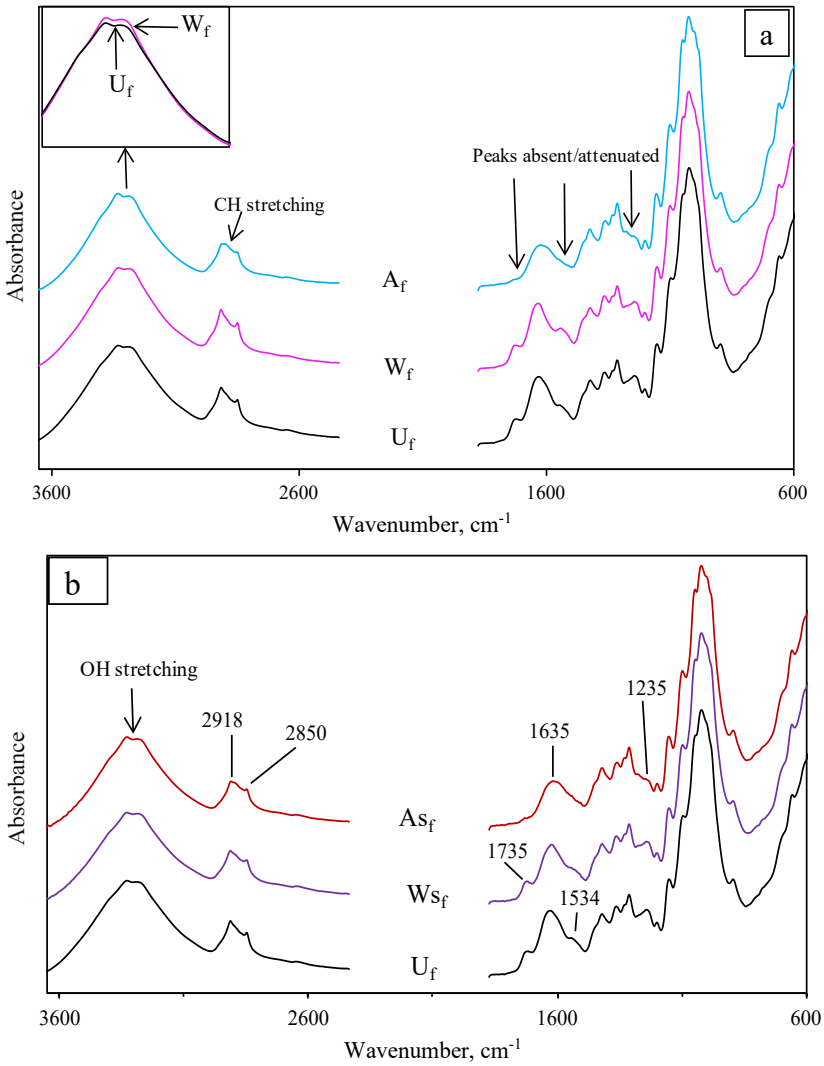

Figure 11. Vertically shifted FTIR spectra for (a) untreated (U_f), distilled water (W_f), and alkali treated (A_f) hemp fibres; (b) U_f, water + silane (Ws_f) and alkali + silane (As_f) treated hemp fibres with the wavenumbers for differences observed (Paper II).

3.1.3 TGA analysis

To support the SEM and FTIR results, the author also conducted a TGA analysis in **Paper II**, because the extraction of amorphous contents from hemp fibres should slightly increase thermal stability due to the lower start of decomposition temperature of hemicelluloses (180–280 °C) and lignin (150–450 °C) (Kabir *et al.*, 2013a) compared to cellulose (325–400 °C).

The TGA curves showed two mass loss levels (see Figures 5a in Paper II). The first mass loss/degradation, at 39–160 °C is mainly due to the evaporation of moisture (Dayo *et al.*, 2018; Viscusi *et al.*, 2020). At this stage, the untreated hemp fibre showed the most mass loss (1.4%), which is indicative of the hydrophilic properties due to the presence of non-cellulosic polysaccharides. The second mass loss occurred from 160–600 °C with a peak of 346 °C, which indicates that the fibre degradation at this level begins with the decomposition of hemicellulose and lignin and peaked with cellulose degradation. To analyse this mass loss, the temperatures T_5 and T_{10} corresponding to a mass loss of 5 and 10% were used (see Table 2 in Paper II). It was found that the untreated hemp fibre presented the lowest T_5 (254 °C) and T_{10} (289 °C), which was increased by about 7 and 4%, respectively following water pretreatment, while the hemp fibres pretreated with alkali recorded the highest values, 292 °C (T_5) and 313 °C (T_{10}). The introduction of silane to water pretreated hemp fibres further increased both T_5 and T_{10} by 2%. The obtained results indicate that for the main degradation temperature 240–350 °C the fibres pretreated with alkali had the lowest mass loss, because of the removal of parts of the hemicelluloses and lignin (Kabir *et al.*, 2013a). Also, the differential thermogravimetric (DTGA) curves in Figure 12a and b show that there is hardly any difference between the temperature peaks at points 240–290 °C for U_f and W_f; however, dTG curve for A_f highlights lower temperature peaks at the same range, which is due to the low presence of decomposable hemicellulosic matter.

The TGA results support the findings of the SEM and FTIR analyses, which shows that alkali pre-treatment was more effective than water pre-treatment in removing amorphous contents, and that water pre-treatment still slightly altered the hemp fibre structure, regardless of the small amount of fibre constituents removed.

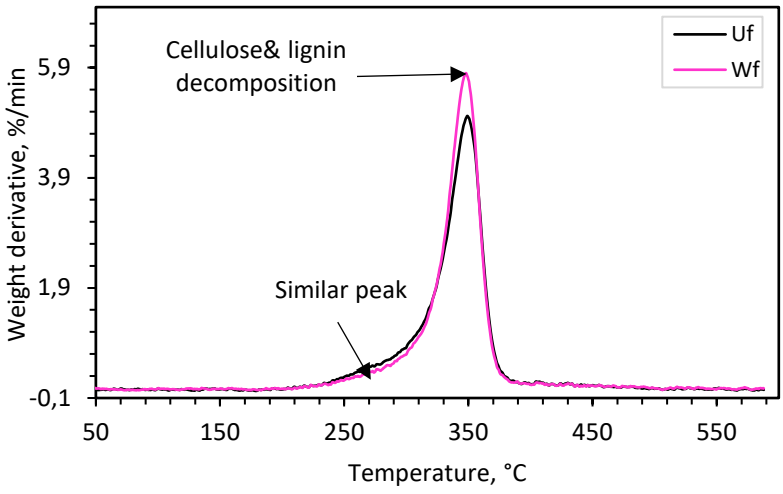

(a)

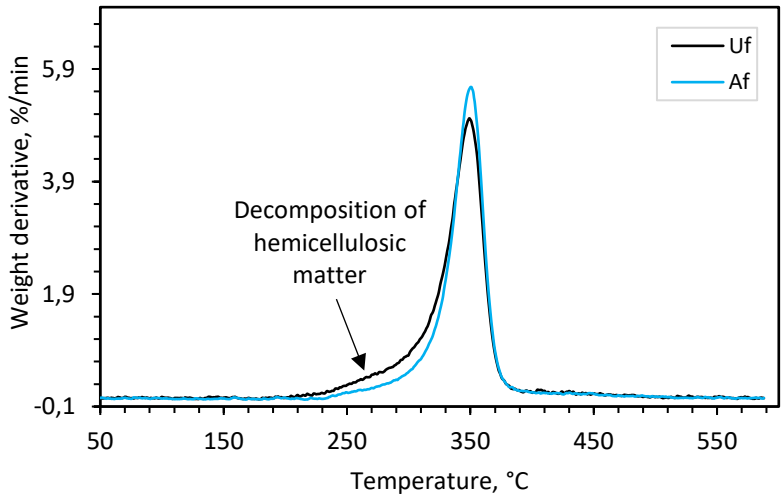

(b)

Figure 12: DTGA curves of a) untreated (U_f) and water pretreated (W_f); (b) U_f and alkali pretreated hemp fibres (A_f) (see Figure 5b in Paper II).

3.1.4 Tensile properties of the hemp fibres

To evaluate the impact of the fibre surface pre-treatments on the mechanical properties, the tensile performance of the fibres was studied from 50 replicas per batch in Paper I and II.

Table 7 presents the mean maximum tensile strength (σ), modulus (*E*), and strain of the hemp fibres. The σ (500 ± 239 MPa) of the untreated hemp fibre (see Table 2 in Paper I) was found to be in the middle range (285–969 MPa) of published data (Bourmaud *et al.*, 2018) and the *E* (16.6 ± 8.5 GPa) is at the lower range (14.4–51 GPa) (Bourmaud *et al.*, 2018; Gregoire *et al.*, 2019). This low strength performance by the hemp fibres is

suggested to be due to the low lignification (Liu, Baum, *et al.*, 2017) compared to the level reported for Western European Tisza variety (2–6%). When the strength of the fibre is compared after modification, statistical analysis (see Table 4 in Paper II) showed that the water and alkali pre-treatments both significantly caused a reduction in the σ and elongation at break but did not affect the *E*. Although, there was no meaningful difference in the tensile properties when water and alkali pre-treatments are considered.

The decrease in σ following the water pre-treatment is suggested to be due to the high-water retention ability of the fibre and component rearrangement in the S2 layer because of the partial removal of pectins and hemicelluloses from the fibre surface, cell wall and middle lamella. According to Pejic *et al.* (2008) high water retention of hemp fibre can be influenced by low lignin content, which was identified by the chemical analysis of Estonia grown hemp fibre while studies by Le Duigou *et al.* (2012) noted alteration of the structural cohesion (cell-wall peeling process) of a flax fibre after water treatment. However, the decrease in the fibre mechanical properties experienced after alkali pre-treatments can be due to a reduction of lignin and hemicellulose amounts (Le Duigou *et al.*, 2012; Garat *et al.*, 2020), transformation of cellulose II to cellulose I (Sair *et al.*, 2017) and an increase of the cellulose crystallinity (Islam, Pickering and Foreman, 2010).

Furthermore, Table 7 also shows that the silane treatment increased the tensile properties of the hemp fibres pre-treated with water and silane, though no meaningful change in the MOE was observed for that with alkali pre-treatment (see Table 4 in Paper II). The reason for the increase in the performance due to silane treatment is reported to be the additional shear resistance brought by the layer of chemicals that are attached to the microfibrils (Kabir *et al.*, 2013a).

Table 7. Means of tensile strength, modulus, and elongation at break (Table 3, Paper II).

Treatment	σ, MPa	*E*, GPa	Strain, %
Untreated	500 ± 239	16.6 ± 8.5	2.93 ± 1.02
Water	376 ± 220	14.3 ± 7.9	2.43 ± 0.78
Alkali	381 ± 189	15.0 ± 5.2	2.42 ± 0.91
Water & silane	490 ± 210	17.2 ± 8.3	2.71 ± 1.16
Alkali & silane	466 ± 287	15.6 ± 9.0	2.81 ± 0.89

3.2 Mechanical performance of the hemp fibre reinforced PLA composite

The mechanical performance of the aligned hemp fibre reinforced PLA composites was studied in **Paper I** and **II**.

3.2.1 Tensile properties of the untreated hemp fibre reinforced PLA composite

In **Paper I**, further to the determination of the fibre properties, the tensile properties of the composites reinforced with 30 and 50 wt.% untreated hemp fibres were evaluated to investigate the applicability of the hemp fibre for composite production. It should be recalled that the blend mix of hemp fibres with PLA fibres in this study was done using a 15 mm width drum carder and fabricated by hot pressing with a 300 x 300 x 4 mm metal form. As seen in Table 8 (same as Table 3 in Paper I) the 30 wt.% reinforcement produced a σ of (51 ± 9 MPa) and *E* of (4.8 ± 0.3 GPa) that represent an 11% and 79% increase, respectively can be compared to the neat PLA (46 MPa and 2.7 GPa, respectively).

However, with 50 wt.% reinforcement, σ decreased by roughly 41% while the *E* increased by 149%. The decrease in the σ at 50 wt.% fibrous reinforcement is attributed to the insufficient wetting of the hemp fibres by the matrix that inhibit the load transfer between the fibres and the matrix (Pickering, Efendy and Le, 2016).

Additionally, since the fibres were found to consist of high number of cortical residues and bundled fibres, it was impossible to attain a good adhesion between the fibres and the PLA at the higher fibre content. The examination of the void/porosity contents also supports this explanation, because the 50 wt.% hemp fibre presented 17% void content that was 10% higher than that at 30 wt.%. According to (Madsen, Hoffmeyer and Lilholt (2007), the higher fibre fraction causes an increase in composite porosity that leads to a decrease in mechanical performance. Although the outcome, especially at 30 wt.% shows the possibility to use the hemps fibres as a composite reinforcement, a high deviation in the σ occurred which may have been due to the inhomogeneous distribution of the hemp fibres due to the presence of high amount of fibre bundles.

Table 8. Average physicomechanical and tensile properties of hemp/PLA composites with 30 and 50 wt.% fibre reinforcement (Paper I).

Fibre content, %	Volume fraction, %	Density, g/cm^3	Porosity, %	σ, MPa	*E*, GPa
30	28	1.26	7	51 ± 9	4.8 ± 0.3
50	48	1.04	17	27 ± 3	6.7 ± 0.6

Following the results of the biocomposite mechanical performance obtained this study, it was found that to improve the composite properties through the following is essential:

- Increasing the fibre individualisation
- Limiting the composite void content through improved manufacturing process, and
- Improving the fibre/matrix adhesion by removing the non-cellulosic/soluble contents.

3.2.2 Effect of the fibre surface modification on the tensile and flexural properties of the reinforced composite

In **Paper II**, to improve the composite mechanical performance based on the recommendations in Paper I, the author fabricated the composites from pre-treated hemp fibres (W_f, A_f, WS_f and AS_f) and compared the performance to U_f reinforced composites at 30 and 50 wt.%. The tensile results are presented in Figure 13a and b (see Figure 11 in Paper II). The σ of the composites reinforced with the untreated hemp fibre (UH) at 30 and 50 wt.% was similar to the results in **Paper I**. Regardless, the results showed that the fibre surface pre-treatments improved the composite mechanical performance, especially at 30 wt.% and significantly for composites reinforced with A_f (AH) and AS_f (ASH), compared to those with W_f (WH) and WS_f (WSH). The *E* shows similar trend as the σ and mirrors the result of the fibre *E*. Other studies have also obtained similar improvements in the properties of the composite following fibre treatments especially with alkali (Hu and Lim, 2007; Kabir *et al.*, 2013b; Väisänen *et al.*, 2018; Pappu, Pickering and Thakur, 2019), but Sepe *et al.* (2018) obtained some depreciation in the composite performance after treating the hemp fibres with 1 and 5wt.% NaOH solution that was ascribed to the ease of fibril pull out due to the substantial removal of hemicellulose and lignin.

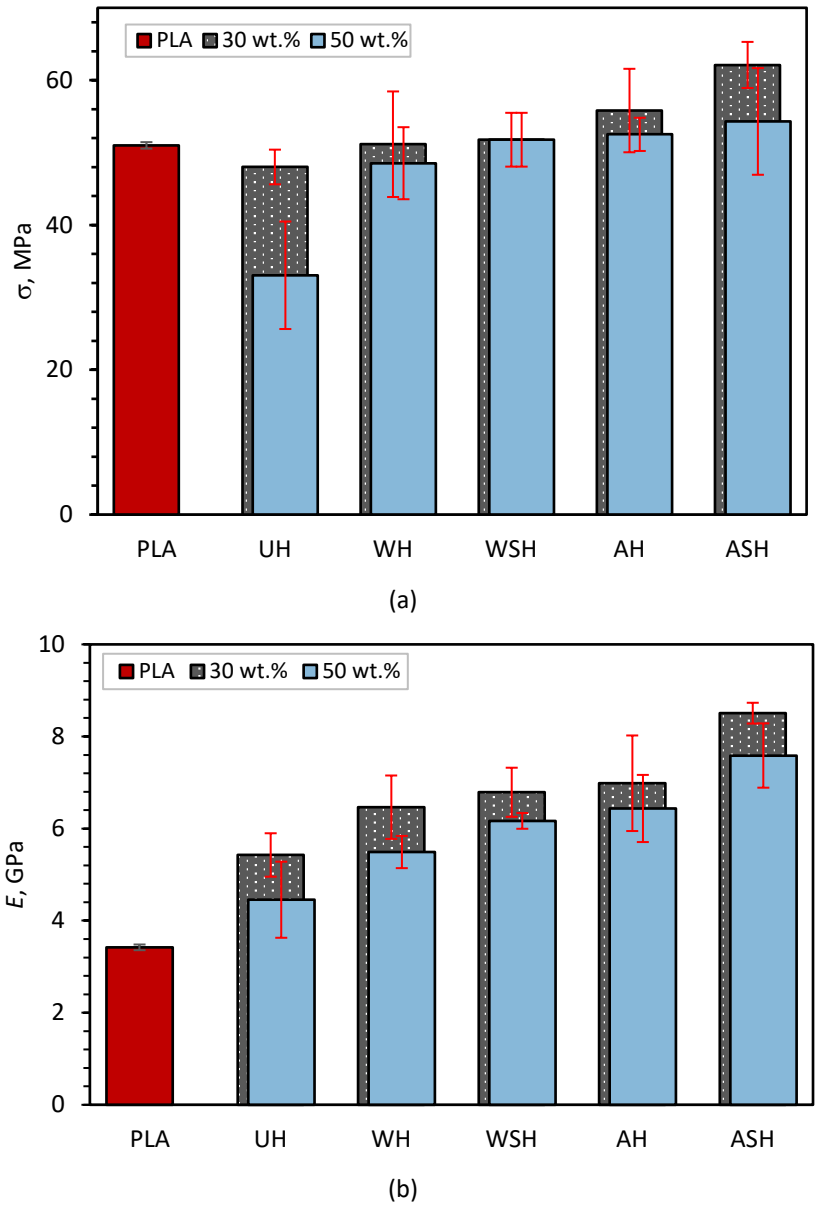

Figure 13. Average maximum (a) tensile strength;(b) modulus (UH) and treated (water (WH), water and silane (WSH), alkali (AH); alkali with silane (ASH) composites at 30 and 50 wt.% hemp fibre content compared to neat PLA.

Figure 14a shows that compared to the neat PLA, flexural strength (MOR) decreased when U_f was used as reinforcement. Although no meaningful change was seen between UH and WH composites, the overall result indicates that the fibre pre-treatments gave some level of improvement in the composite MOR. The most notable improvement in MOR was by AH and ASH. There was a similar reduction in MOR with an increase in the composite fibre content from 30 to 50 wt.%.; at 50 wt.% no notable change was revealed in the MOE when the UH, WH, WSH and AH composites are compared, though at 30 wt.%

the MOE of AH was significantly better (see Figure 14b). The composite flexural performance from this study is consistent with previous studies by (Sawpan, Pickering and Fernyhough, 2011b; Sair *et al.*, 2017; Dayo *et al.*, 2018).

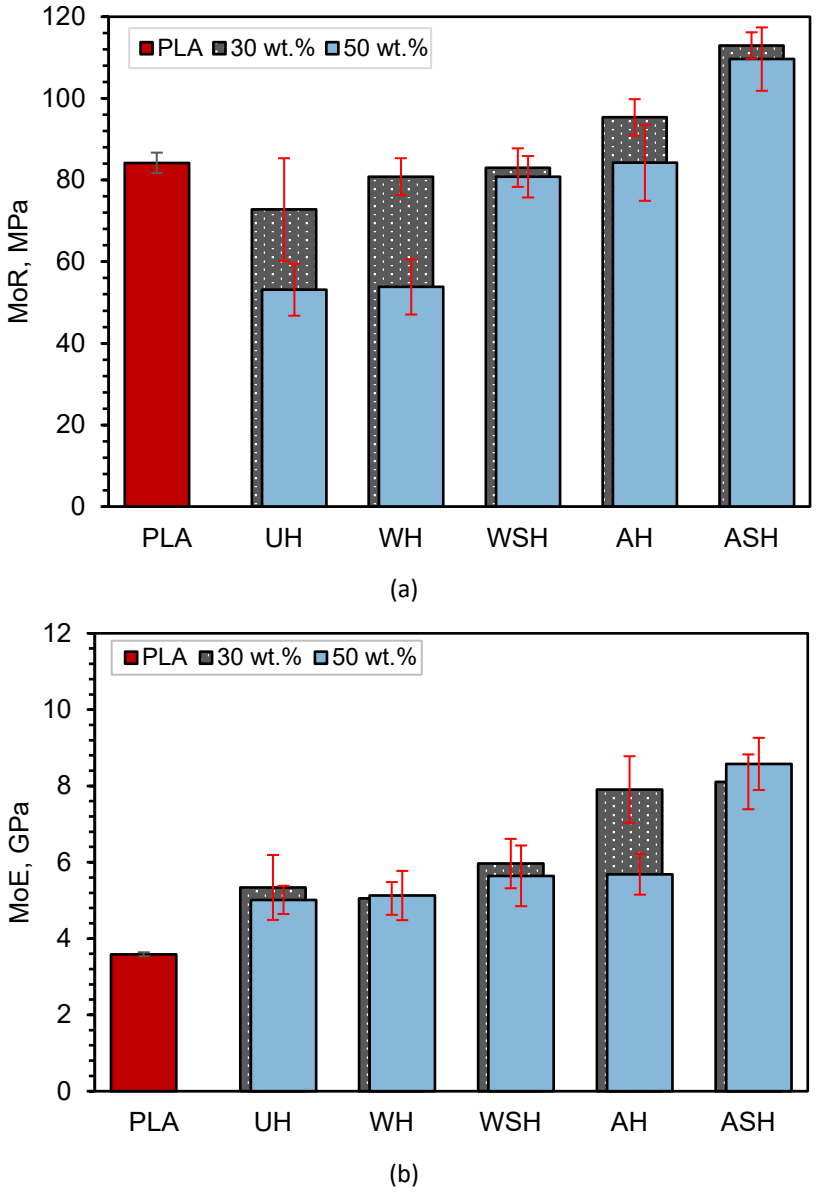

Figure 14. Average maximum (a) MOR; (b) MOE of untreated (UH) and treated (water (WH), water and silane (WSH), alkali (AH); alkali with silane (ASH) composites at 30 and 50 wt.% hemp fibre content compared to neat PLA.

The results revealed that a deterioration in the fibre tensile performance was obtained after the water and alkali pre-treatments. The improvement in the composite mechanical performance showed that the hemp fibres are more individualized and that there is a better interfacial bonding between the fibre and the matrix, which is mainly due to the availability of more cellulose interlocking sites with removal of water-soluble polysaccharides during water pre-treatment (Bourmaud, Morvan and Baley, 2010) and pectin, wax and intercellular contents during alkali pre-treatment. Furthermore, the improved mechanical performance after silane treatment can be related to the higher properties of the fibres themselves and the better adhesion with the PLA matrix brought on by the silane couplings.

The cross-sectional SEM images presented in Figure 7 of **Paper II** as well as Figure 5 in **Paper III** showed evidence of the fibre individualisation and distribution within the matrix after pre-treatments. The AH and ASH composites were found to have smaller fibres that are more dispersed within the PLA matrix and, compared to UH and WH, fewer fibre bundles were present in WSH composites.

3.3 Effect of the hemp fibre modification on the water behaviour of the composite

The hygroscopic moisture adsorption and water absorption of the hemp fibre reinforced PLA composites were analysed in **Paper III**.

3.3.1 Hygroscopic Moisture Adsorption

Figure 15a and b show that the composites' hygroscopic adsorption decreases with fibre surface modification and increases with the fibre content. The highest EMC (11.76%) was by UH (50 wt.%) at 95% RH, which lowered significantly by 18% following alkali pre-treatment and 16% with combined alkali and silane treatments. WSH also produced notably less EMC at both fibre contents than UH and WH composites (see Table 4 in Paper III). The higher adsorption at 50 wt.% compared to 30 wt.% is ascribed to the presence of a higher fibrous ratio with more hydrophilic groups than the PLA matrix and the higher volume of porosities for the composites with 50 wt.% fibres (see Table 3 in Paper III). The reduction in EMC for the composites reinforced with the pre-treated hemp fibre is caused by (i) less free OH groups in the case of combined water and silane treatment, (ii) a change in the fibre microstructure in the case of water and alkali pre-treatments and (iii) the enhanced bonding between the fibre and PLA. These findings very much agree with the results published in Paper II.

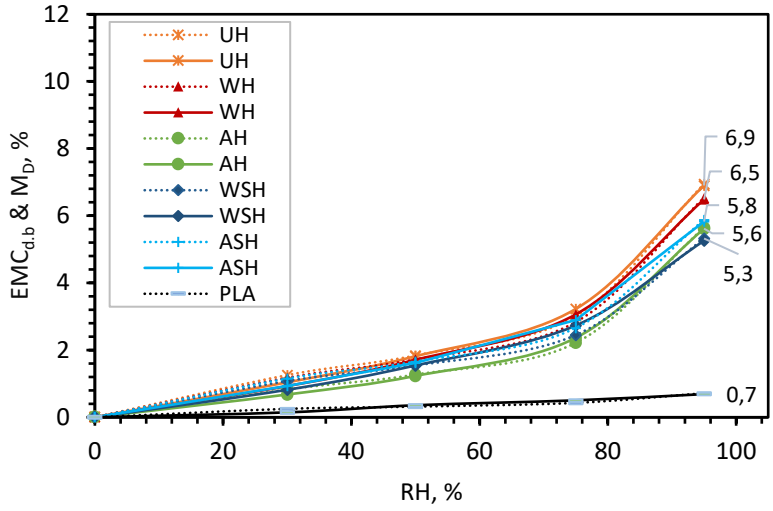

(a)

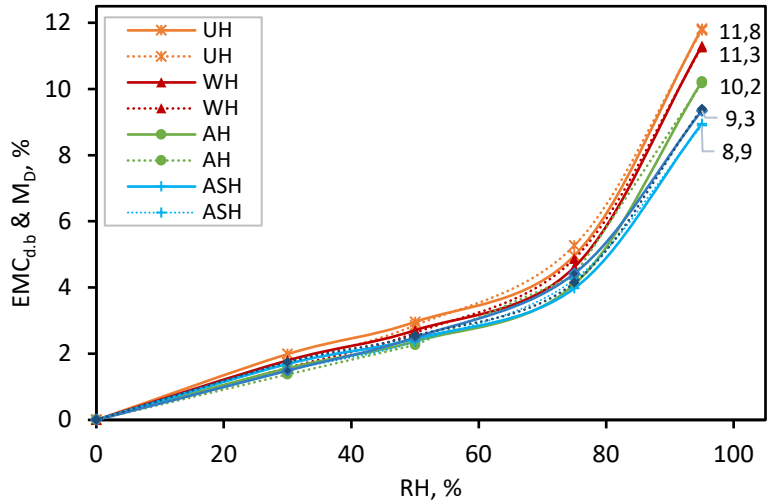

(b)

Figure 15. Adsorption isotherms (predicted M_D (- -) and measured (—) for (a) the neat PLA, the 30 wt.% composites; (b) the 50 wt.% composites of untreated (UH ж), water pre-treated (WH ▲), alkali pre-treated (AH ●) and combined treatment with silane (water (WSH ♦); alkali (ASH+) (Paper III).

3.3.2 Water Absorption (WA) and Thickness Swelling (TS)

The water absorption and thickness swelling of the composites were mostly dependent on the fibre content, illustrated in Figure 16. This is due to the less porosity (see Table 3 in Paper III) and lower hydrophilic character of the composite at 30 wt.%. Comparison of the water absorption and thickness swelling values of UH, WH, WSH, AH, and ASH showed that all the composites with treated hemp fibres had lower water absorption and thickness swelling than UH, which is consistent with result of the hygroscopic sorption as well as, the composite mechanical performance studied in Paper II. The water

pre-treatment slightly increased the composite (WH) water resistance, but composites with alkali pre-treated fibres (AH) produced the most significant resistance. The combined fibre surface modification further decreased the composite affinity for water, though hardly any difference was observed, especially in the thickness swelling of AH compared to ASH. The neat PLA showed no apparent changes in mass or thickness (0%) after 28 days of immersion, so no values are reported.

The changes in the porosity nature of hemp fibres are one cause of the low water reactivity of AH and ASH. After partly eliminating non-cellulosic constituents, alkali pre-treatment of hemp fibres modifies the surface topology, resulting in a more fibre surface roughness (also mentioned in Paper II) that improves mechanical interlocking between the fibre and the matrix. The enhanced bonding between the fibre and the matrix causes adequate packing of the fibres in the composite, lowering the composite porosity (see Table 3 in Paper III) and reducing the water behaviour of the composites (Sreekumar *et al.*, 2009). Another explanation is that alkali pre-treatment enhances matrix accessibility to cellulose and diminishes hydrophilic characteristics due to less amorphous OH available for water molecule interactions.

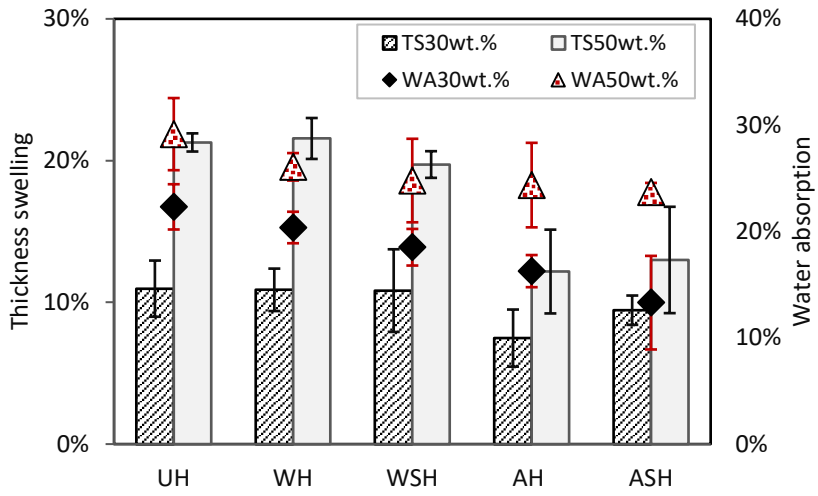

Figure 16. Water absorption and thickness swelling of the hemp reinforced PLA composites (Paper III).

Overall, water pre-treatment showed negligible effect on the studied characteristics of the composite; however, further silane modification produced significantly higher moisture resistance, which may be attributed to the extra removal of the amorphous cell wall content and silane coupling at the hemp fibre surface.

3.4 Effect of the hemp fibre modification on the fire behaviour of the composite

Table 9 shows that the ignition time and temperature of the composites at 30 wt.% was slightly lower and mass loss was higher because of the high PLA content, since the neat PLA showed a fast rate of degradation (180 s) (see Figure 8 in Paper III). However, the hemp fibre surface treatment appears to sustain the composite thermal stability, which is in correlation with the fibre TGA analysis in **Paper II**.

Table 9. The mass loss, ignition time and temperature of the composites compared to neat PLA (Table 6 in Paper III).

Fibre content, %	Samples	Ignition time, s	Ignition temperature, °C	Mass loss, %
30	UH	29 ± 10	112 ± 23	93 ± 2.0
	WH	31 ± 10	117 ± 18	95 ± 0.1
	WSH	30 ± 04	131 ± 28	94 ± 0.4
	AH	44 ± 02	118 ± 08	94 ± 1.0
	ASH	33 ± 03	159 ± 18	94 ± 2.0
50	UH	32 ± 07	129 ± 15	90 ± 1.0
	WH	49 ± 06	134 ± 17	91 ± 2.0
	WSH	46 ± 10	179 ± 29	90 ± 1.0
	AH	51 ± 10	178 ± 18	90 ± 4.0
	ASH	47 ± 09	181 ± 18	89 ± 1.0
0	Neat PLA	37 ± 02	104 ± 04	100 ± 0.0

3.5 Cost analysis of the fibre surface pretreatment & treatment

The results of Papers **II** and **III** demonstrated that alkali pre-treatment of hemp fibres and modification with silane had the highest impact on the composite qualities studied. The substances required for the fibre pre-treatment/treatment were previously mentioned in Section 2.2.2 of Chapter 2. Table 10 shows the current price of these materials. Because of the excessive cost of silane treatment (Table 11) the author concluded in Paper III that treatment of the hemp fibres with alkali should be sufficient, as only minor gains were observed in most cases when the properties of AH composites were compared to ASH. Furthermore, Paper II highlighted that the pre-treatment of the hemp fibre with NaOH solution caused a decrease in the fibre tensile properties. Therefore, it can be assumed that despite the improvement achieved in the composite mechanical performance, there might have been some performance limitations due to the lower fibre strength. Hence, regardless of the presence of a more effective surface area for matrix bonding, the reduction of the hemp fibre strength provides some limitation in the mechanical performance of the biocomposite.

Table 10. The cost of material required for cleaning and modifying the hemp fibre surface.

Materials	Distilled water	NaOH (sigma-Aldrich)	APTES, 98% conc. (Alfa Aesar)	Acetic acid 99.8% G.R (Lach-ner)	Ethanol, 97% conc.
Cost €/Quantity	0.55/1000 ml	5.5/1000 g	128/500 g	7.19/1000 ml	5.8/1000 ml
Water pre-treatment	✓	-	-	-	-
Alkali pre-treatment (NaOH)	✓	✓	-	-	-
Silane treatment (water)	✓	-	✓	✓	✓
Silane treatment (alkali)	✓	✓	✓	✓	✓

Table 11. The cost of pre-treatment/modification required to fabricate a 30 wt.% hemp fibre reinforced composites from a 450 x 450 x 2 mm mould.

Pre-treatment/modification type	Cost, €
Water pre-treatment	0.87
Alkali pre-treatment	1.30
Combined water + silane	9.71
Combined alkali + silane	11.71

It can be concluded from these results that the frost retted hemp fibres from Estonia showed comparably satisfactory results in comparison to the results reported in the literature (Table 4) and thus indicate a derivable potential.

Conclusions

This thesis examined frost-retted Estonian hemp fibre (Cannabis sativa, dioecious Hungarian (Tisza) variety) for potential use in biocomposite materials. The main benefit of using these fibres is that they are a by-product of cannabidiol manufacturing in Estonia and have no practical application today. The application of these fibres in biocomposites might pave the way for the increased adoption of renewable materials in the transportation and construction industries, which will enhance a more circular and sustainable economy. To that end, the hemp fibres were manually detached from the shives and carded, the chemical and mechanical properties were analysed, and various surface modifications (water pre-treatment, alkali pre-treatment, and combined treatments with silane) were applied to improve the properties of the fibre to produce a robust biocomposite that was characterised by the mechanical performance (tensile and flexural), hygroscopic moisture adsorption and water absorption, and fire resistance behaviour. The following conclusions may be drawn from the research results:

1. Chemical analysis showed that the frost-retted Estonian hemp fibre has a high soluble (pectin) content (12.6 ± 0.4%) as well as a low lignin level (1.4%) compared to the values reported in Western European hemp varieties (2–6%). The high soluble content is attributed to the limited activity of microbes and enzymes during the low-temperature retting period in Estonia, whereas the low lignin concentration is due to the short daylight duration during the hemp's later development stage. Although the fibre contained a high cellulose content (77.4 ± 0.3), the tensile strength of the unitary fibre (500 ± 239 MPa) and modulus (16.6 ± 8.5 GPa) were respectively found to be in the middle (285–969 MPa) and lower (14.4–51 GPa) range of data from past studies. These low mechanical properties were attributed to the measured low lignin content of the hemp fibre.
2. The high concentration of solubles impacted fibre separation, resulting in many bundled fibres in the stem, both of which affected the hemp fibre's ability to give an acceptable performance at the composite level, as shown by the low tensile strength (27 ± 3 MPa) and (51 ± 9 MPa) at 30 and 50 wt.% respectively, necessitating the need for fibre surface treatment to remove the cortical residues and separate the fibre bundles.
3. FTIR, TGA and SEM analyses of the pretreated (water; alkali) and treated (water-silane, alkali-silane) hemp fibres found structural alterations that are due to the removal of targeted component. But these analyses, together with the fibre mass loss (4 ± 0.3%), confirmed that the water pretreatment was the least effective modification. However, despite the small amount of non-cellulosic fibre contents extracted by the water pre-treatment, the resulting structural changes were influential on the mechanical properties of the fibre by reducing the tensile strength and elongation at the break of the fibre by 28% and 17%, respectively. This was ascribed to high water retention ability due to the low lignin content that allows the fibre to store more moisture as bound water, removal of cortical residues and alterations in the S2 layer of the secondary cell wall of the hemp fibre.
4. There was also a 20% and 17% decrease in the hemp fibre tensile strength and elongation at break, respectively, after alkali pretreatment, due to the reduction

of lignin and hemicellulose amounts and the potential degradation of cellulose chains/transformation of cellulose II to cellulose I. On the other hand, silane treatment improved these properties because of the additional shear resistance by the layer of chemicals attached to the microfibrils after silane modification.

5. Regardless of the negative impact of the water and alkali pretreatment on the hemp fibre tensile performance, the composites of water and alkali pretreated hemp fibres produced a better tensile strength and modulus compared to the composites reinforced with untreated hemp fibres. This performance improvement was due to the better level of fibre individualisation and improved fibre/PLA bonding caused by the extraction of water soluble polysaccharides in the case of water pretreatment and the extraction of a substantial portion of the pectins, wax, and other non-cellulosic contents, during alkali pretreatment. The additional boost in mechanical performance occurred with silane treatment in both cases because of the higher performance of the fibres themselves and the better adhesion with the polymer matrix induced by silane couplings.
6. Water pretreatment had insignificant effect on protecting the composite when exposed to wet conditions. But, with additional silane modification, the composites offered more resistance, which could be because of the extra removal of amorphous cell wall content and silane coupling at the hemp fibre surface. The alkali pretreatment and combined silane treatment produced no significant differences in these water related properties. The composite reinforced with 30 wt.% alkali pretreated hemp fibres had the lowest thickness swelling (7.5%), representing a 32% improvement compared to composites of untreated hemp fibre. Combined alkali and silane treatment absorbed water the least (13.3%) that was at 30 wt.% fibre content and denoting a 40% decrease compared to the untreated variant.
7. A higher fibre content (50 wt.%) had no positive impact on the mechanical performance of the composites due to insufficient wetting of the fibres by the PLA, especially following alkali pretreatment and caused a reduction in the composite's resistance to wet conditions, because of an increase in hydrophilic properties and porosity. However, where fire reaction is essential, a higher fibre content appears to be satisfactory.
8. Overall, the hemp fibre surface treatments with joint alkali and silane produced a composite with the best performance. Yet, due to the cost, 9 times higher compared to alkali and, because mostly only slight improvements were achieved compared to alkali pretreatment, alkali treatment was considered a suitable approach to enhance the composite robustness during service.

The current study successfully characterised the properties of frost-retted hemp fibre obtained from industrial hemp cultivated in Estonia and demonstrates the potential to use this locally obtained resource to develop biocomposites adequate for the transportation and construction sectors, allowing for a decrease in CO_2 emissions, more upcycling and providing the opportunity to achieve the EGD commitments. However, product prototype testing is necessary and further studies are needed to improve the biocomposite fire resistance, as well as an automated fabrication process that reduces fabrication errors.

List of figures

List of tables

References

Alao, P. F. *et al.* (2019) 'Effect of hemp fibre length on the properties of polypropylene composites', *Agronomy Research*, 17(4), pp. 1517–1531. doi: 10.15159/AR.19.146.

Alix, S. *et al.* (2009) 'Effect of chemical treatments on water sorption and mechanical properties of flax fibres', *Bioresource Technology*. Elsevier, 100(20), pp. 4742–4749. doi: 10.1016/j.biortech.2009.04.067.

Baghaei, B. *et al.* (2014) 'Novel aligned hemp fibre reinforcement for structural biocomposites: Porosity, water absorption, mechanical performances and viscoelastic behaviour', *Composites Part A: Applied Science and Manufacturing*. Elsevier, 61, pp. 1–12. doi: 10.1016/j.compositesa.2014.01.017.

Baghaei, B., Skrifvars, M. and Berglin, L. (2013) 'Manufacture and characterisation of thermoplastic composites made from PLA/hemp co-wrapped hybrid yarn prepregs', *Composites Part A: Applied Science and Manufacturing*. Elsevier Ltd, 50, pp. 93–101. doi: 10.1016/j.compositesa.2013.03.012.

Bhattacharyya, D., Subasinghe, A. and Kim, N. K. (2015) *Natural fibers: Their composites and flammability characterizations*, *Multifunctionality of Polymer Composites: Challenges and New Solutions*. Elsevier Inc. doi: 10.1016/B978-0-323-26434-1.00004-0.

Bourmaud, A. *et al.* (2018) 'Towards the design of high-performance plant fibre composites', *Progress in Materials Science*. Elsevier, 97(May), pp. 347–408. doi: 10.1016/j.pmatsci.2018.05.005.

Bourmaud, A., Morvan, C. and Baley, C. (2010) 'Importance of fiber preparation to optimize the surface and mechanical properties of unitary flax fiber', *Industrial Crops and Products*. Elsevier B.V., 32(3), pp. 662–667. doi: 10.1016/j.indcrop.2010.08.002.

British Columbia Ministry of Agriculture and Food (1999) 'Industrial Hemp Factsheet', (September), p. 20. Available at: https://foodsecurecanada.org/sites/foodsecurecanada.org/files/hempinfo.pdf.

Brochier Salon, M. C. *et al.* (2005) 'Silane adsorption onto cellulose fibers: Hydrolysis and condensation reactions', *Journal of Colloid and Interface Science*, 289(1), pp. 249–261. doi: 10.1016/j.jcis.2005.03.070.

Cyras, V. P. *et al.* (2004) 'Effect of chemical treatment on the mechanical properties of starch-based blends reinforced with sisal fibre', *Journal of Composite Materials*, 38(16), pp. 1387–1399. doi: 10.1177/0021998304042738.

Dayo, A. Q. *et al.* (2018) 'The influence of different chemical treatments on the hemp fiber/polybenzoxazine based green composites: Mechanical, thermal and water absorption properties', *Materials Chemistry and Physics*. Elsevier Ltd, 217, pp. 270–277. doi: 10.1016/j.matchemphys.2018.06.040.

Demir, H. *et al.* (2006) 'The effect of fiber surface treatments on the tensile and water sorption properties of polypropylene-luffa fiber composites', *Composites Part A: Applied Science and Manufacturing*. Elsevier, 37(3), pp. 447–456. doi: 10.1016/j.compositesa.2005.05.036.

Douglas D. Stokke, Qinglin Wu, Guangping Han, and C. V. S. (2013) *Introduction to Wood and Natural Fiber Composites*. John Wiley & Sons, Incorporated. Available at: http://ebookcentral.proquest.com/lib/tuee/detail.action?docID=1498520.

Le Duigou, A. *et al.* (2012) 'Improving the interfacial properties between flax fibres and PLLA by a water fibre treatment and drying cycle', *Industrial Crops and Products*, 39(1), pp. 31–39. doi: 10.1016/J.INDCROP.2012.02.001.

Fiore, V., Di Bella, G. and Valenza, A. (2015) 'The effect of alkaline treatment on mechanical properties of kenaf fibers and their epoxy composites', *Composites Part B: Engineering*. Elsevier Ltd, 68, pp. 14–21. doi: 10.1016/j.compositesb.2014.08.025.
Garat, W. *et al.* (2020) 'Swelling of natural fibre bundles under hygro- and hydrothermal conditions: Determination of hydric expansion coefficients by automated laser scanning', *Composites Part A: Applied Science and Manufacturing*. Elsevier Ltd, 131. doi: 10.1016/J.COMPOSITESA.2020.105803.
Gregoire, M. *et al.* (2019) 'Study of solutions to optimize the extraction of hemp fibers for composite materials', *SN Applied Sciences*. Springer International Publishing, 1(10), pp. 1–6. doi: 10.1007/s42452-019-1332-4.
Hapuarachchi, T. D. *et al.* (2007) 'Fire retardancy of natural fibre reinforced sheet moulding compound', *Applied Composite Materials*, 14(4), pp. 251–264. doi: 10.1007/s10443-007-9044-0.
Hu, R. and Lim, J.-K. (2007) 'Fabrication and Mechanical Properties of Completely Biodegradable Hemp Fiber Reinforced Polylactic Acid Composites', *Journal of COMPOSITE MATERIALS*, 41(13). doi: 10.1177/0021998306069878.
Hussain, A. *et al.* (2019) 'Hygrothermal and mechanical characterisation of novel hemp shiv based thermal insulation composites', *Construction and Building Materials*. Elsevier Ltd, 212, pp. 561–568. doi: 10.1016/j.conbuildmat.2019.04.029.
Islam, M. S., Pickering, K. L. and Foreman, N. J. (2010) 'Influence of alkali treatment on the interfacial and physico-mechanical properties of industrial hemp fibre reinforced polylactic acid composites', *Composites Part A: Applied Science and Manufacturing*. Elsevier Ltd, 41(5), pp. 596–603. doi: 10.1016/j.compositesa.2010.01.006.
Islam, M. S., Pickering, K. L. and Foreman, N. J. (2011) 'Influence of alkali fiber treatment and fiber processing on the mechanical properties of hemp/epoxy composites', *Journal of Applied Polymer Science*, 119(6), pp. 3696–3707. doi: 10.1002/app.31335.
Islam, S. and Bhat, G. (2019) 'Environmentally-friendly thermal and acoustic insulation materials from recycled textiles', *Journal of Environmental Management*. Elsevier, 251(April), p. 109536. doi: 10.1016/j.jenvman.2019.109536.
Kabir, M. M. *et al.* (2013a) 'Effects of chemical treatments on hemp fibre structure', *Applied Surface Science*. Elsevier B.V., 276, pp. 13–23. doi: 10.1016/j.apsusc.2013.02.086.
Kabir, M. M. *et al.* (2013b) 'Tensile properties of chemically treated hemp fibres as reinforcement for composites', *Composites Part B: Engineering*. Elsevier Ltd, 53, pp. 362–368. doi: 10.1016/j.compositesb.2013.05.048.
Ku, H. *et al.* (2011) 'A review on the tensile properties of natural fiber reinforced polymer composites', *Composites Part B: Engineering*. Elsevier, 42(4), pp. 856–873. doi: 10.1016/J.COMPOSITESB.2011.01.010.
Liu, M., Silva, D. A. S., *et al.* (2016) 'Controlled retting of hemp fibres: Effect of hydrothermal pre-treatment and enzymatic retting on the mechanical properties of unidirectional hemp/epoxy composites', *Composites Part A: Applied Science and Manufacturing*. Elsevier Ltd, 88, pp. 253–262. doi: 10.1016/j.compositesa.2016.06.003.
Liu, M., Meyer, A. S., *et al.* (2016) 'Effect of pectin and hemicellulose removal from hemp fibres on the mechanical properties of unidirectional hemp/epoxy composites', *Composites Part A: Applied Science and Manufacturing*. Elsevier Ltd, 90, pp. 724–735. doi: 10.1016/j.compositesa.2016.08.037.

Liu, M., Baum, A., *et al.* (2017) 'Oxidation of lignin in hemp fibres by laccase: Effects on mechanical properties of hemp fibres and unidirectional fibre/epoxy composites', *Composites Part A: Applied Science and Manufacturing*. Elsevier Ltd, 95, pp. 377–387. doi: 10.1016/j.compositesa.2017.01.026.
Liu, M., Thygesen, A., *et al.* (2017) 'Targeted pre-treatment of hemp bast fibres for optimal performance in biocomposite materials: A review', *Industrial Crops and Products*, 108(July), pp. 660–683. doi: 10.1016/j.indcrop.2017.07.027.
Lu, N., Swan, R. H. and Ferguson, I. (2012a) 'Composition, structure, and mechanical properties of hemp fiber reinforced composite with recycled high-density polyethylene matrix', *Journal of Composite Materials*, 46(16), pp. 1915–1924. doi: 10.1177/0021998311427778.
Lu, N., Swan, R. H. and Ferguson, I. (2012b) 'Composition, structure, and mechanical properties of hemp fiber reinforced composite with recycled high-density polyethylene matrix', *Journal of Composite Materials*, 46(16), pp. 1915–1924. doi: 10.1177/0021998311427778.
Madsen, B., Hoffmeyer, P. and Lilholt, H. (2007) 'Hemp yarn reinforced composites - II. Tensile properties', *Composites Part A: Applied Science and Manufacturing*, 38(10), pp. 2204–2215. doi: 10.1016/J.COMPOSITESA.2007.06.002.
Manaia, J. P., Manaia, A. T. and Rodriges, L. (2019) 'Industrial hemp fibers: An overview', *Fibers*, 7(12), pp. 1–16. doi: 10.3390/?b7120106.
Marrot, L. *et al.* (2013) 'Analysis of the hemp fiber mechanical properties and their scattering (Fedora 17)', *Industrial Crops and Products*. Elsevier B.V., 51, pp. 317–327. doi: 10.1016/j.indcrop.2013.09.026.
Mazian, B. *et al.* (2018) 'Influence of field retting duration on the biochemical, microstructural, thermal and mechanical properties of hemp fibres harvested at the beginning of flowering', *Industrial Crops and Products*, 116(February), pp. 170–181. doi: 10.1016/j.indcrop.2018.02.062.
Merkel, K. *et al.* (2014) 'Processing and characterization of reinforced polyethylene composites made with lignocellulosic fibres isolated from waste plant biomass such as hemp', *Composites Part B: Engineering*. Elsevier Ltd, 67, pp. 138–144. doi: 10.1016/j.compositesb.2014.06.007.
Mohd Ishak, Z. A. and Mat Taib, R. (2015) *Multifunctional polymer composites using natural fiber reinforcements*, *Multifunctionality of Polymer Composites: Challenges and New Solutions*. Elsevier Inc. doi: 10.1016/B978-0-323-26434-1.00003-9.
Naughton, A., Fan, M. and Bregulla, J. (2014) 'Fire resistance characterisation of hemp fibre reinforced polyester composites for use in the construction industry', *Composites Part B: Engineering*, 60. doi: 10.1016/j.compositesb.2013.12.014.
Nilsson, D., Svennerstedt, B. and Wretfors, C. (2005) 'Adsorption equilibrium moisture contents of flax straw, hemp stalks and reed canary grass', *Biosystems Engineering*. Academic Press, 91(1), pp. 35–43. doi: 10.1016/j.biosystemseng.2005.02.010.
Oksman, K., Skrifvars, M. and Selin, J. F. (2003) 'Natural fibres as reinforcement in polylactic acid (PLA) composites', *Composites Science and Technology*, 63(9), pp. 1317–1324. doi: 10.1016/S0266-3538(03)00103-9.
Panaitescu, D. M. *et al.* (2015) 'Influence of compatibilizing system on morphology, thermal and mechanical properties of high flow polypropylene reinforced with short hemp fibers', *Composites Part B: Engineering*. Elsevier Ltd, 69, pp. 286–295. doi: 10.1016/j.compositesb.2014.10.010.

Panaitescu, D. M. *et al.* (2020) 'Effect of hemp fiber length on the mechanical and thermal properties of polypropylene/SEBS/hemp fiber composites', *Journal of Materials Research and Technology*. Elsevier BV, 9(5), pp. 10768–10781. doi: 10.1016/j.jmrt.2020.07.084.
Pappu, A., Pickering, K. L. and Thakur, V. K. (2019) 'Manufacturing and characterization of sustainable hybrid composites using sisal and hemp fibres as reinforcement of poly (lactic acid) via injection moulding', *Industrial Crops and Products*. Elsevier B.V., 137, pp. 260–269. doi: 10.1016/j.indcrop.2019.05.040.
Pasila, A. (2000) 'The effect of frost on fibre plants and their processing', *Molecular Crystals and Liquid Crystals Science and Technology, Section A: Molecular Crystals and Liquid Crystals*, 353, pp. 11–22. doi: 10.1080/10587250008025644.
Pejic, B. M. *et al.* (2008) 'The effects of hemicelluloses and lignin removal on water uptake behavior of hemp fibers', *Bioresource Technology*. Elsevier, 99(15), pp. 7152–7159. doi: 10.1016/j.biortech.2007.12.073.
Pereira, P. H. F. *et al.* (2015) 'Vegetal fibers in polymeric composites: A review', *Polimeros*, pp. 9–22. doi: 10.1590/0104-1428.1722.
Pickering, K. L., Efendy, M. G. A. and Le, T. M. (2016) 'A review of recent developments in natural fibre composites and their mechanical performance', *Composites Part A: Applied Science and Manufacturing*, 83, pp. 98–112. doi: 10.1016/j.compositesa.2015.08.038.
Pil, L. *et al.* (2016) 'Composites : Part A Why are designers fascinated by flax and hemp fibre composites ?', *Composites Part A*. Elsevier Ltd, 83, pp. 193–205. doi: 10.1016/j.compositesa.2015.11.004.
Réquilé, S. *et al.* (2021) 'Exploring the dew retting feasibility of hemp in very contrasting European environments: Influence on the tensile mechanical properties of fibres and composites', *Industrial Crops and Products*, 164(August 2020). doi: 10.1016/j.indcrop.2021.113337.
Sair, S. *et al.* (2017) 'Effect of surface modification on morphological, mechanical and thermal conductivity of hemp fiber: Characterization of the interface of hemp - Polyurethane composite', *Case Studies in Thermal Engineering*. Elsevier Ltd, 10, pp. 550–559. doi: 10.1016/j.csite.2017.10.012.
Sawpan, M. A., Pickering, K. L. and Fernyhough, A. (2011a) 'Effect of fibre treatments on interfacial shear strength of hemp fibre reinforced polylactide and unsaturated polyester composites', *Composites Part A: Applied Science and Manufacturing*. Elsevier Ltd, 42(9), pp. 1189–1196. doi: 10.1016/j.compositesa.2011.05.003.
Sawpan, M. A., Pickering, K. L. and Fernyhough, A. (2011b) 'Improvement of mechanical performance of industrial hemp fibre reinforced polylactide biocomposites', *Composites Part A: Applied Science and Manufacturing*. Elsevier Ltd, 42(3), pp. 310–319. doi: 10.1016/j.compositesa.2010.12.004.
Sepe, R. *et al.* (2018) 'Influence of chemical treatments on mechanical properties of hemp fiber reinforced composites', *Composites Part B: Engineering*. Elsevier Ltd, 133, pp. 210–217. doi: 10.1016/j.compositesb.2017.09.030.
Sgriccia, N., Hawley, M. C. and Misra, M. (2008) 'Characterization of natural fiber surfaces and natural fiber composites', *Composites Part A: Applied Science and Manufacturing*. Elsevier, 39(10), pp. 1632–1637. doi: 10.1016/j.compositesa.2008.07.007.
Sood, M. and Dwivedi, G. (2018) 'Effect of fiber treatment on flexural properties of natural fiber reinforced composites: A review', *Egyptian Journal of Petroleum*. Egyptian Petroleum Research Institute, pp. 775–783. doi: 10.1016/j.ejpe.2017.11.005.

Sreekumar, P. A. *et al.* (2009) 'Effect of fiber surface modification on the mechanical and water absorption characteristics of sisal/polyester composites fabricated by resin transfer molding', *Composites Part A: Applied Science and Manufacturing*. Elsevier, 40(11), pp. 1777–1784. doi: 10.1016/j.compositesa.2009.08.013.
Tavares, T. D. *et al.* (2020) 'Biofunctionalization of natural fiber-reinforced biocomposites for biomedical applications', *Biomolecules*, 10(1). doi: 10.3390/biom10010148.
Thiagamani, S. M. K. *et al.* (2019) 'Investigation into mechanical, absorption and swelling behaviour of hemp/sisal fibre reinforced bioepoxy hybrid composites: Effects of stacking sequences', *International Journal of Biological Macromolecules*. Elsevier B.V., 140, pp. 637–646. doi: 10.1016/j.ijbiomac.2019.08.166.
Väisänen, T. *et al.* (2018) 'Modification of hemp fibers (Cannabis Sativa L.) for composite applications', *Industrial Crops and Products*. Elsevier B.V., 111, pp. 422–429. doi: 10.1016/j.indcrop.2017.10.049.
Viscusi, G. *et al.* (2020) 'Natural fiber reinforced inorganic foam composites from short hemp bast fibers obtained by mechanical decortation of unretted stems from the wastes of hemp cultivations', *Materials Today: Proceedings*. Elsevier BV. doi: 10.1016/j.matpr.2020.02.672.
Xie, Y. *et al.* (2010) 'Silane coupling agents used for natural fiber/polymer composites: A review', *Composites Part A: Applied Science and Manufacturing*. Elsevier Ltd, 41(7), pp. 806–819. doi: 10.1016/j.compositesa.2010.03.005.
Zegaoui, A. *et al.* (2018) 'Morphological, mechanical and thermal properties of cyanate ester/benzoxazine resin composites reinforced by silane treated natural hemp fibers', *Chinese Journal of Chemical Engineering*. Chemical Industry Press, 26(5), pp. 1219–1228. doi: 10.1016/j.cjche.2018.01.008.

Acknowledgements

I would like to appreciate my supervisors, Prof. Jaan Kers and Dr. Triinu Poltimäe for their support and advice in ensuring the successful completion of this research work. Additionally, I extend my gratitude to Dr. Heikko Kallakas for his support and motivation to do this research. I am very thankful to all co-authors of the scientific papers, especially Dr. Laetitia Marrot for her splendid contributions to the research.

I am also grateful to all my colleagues in the Laboratory of Wood Technology, in textiles and polymer technology who offered technical support and advice during the research. I am also acknowledging my friends and families for their motivational support throughout the doctoral study.

This research was funded by the European Regional Development Fund under the Dora Plus Action 2.1. “Mobility scholarship for foreign PhD students”.

The research was also partially supported by ASTRA “TUT Institutional Development Programme for 2016-2022” Graduate School of Functional Materials and Technologies (2014-2020.4.01.16-0032). Short-term conference attendance during doctoral studies were supported by Archimedes Foundation. As well as investment from the Republic of Slovenia and ARRS (Slovenian Research Agency) Bilateral Project Slovenia—Estonia (grant agreement number BI-EE/20-22-007).

Abstract

Characterisation of Frost-Retted Hemp Fibres for Use as Reinforcement in Biocomposites

To achieve the EU Green Deal (EGD) aims, there is a need to utilise more locally sourced materials and obtain suitable alternatives to synthetic products. Given this, there is a need for redesigning of processes and product utilisation by the industrial sectors, which causes a higher inclination to use biobased, healthy, sustainable, biodegradable, and renewable resources. Natural fibres (plant based materials) have thus gained more attention. In particular, industrial hemp shows high potential and is considered to be one of the ways to achieve the EGD targets. Currently, the demand for hemp is driven on the market mainly by the need for cannabidiol (CBD), although there is growing interest in the application of the fibres (by-product) as reinforcement in polymeric matrix composites in construction, automobile, packaging, and cosmetic industry, due to the high stiffness and strength compared to the available natural fibres. However, performance and durability concerns in service limit their adaptation. In addition, there is a lack of adequate information or resources in some cases about the performance or applicability of hemp fibres.

Hence, this PhD research seeks to fill this gap and investigates the applicability of frost-retted hemp fibres from Estonia as reinforcing materials in biocomposites. The study aimed to augment the contribution to a carbon-neutral environment by applying the underutilised hemp plants (dioecious Hungarian variety) from Estonia as reinforcements in enhancing the technological and physicomechanical properties of sustainable biocomposites. The novelty of current research is based on the characteristics of frost-retted hemp fibres grown in Estonia which is not reported in the literature. Their utilisation will lead to valorisation of local resources. Furthermore, this research applied a uniquely comprehensive approach with double scale analysis, involving the examination of the characteristics of the unmodified and chemically modified hemp fibres on a micro-scale and their influence on a macro-scale (the biocomposite's physicomechanical performance).

In this regard, the chemical composition, strength properties and morphological features of the hemp fibre were first examined, biocomposites were fabricated by thermocompression from 30 and 50 wt.% fibre reinforcing polylactic acid (PLA), and the biocomposite tensile performance were evaluated.

The research outcome revealed that the hemp fibres grown in Estonia had lower lignification (1.4%), compared to values reported for Western European regions, resulting from short daylight during the latter growth stage and high soluble content (12 ± 0.4%), because of limited microbial activities during frost-retting, which causes more bundled fibres that affect the mechanical performance of the biocomposites. Subsequently, four fibre modification methods (water immersion for 72 hours, alkali pretreatment with 5 wt.% NaOH solution for 4 hours, combined water with silane and combined alkali with silane treatment) were applied to alter the fibre properties and improve the performance of the biocomposite. The pre and post-modification characterisation of the hemp fibre done with a scanning electron microscope (SEM), Fourier transform infrared (FTIR) and thermogravimetric analysis (TGA) showed the relative effectiveness of the treatments in changing the fibre properties, due to the amount of non-cellulosic fibre components (pectin, wax, lignin, and hemicelluloses)

extracted. The fabricated biocomposite microscopic cross-sectional observation also showed that the treatments caused better fibre individualisation and homogeneity within the PLA matrix. Furthermore, the physicomechanical performance of the biocomposites at 30 and 50 wt.% fibre content indicated that the reinforcement of the PLA at 50 wt.%, caused a decrease in mechanical performance because of more fibre-fibre contact, especially after modification and in general, the inadequate wetting of the fibres by the PLA caused more porosity and poor stress transfer. The biocomposite performance also decreased at the high fibre content in wet conditions due to the more hydrophilic affinity and the presence of more voids. However, considering the future applications of the biocomposites such as in the building and transportaton sectors where fire reaction properites are essential, a higher fibre content appears to be satisfactory. Concerning biocomposites with modified hemp fibre, the combined alkali and silane treatment produced the most promising results, with a tensile strength of 62 MPa, modulus of rupture of (113 MPa) and modulus of elasticity of 7.6 GPa at 30 wt.%, but the rupture modulus though slightly higher at 50 wt.% (5.8%) was not significant. In wet conditions, a similar improvement was obtained, although the results were not better when compared to biocomposites reinforced with the fibres treated only with NaOH solution.

Considering that combined alkali and silane modification of hemp fibres is nine times more expensive than alkali treatment and that the improvement in the results was not significant in most cases, the study recommended that the fibre treatment with NaOH solution would be most preferable.

Finally, this study successfully characterised the Estonian hemp fibre (dioecious Hungarian variety) and developed biocomposites with improved performance, which will contribute to the reduction of CO_2 emissions, promote the use of locally obtained resources, and provide the opportunity to realise a sustainable environment. However, to scale up there is a need to improve the manufacturing technology to ensure the consistency in composite performance and therefore the use of an automated manufacturing strategy would assure product performance uniformity.

Lühikokkuvõte

Külmligu kanepikiudude karakteriseerimine kasutamiseks sarrusena biokomposiitides

Euroopa Liidu roheleppe eesmärkide saavutamiseks on vaja otsida sobivaid alternatiive sünteetilistele toodetele kasutades selleks rohkem kohaliku päritoluga materjale. Selle eesmärgi saavutamiseks on vajalik ümberkujundada tootmises kasutuselolevad protsessid, mis võimaldaksid säästvamalt ja efektiivsemalt kasutada biopõhiseid, tervislikke, taastuvaid ja biolagunevaid ressursse. Looduslikud kiud (sh taimsed kiud) on pälvinud suurt tähelepanu. Roheleppe eesmärkide saavutamisel nähakse suurt potentsiaali tööstuslikul kanepil. Praegu on nõudlus kanepi järele peamiselt tingitud vajadusest kannabidiooli järele. Kuna kanepikiul on võrreldes teiste looduslike kiududega suurem jäikus ja tugevus, siis on suurenenud huvi kiu (kõrvalsaaduse) kasutamise vastu polümeersete komposiitide armeerimisel ehituses, autotööstuses, pakendites.

Kasutuse laiendamist piiravad nii adekvaatse info puudumine kanepikiudude kasutusomaduste ja materjali suutlikkuse kohta kui ka kasutuses olevate materjalide kasutusea ja vastupidavusega seotud probleemid.

Käesolev uurimustöö püüab neid lünki täita. Doktoritöös uuritakse Eestis kasvatatud kiukanepivartest (Ungari Tisza) üle talve seismisega külmligu töödeldud kanepikiudude kasutatavust biokomposiitide sarrusena.

Uuringu eesmärgiks oli panustada keskkonna süsinikuneutraalseks muutmisesse läbi Eestis kasvatatud kanepitaimedest (Ungari sort Tisza) saadud ja seni alakasutatud kanepikiude rakendamise jätkusuutlike biokomposiitide tehnoloogiliste ja füüsikalis-mehaaniliste omaduste parendamiseks.

Käesoleva uurimistöö uudsus seisneb Eestis kasvatatud külmligu kanepikiudude omaduste karakteriseerimises, kuna selle kohta teaduskirjanduses info puudus. Nende kasutamine suurendab kohalike ressursside väärindamist. Uuringus kasutati kanepikiu omaduste analüüsil ainulaadset terviklikku kahe skaalalist lähenemisviisi, mis hõlmas modifitseerimata ja keemiliselt modifitseeritud kanepikiudude omaduste uurimist mikroskaalal ja nende mõju uurimist biokomposiidi füüsikalis-mehaanilistele omadustele makroskaalal.

Esmalt uuriti kanepikiu keemilist koostist, tugevus- ja morfoloogilisi omadusi. Seejärel valmistati polüpiimhappe (PLA) ja kanepikiududest biokomposiidid 30 ja 50 massiprotsendilise (m.%) armeerivate kiudude sisaldusega ning hinnati nende tõmbetugevust ja tõmbeelastsusmoodulit.

Uuringu tulemused näitasid, et Eestis kasvanud kanepikiu rakuseinte lignifitseerumine oli madalam (1,4%) võrreldes Lääne-Euroopas kasvatatud kanepiga, mis tulenes lühikesest päevavalguse ajast viimases kasvufaasis ja kõrgest lahustuvate ainete sisaldusest (12 ± 0,4%). Mikroobide tegevuse piiratuse tõttu külmleotuse ajal halvenes üksikute kiudude eraldamine kiukimpudest, mis vähendas biokomposiitide mehaanilist tugevust. Peale kanepikiudude eraldamist kiukimpudest kasutati kiu omaduste muutmiseks ja biokomposiidi tugevusomaduste parandamiseks nelja kiudude keemilise modifitseerimise meetodit (72-tunnine vees leotamine, 4-tunnine leeliseline eeltöötlemine 5 m.% NaOH lahusega, kombineeritud vesi-silaan ja leelis-silaan töötlemine). Kanepikiu keemilise eel- (vee või leelisega) ja järeltöötluse (silaaniga) mõju kiu omadustele uuriti skaneeriva elektronmikroskoobi (SEM), Fourier' transformatsiooniga infrapuna spektromeetri (FTIR) ja termogravimeetrilise analüüsiga

(TGA). Analüüsi tulemused näitasid keemilise töötluse suhtelist tõhusust kiu omaduste modifitseerimisel, mis oli tingitud mittetselluloossete ainete (pektiin, vaha, ligniin ja hemitselluloosid) osalisest ekstraheerimisest. Biokomposiidi ristlõike mikroskoopilised uuringud näitasid, et eeltöötlemine tagas parema kiudude jaotumise ja homogeensuse PLA maatriksis. Lisaks näitasid 30 ja 50 m.% kiusisaldusega biokomposiitide füüsikalis-mehhaanilined katsetused, et 50 m.% kiusisaldusega biokomposiitide puhul mehaaniline tugevus vähenes, kuna PLA maatriks ei suutnud kõiki kiude enam siduda ja kiudude omavaheline kontakt oli suurem, eriti pärast modifitseerimist. Kiudude ebapiisav märgumine PLA-ga põhjustas biokomposiidi suuremat poorsust ja ebaühtlase pingete jaotumise komposiidis.

Biokomposiidi töökindlus ja tugevus vähenesid märgades oludes kõrge kiusisalduse korral kiudude suurema hüdrofiilsuse ja suurema tühimike arvu tõttu. Kuid arvestades biokomposiitide tulevasi rakendusi, näiteks ehitus- ja transpordisektoris, kus tuletõkke omadused on olulised, võiks suurem kiusisaldus anda rahuldava tulemuse. Modifitseeritud kanepikiuga biokomposiitide puhul andis 30% kiusisalduse juures kõige paremaid tulemusi kombineeritud töötlemine leelise ja silaaniga, kus komposiidi tõmbetugevus oli 62 MPa, paindetugevus 113 MPa ja elastsusmoodul 7,6 GPa. 50% kiusisaldusega suurenes paindetugevus ainult 5,8%. Kanepikiudude eeltöötlusel veega saavutati sarnane kiu omaduste paranemine, kuid tulemused ei olnud oluliselt paremad võrreldes NaOH lahusega keemiliselt töödeldud kiududega tugevdatud biokomposiitidega. Arvestades, et leelise ja silaaniga kombineeritud modifitseerimine on 9 korda kallim kui leelisega töötlemine ning tulemuste paranemine ei olnud enamikul juhtudel märkimisväärne, soovitati uuringus eelistada kiudude töötlemist NaOH lahusega.

Kokkuvõtteks võib öelda, et doktoritöös karakteriseeriti Eestis kasvanud ja külmligu meetodil töödeldud kanepikiu (Ungari Tizsa) omadusi ja töötati välja suurema mehaanilise tugevusega biokomposiidid, mis aitavad kaasa CO_2 emissiooni vähendamisele ja soodustavad kohapeal kasvatatud ressursside keskkonnasäästlikku kasutamist. Suuremate komposiitplaatide tootmiseks ja materjali tugevusomaduste ühtlustamiseks on vaja täiustada tootmistehnoloogiat protsessi automatiseerimisega.

Appendix 1

Publication I

Marrot, L.; Alao, P.F.; Mikli, V.; Kers, J. Properties of Frost-Retted Hemp Fibers for the Reinforcement of Composites. Journal of Natural Fibers 2021, 1–12.

JOURNAL OF NATURAL FIBERS
https://doi.org/10.1080/15440478.2021.1904474

Taylor & Francis
Taylor & Francis Group

ARTICLE

OPEN ACCESS Check for updates

Properties of Frost-Retted Hemp Fibers for the Reinforcement of Composites

Laetitia Marrot[1,2], Percy Festus Alao[3], Valdek Mikli[3], and Jaan Kers[3]

[1]Renewable Materials Composites Group, InnoRenew CoE, Izola, Slovenia; [2]University of Primorska, Koper, Slovenia; [3]Department of Polymer Materials, Tallinn University of Technology, Tallinn, Estonia

ABSTRACT

Frost-retted hemp fibers were investigated to assess their suitability for composite applications. Chemical analysis of frost-retted hemp fibers highlighted a high amount of solubles (pectins) at the fibers surface and a low lignin content in the fibers that was attributed to an unfavorable synthesis of lignin in the cell wall due to the particularly cold temperature during hemp growth in the Nordic countries. The fibers tensile properties were considered at two different scales and the performances of hemp/PLA composites were assessed. Recommendations were provided for the use of frost-retted hemp fibers in the reinforcement of thermoplastic composites.

摘要

研究了霜脱胶大麻纤维对复合材料的适用性. 对霜脱胶大麻纤维的化学分析表明, 纤维表面有大量的可溶物（果胶）, 纤维中的木质素含量较低, 这是由于北欧国家大麻生长期间温度特别低, 不利于细胞壁木质素的合成. 研究了纤维在两种不同尺度下的拉伸性能, 并对大麻/聚乳酸复合材料的性能进行了评价. 提出了霜麻纤维增强热塑性复合材料的建议.

KEYWORDS

Hemp; frost-retting; nordic country; tisza variety; PLA composite; polylactic acid composite

关键词

大麻; 霜冻脱胶; 北欧国家; 提萨品种; 复合材料; 聚乳酸复合材料

Introduction

Natural plant fibers as reinforcement of composites have received a growing interest from the scientific community for the last 15 years (Bourmaud et al. 2018). Industrial hemp (*Cannabis sativa*) is an annual crop that requires low input for its cultivation (Horne 2020), fitting into sustainable farming systems (Ranalli and Venturi 2004). In Nordic countries, hemp is primarily cultivated to produce cannabidiol for medicine application. Flowers and leaves are harvested in September while the straws (including fibers and shives) are considered as a waste or low-value product. Hemp fibers are extracted from the straws through a mechanical defibration process that crushes the stems. Prior to the decortication, the straws can undergo a retting process (1) to loosen bonding between fiber-fiber and bundle-bundle by degrading the non-cellulosic components in the bast fiber layer, particularly the pectic polysaccharides (Horne 2020); and (2) to facilitate fiber separation and to avoid fiber breakage during following mechanical processing (e.g. scutching) and to preserve the fibers quality (Gregoire et al. 2019). Western European field retting consists of leaving purposefully the stems in the field after the autumn harvest to be decorticated under the actions of microorganisms. The time of field retting depends on the geographic location and weather conditions. In Nordic countries, autumn is a cold and rainy period. If harvested at that time, due to the high moisture content, hemp stems require a high amount of energy to dry and avoid the formation of mold that could destroy the quality of the raw material (Pasila 2000). Pasila (Pasila 2000) suggested harvesting the straw in spring, which is the driest time of the year. Hemp straws harvested in spring are defined as “frost-retted”. Under frost-retting, the

CONTACT Laetitia Marrot laetitia.marrot@innorenew.eu Renewable Materials Composites Group, InnoRenew CoE, Livade 6, Izola 6310, Slovenia.

fiber separation from the stem is induced by the daily changes of temperature above and below the zero in the springtime. The water freezes and melts in the plant cell structures, which leads to an enlarging movement that loosens the bast fiber from the stem (Pasila 2000). The main goal of this paper is to assess the suitability of frost-retted hemp fibers for composite applications in order to value this by-product of the Nordic hemp industry. The study will present the chemical composition and the mechanical properties of hemp fibers (*Cannabis sativa*, dioecious Hungarian variety Tisza) that underwent a frost-retting process, and the mechanical performances of Polylactic acid (PLA) composites using these frost-retted fibers as reinforcement. This study will provide data on the Tisza variety, which is not often reported in the literature. The mechanical analysis of the frost-retted hemp fibers will be performed for two scales of reinforcement (unitary fibers and strands), and the performances of the corresponding PLA composites will be investigated to provide good practices for the manufacture of sustainable composites using frost-retted fibers.

Materials and methods

Materials

Hemp fibers (*Cannabis sativa*, dioecious Hungarian variety Tisza) were supplied by Hempson OÜ. They were sown the 10 June 2016 in Estonia on the Saaremaa island. Growth lasted until October 2016, and, after senescence, the stems stood in the field until 4 May 2017 before being harvested. Between June and October 2016, the average monthly temperatures were 15, 18, 17, 15 and 7°C, and the average monthly light were 13.0, 11.5, 8.9, 8.6, 4.0 hours/day. During the frost-retting period (November 2016 – May 2017), the average monthly temperatures were 3, 3, 0, 0, 2, 4, 9°C. The stems were then industrially decorticated by a mechanical process.

PLA fibers (Ingeo™) from Trevira® GmbH were used for the manufacture of composites. The fibers were 60 mm long, with a round cross-section, a finesse of 6.7 dtex, and a density of 1.25 g/cm^3.

Microscopic analysis of hemp fibers

Fibers surface and individualization were observed with a high-resolution Zeiss Ultra 55 Scanning Electron Microscope (SEM). Prior to the observation, the fibers were vacuum coated with an alloy of gold/palladium (80/20). The machine was operated between 4 and 20 kV, scanning depth up to 100 nm, and magnification up to 50000.

The individualization of the fibers was quantified by image analysis. The fibers were first embedded in epoxy resin, then the cross-section of the sample was polished and observed with a digital microscope Keyence VHX-6000. The images were analyzed with the ImageJ software. The type was converted into 8-bit, a threshold was applied, and the image was processed to reduce noise and fill the holes before analyzing the particles. The particle analysis provided surface areas of 671 fibers and bundles units, and corresponding equivalent diameters of these units were estimated by considering a circular shape for their cross-section.

Chemical analysis of hemp fibers

Chemical composition of the untreated hemp batch was determined by the Van Soest method, based on standards NF EN ISO 13906 and NF V18-122. This method uses a successive and differential solubilization of the constituents of the samples (constituents of the plant cell walls mainly) in 3 detergents followed by a calcination. The Neutral Detergent Fiber (NDF) attack ensures a partial removal of pectins. NDF composition is 30 g/L of sodium dodecyl sulfate, 18.61 g/L of ethylenediaminetetraacetic acid (EDTA), 6.81 g/L of sodium borate, and 4.56 g/L of disodium hydrogenophosphate dihydrate. The Acid Detergent Fiber (ADF) attack then eliminates pectins and hemicelluloses. ADF is made of 20 g/L of cetyl trimethylammonium bromide in H_2SO_4 at 0.5 mol/L. Each extraction

lasts for 1 h at 100°C and is followed by 2 rinsing steps for 1 h with boiling water. The Acid Detergent Lignin (ADL) attack on ADF residues consists of an acidic solution of 72% H_2SO_4 (12 mol/L) and allows the elimination of cellulose. The last calcination step eliminates lignin in ADL residues. Monitoring the mass of the samples during these successive specific attacks makes it possible to obtain sequentially the cellulose content, an estimate of the hemicelluloses content, an estimate of the soluble content (part of pectins), the lignin content, and the ash content (inorganic matter). In practice, the chemical analysis of the hemp fibers was performed with FIBRETHERM® equipment (Gerhardt) including a control sample and allowed accurate result with a precision of 0.1% for the components content. The chemical composition corresponds to the average and standard deviation of duplicates.

Composite preparation and evaluation of fibers orientation

Hemp fibers and PLA fibers were dried in an oven for 24 hours at a temperature of 80°C prior to the composite preparation. Two ratios hemp fibers/PLA (30 and 50 wt% regarding hemp fibers weight) were prepared. Hemp and PLA fibers were weighed using a Mettler Toledo PL202-s and then combined using a drum carder of 100 mm width. Aligned hemp and PLA fibers were then mixed and placed in a metal mold of dimensions 300 × 300 x 4 mm. The mixture was compressed for 10 min at a temperature of 180°C and a pressure of 3 MPa. Finally, the composite product was conditioned at room temperature (23°C) before removal from the form.

Within the composites, the fibers are unidirectionally aligned, but, given their inhomogeneity in terms of dimensions and their entanglement, there is a clear misalignment that needs to be taken into account. For this purpose, surface analysis on the longitudinal section of the composites was operated under a digital microscope Keyence VHX-6000. Considering that the average misalignment is the same within the thickness of the composites, the misorientation of the fibers and strands in regard to the loading direction was measured. A total of 105 angle measurements were taken on the samples machined for tensile tests.

Mechanical characterization of fibers and composites

Natural fibers can be mechanically characterized either at the unitary fiber scale or at the bundle of fibers (strands) scale. Dispersion of the mechanical properties of hemp and flax unitary fibers has been discussed in the literature (Lefeuvre et al. 2014; Marrot et al. 2013). To reduce variability, Barbulée et Gomina (Barbulée and Gomina 2017) suggest testing strands that gather hundreds of unitary fibers. They obtain a convergence of the average deformation with about 1% accuracy when testing 15 strands (Barbulée and Gomina 2017). In this study, the mechanical properties of the fibrous reinforcement were tested at two scales (unitary fiber and strand) to consider the influence of the fiber dimensions on the reported values and dispersion. Tensile tests on unitary hemp fibers and strands were carried out on a universal testing machine Zwick Roell Z010 at 23 ± 1°C and 50 ± 2% RH. The tensile test on unitary fibers has been carried out in accordance with the NF T25-501-3 standard describing the determination of tensile properties of flax unitary fibers for application in the reinforcement of plastic composites. To the best of the authors knowledge, there is no equivalent standard for the mechanical characterization of hemp fibers. The machine was equipped with a 20 N load cell, gauge length was taken at 10 mm, deformation was obtained using cross-head travel, and strain rate was set at 1 mm/min. Before testing, the mean diameter was determined as the average of 3 diameter measurements. A total of 64 unitary fibers were tested among which 19 were not exploitable (break in the jaws). For the tensile test on strands, the machine was equipped with a 10 kN load cell, gauge length was fixed at 50 mm, and strain rate was set at 1 mm/min. The choice of the gauge length resulted in taking the maximal length allowing homogeneous fineness along the whole length of the strand. 42 strands were tested (1 sample was not exploitable). Prior to the test, the mass of the strands with a length of 10 cm was measured with a Mettler Toledo XPR303S scale (1 mg precision), and the corresponding average

diameter of the strands was calculated by using the density of the hemp fibers estimated by Bourmaud et al (Bourmaud et al. 2019) at 1,38 g/cm^3 with the buoyancy method.

Five composite samples were tested following EN–ISO 527–4 using an INSTRON 5688 tensile machine. The test condition was at a temperature of 24°C, relative humidity of 40%, and test rate of 2 mm/min. The specimens were conditioned in the room for 24 h before the test, and the test results were averaged arithmetically.

Fiber massic fraction (M_f %) was determined as the weight of the fibrous reinforcement (W_f) divided by the total weight of the composite ($W_f + W_m + W_p$), f, m and p indexes standing, respectively, for fiber, matrix and porosity. Since the weight of the voids Wp is taken as 0:

$$M_f\% = \frac{W_f}{W_f + W_m + W_p} = \frac{W_f}{W_f + W_m}$$

The fiber volume fraction (V_f %) is given by the relation:

$$V_f\% = \frac{M_f\%}{M_f\% + \left(\frac{\rho_f}{\rho_m}\right)\left(1 - M_f\%\right)}$$

With ρ_f as the density of fibrous reinforcement (1.38 according to (Bourmaud et al. 2019) as mentioned above) and ρ_m as the density of the PLA matrix (1.25 according to the FDS).

Composites density (ρ_c) was calculated using the weight and volume of the samples. The void fraction (V_p%) was then calculated from the measured weights and densities:

$$V_p\% = 1 - \frac{\frac{W_f}{\rho_f} + \frac{W_c - W_f}{\rho_m}}{\frac{W_c}{\rho_c}}$$

Results and discussion

Investigation of biochemical composition

Chemical composition of the frost-retted hemp fibers is presented in Table 1. Cellulose content (77.4 ± 0.3% w/w) is in accordance with results from the literature (Liu et al. 2015; Marrot et al. 2013). Pectins content is related to the soluble content extracted by the Van Soest method. In this study, the soluble content (12.6 ± 0.4% w/w) is relatively high compared to values from the literature. Marrot et al (Marrot et al. 2013) reported a pectins content of 3.0% w/w. Liu et al (Liu et al. 2015) noted a reduction of the pectin deposition (indicated by galacturonic acid content) from 6.3 for un-retted fibers to 3.1–5.4% w/w for field-retted fibers. However, in the case of frost-retting, the separation of the fibers from the stem is due to the variation of volume of alternatively liquid and solid water in the cell plant structure under the effect of negative temperatures. Under such low temperature conditions, the activity of microorganisms and enzymes is limited, and the pectic substances are less prone to degradation than in the case of dew-retting. Lignin content in this study (1.4% w/w) is particularly low compared with values reported in the literature (between 2 and 6% of dry matter (Angelini, Tavarini, and Di Candilo 2016; Müssig et al. 2020)). The phenological development of hemp is conditioned by climatic conditions, in particular to light and temperature (Hall, Bhattarai, and Midmore 2014). As lignin is a component which is biosynthesized in the final stage of the fiber-cell wall remodeling (Crônier, Monties, and Chabbert 2005), the relatively cold temperature and short

Table 1. Chemical composition of the frost-retted hemp fibers.

Cellulose (%)	Hemicellulose (%)	Lignin (%)	Soluble (%)	Inorganic matter (%)
77.4 ± 0.3	8.3 ± 0.3	1.4 ± 0.0	12.6 ± 0.4	0.3 ± 0.0

daily light period at this stage in Estonia may be responsible for an unfavorable synthesis of lignin in the cell wall, resulting in a lower content as the one usually reported for Western European hemp varieties. Similarly, authors (Gindl, Grabner, and Wimmer 2000) reported the influence of climatic variability on the lignification of the cell wall in latewood of Norway spruce.

Hemp fibers individualization

SEM observations of the frost-retted hemp fibers highlighted the presence of large bundles, up to 300 μm in diameter, mixed with unitary fibers (Figure 1A). Significant amounts of impurities (cortical residues, pectins, and wax) were observed on the bundles surface (Figure 1B), preventing their further individualization. This observation is in good agreement with the high soluble content highlighted by the chemical analysis of the fibers.

The image analysis of the cross-section of the fibers highlighted a broad repartition of fiber equivalent diameters from 11 μm to 525 μm. The number of fiber or bundle units per equivalent diameter range is presented on the Figure 2. Unitary fibers (with equivalent diameter in the range 11–30 μm) represent 12.5% of the total number, and 0.5% of the total surface area of the fibrous units. Small bundles (with equivalent diameter in the range 31–110 μm) represent 49.6% of the total number, and 11.7% of the total surface area of the fibrous units. Large bundles (with equivalent diameter higher than 111 μm) represent 37.9% of the total number, and 87.8% of the total surface area of the fibrous units.

Tensile mechanical properties of unitary fibers and strands

The force–deformation curves of a unitary fiber and a strand under tension are presented, respectively, in Figures 3 and 4. In the case of loading for a unitary fiber, the non-linear region observed in the beginning of the curve is typical to plant fibers and corresponds to the alignment of the microfibrils with the fiber axis (Baley 2002; Marrot et al. 2013). The apparent modulus of the unitary fiber is taken in the second region of the loading curve, which is linear and characteristic of an elastic behavior (Figure 3).

In the case of loading for a strand (Figure 4), one or several bundles of fibers are solicited.

Two types of rupture are observed (Figure 4). The first one is a brittle fracture of the strand; the constitutive fibers are linked strongly enough by the pectic interphase to be loaded simultaneously, which results in a single linear region on the loading curve where the apparent modulus is taken. When maximal load is reached, the fibers show a simultaneous brittle fracture. For the second type of rupture, once the bundles reach an equal strain, the loading curve displays a first linear region that corresponds to an elastic behavior. The apparent modulus is measured in this elastic domain (Figure 4). Then the curve shows a non-linear zone ending by the first breakdown of a fiber bundle. The load is then carried by the remaining bundles until the failure of another fiber bundle, and so on. until the break of the last bundle. This succession of breaks and load recovery gives a typical saw-tooth shape to the loading curve, previously described by Barbulée et al (Barbulée et al. 2014) for tension of flax slivers. These authors (Barbulée et al. 2014) observed three types of damage mechanisms in the non-linear zone thanks to acoustic emission analysis: first bundles delamination by breakage of the pectin links between ultimate fibers, then delamination among adjacent bundles, and finally successive ruptures of the bundles occur (Barbulée et al. 2014). The two types of fracture highlight the heterogeneity of the frost-retted strands, which gather bundles strongly connected to each other and bundles with poor cohesion due to degradation of the middle lamellae during the retting process.

In Figure 5, strength at break is plotted versus apparent modulus for unitary fibers and bundles of frost-retted hemp fibers tested in this study. The linear tendency reported in the literature (Bourmaud et al. 2018; Marrot et al. 2013) for this plot is visible for the unitary fibers, with a determination coefficient r^2 at 0.61. For the strands, the linear tendency is not confirmed ($r^2 = 0.06$). Unlike unitary

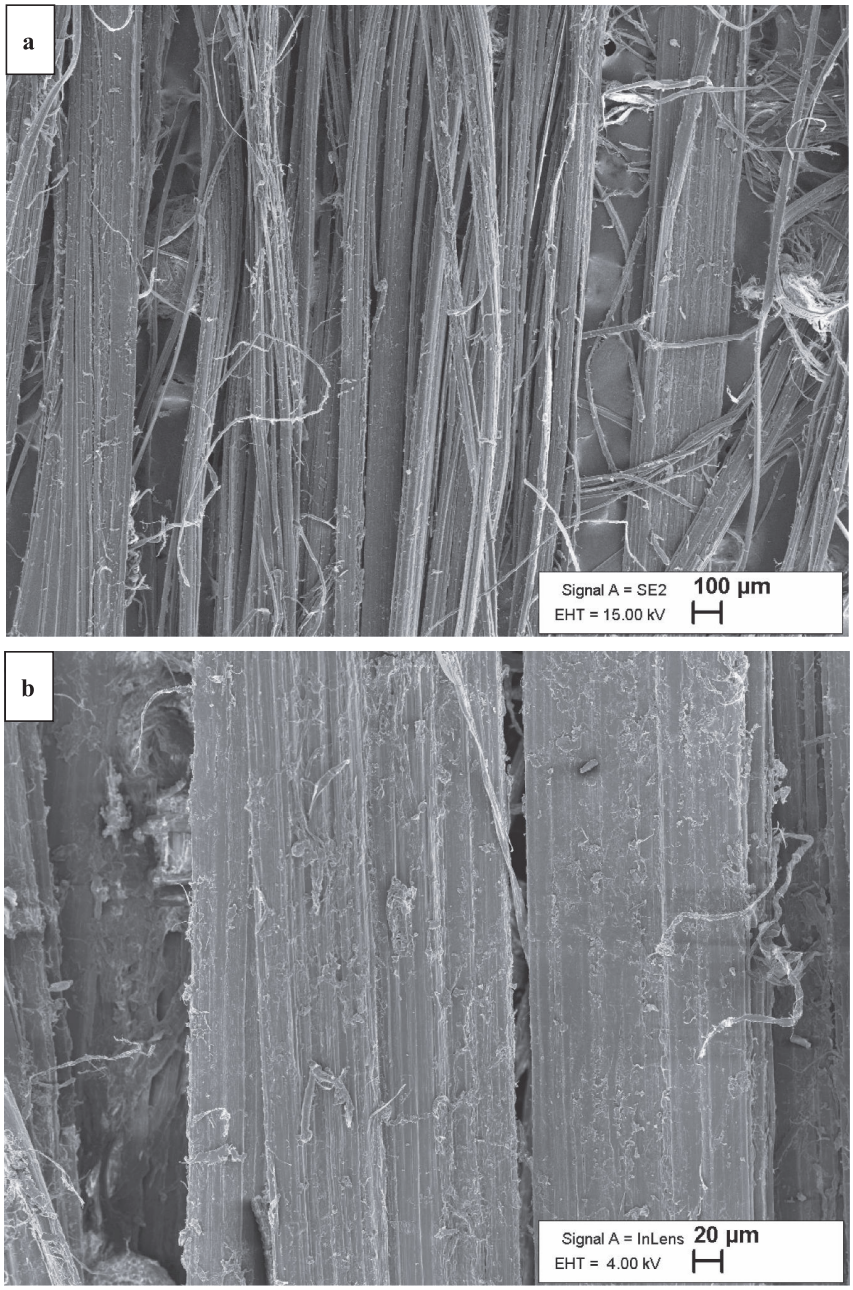

Figure 1. SEM observation of the frost retted hemp fibers: a) Presence of large bundles of fibers mixed with single fibers b) Cortical residues on the hemp fibers surface.

fibers, strands are heterogeneous materials where several types of damages occur during breakage, which explains why apparent modulus and strength at break are not strongly correlated.

The average tensile properties of the two materials are presented in Table 2.

Regarding unitary fibers, in spite of their high cellulose content observed during the chemical composition analysis in the section 5.1, the average value for apparent modulus (16.6 ± 8.5 GPa) is in the lower range of the data from the literature (14.4–51 GPa (Bourmaud et al. 2018; Gregoire et al.

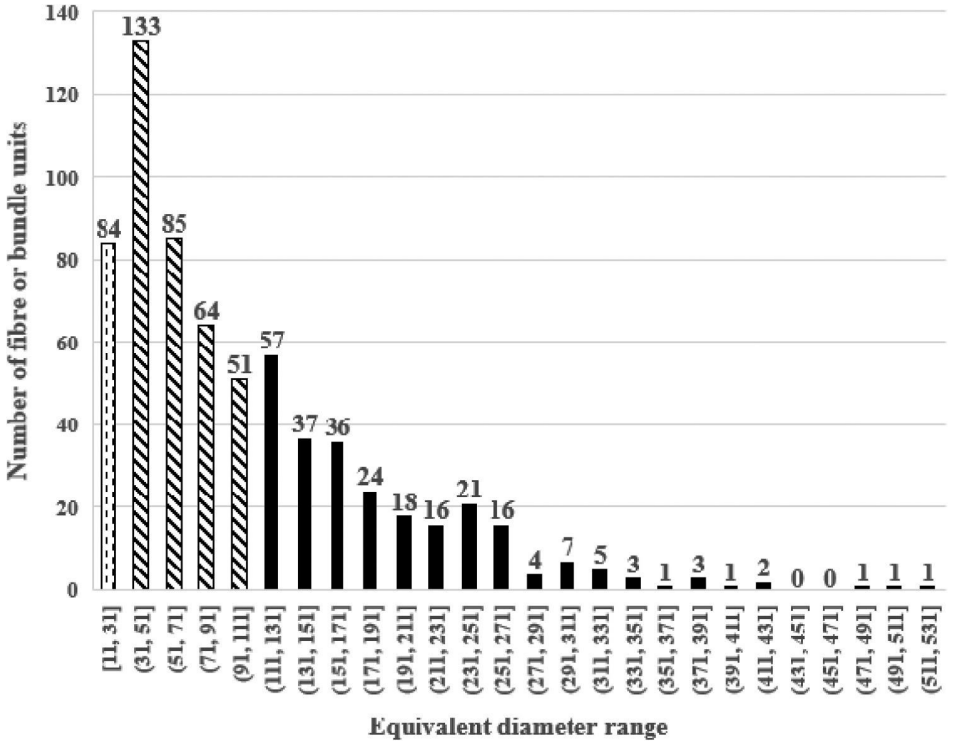

Figure 2. Number of fiber or bundle units per equivalent diameter range.

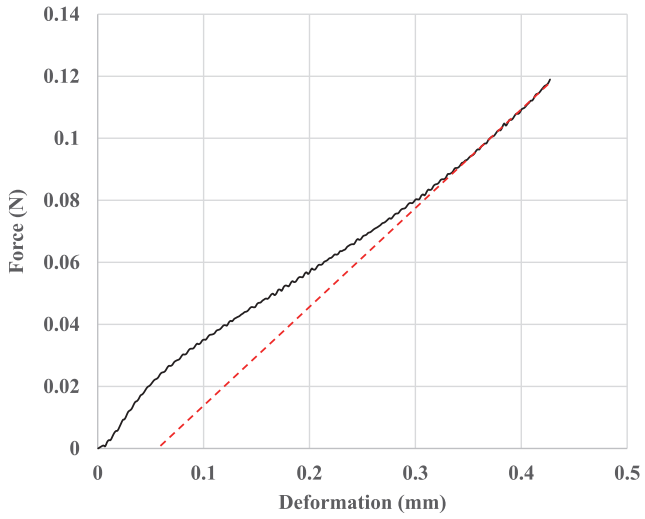

Figure 3. Force-deformation curves of a single fiber.

2019)), and the average value for the strength (500 ± 239 MPa) is in the middle range of the data available in the literature (285–969 MPa) (Bourmaud et al. 2018). The relatively low mechanical properties might be related to the low lignin content measured in our fibers from the Tisza variety compared to the values usually reported for Western European hemp varieties. Indeed, Liu et al (Liu

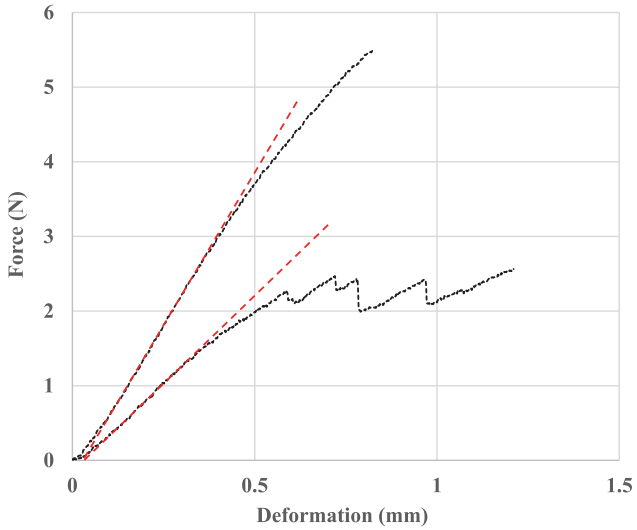

Figure 4. Force-deformation curves of strands under tension.

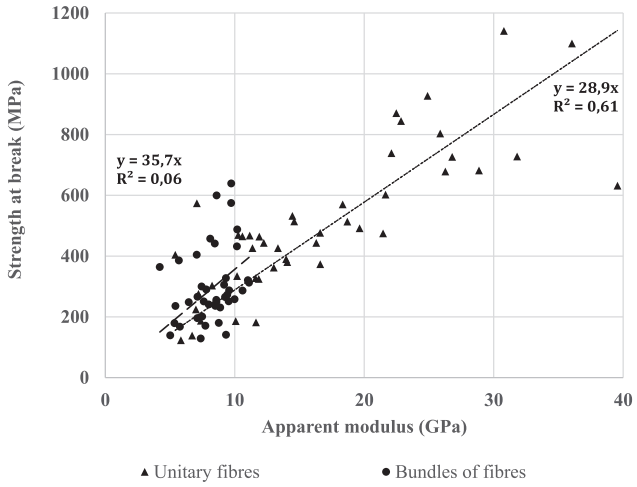

Figure 5. Tensile properties of frost retted hemp unitary fibers and strands.

Table 2. Average tensile properties of unitary fibers and strands of frost-retted hemp fibers.

Material	Number	Diameter (µm)	Modulus (GPa)	Strength (MPa)	Strain at break (%)
Unitary fibers	45	18 ± 5	16.6 ± 8.5	500 ± 239	2.9 ± 1.0
Strands	41	190 ± 64	8.2 ± 1.7	298 ± 123	1.9 ± 0.9

et al. 2017) showed the important role of lignin polymerization in the increase of the mechanical properties of their fibers.

The tensile test of the strands results in lower mechanical properties than the ones measured on unitary fibers: average apparent modulus is 8.2 ± 1.7 GPa and average tensile strength is 298 ± 123 MPa. Different composition and size of the tested materials might have contributed to this result. First, the length of a unitary fiber was found to be around 15 mm during their extraction from the strands prior to the tensile test. The gauge length for the tensile test is taken at 10 mm, i.e. shorter than the

length of a unitary fiber so there likely is only one unitary fiber tested between the clamps. Since the gauge length is fixed at 50 mm for the strands (so roughly 3 times the unitary fiber length) and the average diameter of the strands is found to be slightly higher than 10 times the average diameter of the unitary fibers (see Table 2), a strand gathers at least 300 unitary fibers. The middle lamella, pectin interphase between unitary fibers, is a critical area where failure may happen under tension load (Bos, Van Den Oever, and Peters 2002). The strands tensile properties are then dictated by both unitary fibers and middle lamella resistances. The contribution of the middle lamella in the flax bundle strength has previously been highlighted by Charlet et Beakou (Karine Charlet and Béakou 2011); the authors observed a decrease of the tensile strength while increasing the sample gauge length above the length of the elementary fibers. In this study, we fixed the gauge length at 50 mm to ensure a homogeneity of the fineness along the length of the strand. Nevertheless, for longer gauge lengths, the strength at break would likely decrease, as depicted in the literature (Romhány, Karger-Kocsis, and Czigány 2003), for the reasons described above. Réquilé et al (Réquilé et al. 2018) measured the tensile mechanical properties of hemp fiber-rich outer-tissues including epidermis, fiber bundles, and phloem. With the same gauge length of 50 mm and despite the presence of epidermis and cortical parenchyma in addition to the bundles, the authors (Réquilé et al. 2018) obtained performances in the same range as the ones presented in this study (10.27 ± 1.83 GPa for the apparent modulus and 172.4 ± 76.7 MPa for the tensile strength of dew-retted hemp fiber-rich outer tissues).

Moreover, due to averaging effect of the important number of fibers within a strand, the standard deviation is lower in the case of strands compared with unitary fibers. The dispersion is particularly reduced for the apparent modulus (20% for strands and 51% for unitary fibers, respectively) and, to a lower extent, for the tensile strength (41% and 47%, respectively). The dispersion is clearly visible on the curves of apparent modulus (Figure 6) and tensile strength at break (Figure 7) plotted versus the equivalent diameter of the fibrous unit (unitary fibers and strands together). Both variables decrease when the equivalent diameter increase. For unitary fibers, the decrease of tensile strength at break with increasing diameter is due to the increasing probability of having a flaw in the fiber. This phenomena was first highlighted by Griffith in the frame of the rupture mechanics of fragile materials (Griffith and Taylor 1921) and the weakest link model describes statistically the higher chances of finding a critical flaw when increasing the diameter of the fiber. The decrease of apparent modulus with the diameter of the unitary fibers is attributed to an overestimation of effective cross-section due to the presence of the lumen (void) in the fiber which is not considered. At the bundle

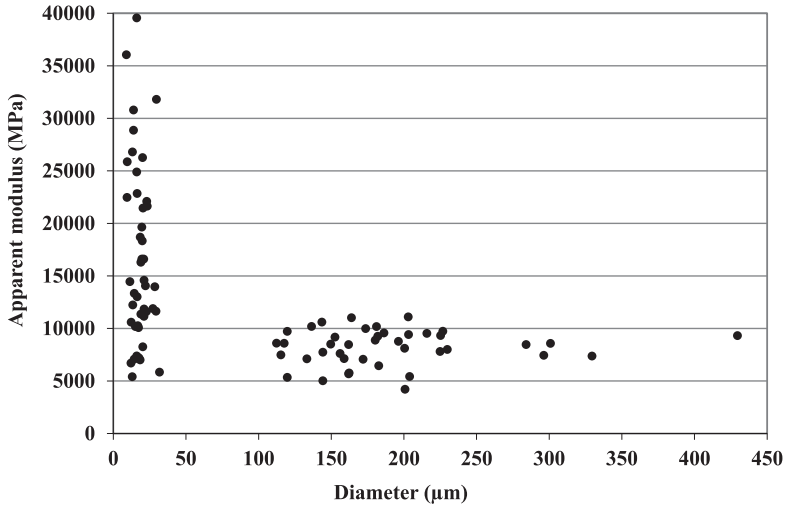

Figure 6. Apparent modulus depending on the diameter of the fibrous unit (unitary fiber or strand).

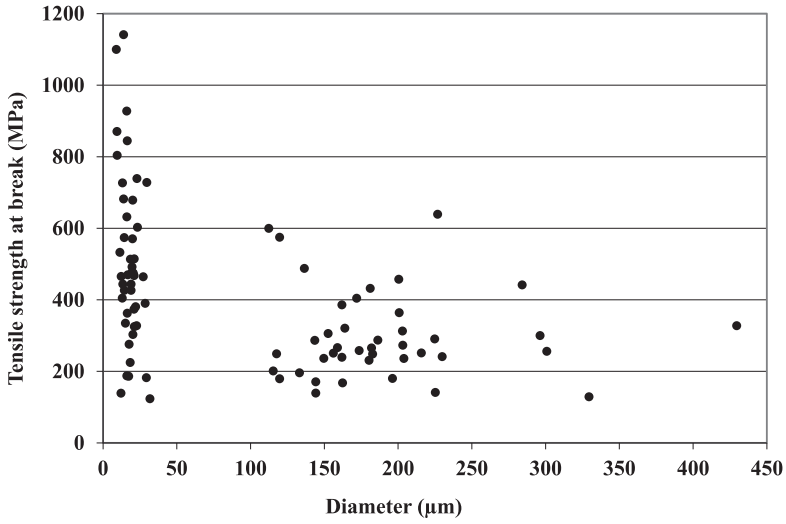

Figure 7. Tensile strength at break depending on the diameter of the fibrous unit (unitary fiber or strand).

scale, the decrease of both variables with diameter is due to the combined types of damages occurring during breakage, as described above.

Properties of aligned hemp/PLA composites

Under a unidirectional tensile load, an optimum reinforcement is achieved when the fibers are perfectly aligned, individualized (Coroller et al. 2013; Marrot et al. 2014), and homogeneously distributed in the matrix. In this study, the average misalignment of the fibers regarding the load direction was estimated at 25° by image analysis. Additionally, we detailed the level of hemp fibers individualization in section 2. We observed that the fibrous reinforcement is mainly constituted of small and large bundles of fibers (99.5% of the total surface area of the fibers cross-section), and we highlighted in section 5.3 the different performances at the unitary fiber scale and the strands scale and provided average mechanical properties for both types of reinforcement. Under these conditions, the mechanical properties of hemp/PLA composites with 30 and 50 wt% of hemp fibers were investigated by tensile tests. Table 3 gathers the experimental average tensile mechanical properties measured for the hemp/PLA composites. The Young modulus of the composites with 30 wt% and 50 wt% is, respectively, 79 and 149% higher than the modulus of the unreinforced PLA (2.7 GPa). This significant increase can be attributed to the higher modulus of the fibers compared to PLA and shows that the Young modulus of the composites is mainly governed by the fiber content and less dependent on the fiber/matrix interface. The strength at break of the composites was increased by 12% with 30 wt% fibers but decreased by 40% with 50 wt% fibers (strength at break of the unreinforced PLA was found to be 46 MPa). In the first case, with 30 wt% reinforcement, the standard deviation is quite high (18%) suggesting poor uniformity of fiber distribution throughout the composite and fiber agglomeration. In the case of 50 wt% fibers, the standard deviation is smaller (9%), and the decrease in strength can be attributed to insufficient wetting of the fibers by the matrix and limited load transfer between the fibers

Table 3. Average tensile mechanical properties of hemp/PLA composites with 30 and 50% of hemp fibers by weight.

M_f (%wt)	V_f (%vol)	ρ_c (g/cm^3)	V_p (%)	ε_c (%)	$\sigma_{c,exp}$ (MPa)	$E_{c,exp}$ (GPa)
30	28	1.26	7	2.2 ± 0.5	51 ± 9	4.8 ± 0.3
50	48	1.04	17	2.6 ± 0.5	27 ± 3	6.7 ± 0.6

and matrix. The high amount of impurities highlighted by the microscopical observations and confirmed by the level of insolubles by chemical analysis prevents a good adhesion between fibers and matrix and is a weak point in the interface. The void fraction is estimated at 7% in the case of the composite reinforced by 30 wt% of hemp fibers and at 17% for the composites reinforced by 50 wt% of hemp fibers. The high void fraction observed at 50 wt% is due to the difficult wetting of the fibers during manufacturing. Poor wetting in non-woven hemp/PLA composites has been reported by Pickering et Aruan Efendy (Pickering and Aruan Efendy 2016) for fiber fraction higher than 30 wt %. It is commonly observed in the literature that the higher the volume fraction of fibers in composites, the higher the fraction of porosities, leading to an inherent reduction in mechanical properties (Madsen, Hoffmeyer, and Lilholt 2007). A way of improving the wetting of the fibers is to reduce the viscosity of the matrix during processing (Pickering and Aruan Efendy 2016). Following the analysis of the composite performances, the authors recommend to improve stress transfer in several ways: 1) avoiding agglomeration of fibers by using fibrous reinforcement that is more individualized, 2) limiting the creation of voids during the manufacturing process by improving the wetting of the fibers and using matrix with adequate viscosity, 3) improving the fiber/matrix adhesion by cleaning the fiber surface to limit the presence of impurities.

Conclusions

The mechanical properties of frost-retted hemp fibers were investigated to assess their suitability for composite applications. Chemical analysis of frost-retted hemp fibers highlighted a high amount of solubles (pectins) at the fibers surface and a low lignin content in the fibers that was attributed to an unfavorable synthesis of lignin in the cell wall due to the particularly cold temperature at this stage of hemp growth in Estonia. Tensile properties measured at two different scales showed values in the lower range of data available in the literature for unitary fibers and values comparable to the literature at the strands scale, and displaying a reduced standard deviation in the case of strands compared with unitary fibers. Hemp/PLA composites were manufactured by thermocompression with 30 and 50 wt% of fibers. Compared to the unreinforced matrix performances, composites' Young moduli were significantly improved by the addition of fibers. However, composites manufactured with 50 wt% of fibers displayed a high level of porosities that greatly impacted their tensile strength. In order to use frost-retted hemp fibers for composite applications, the authors recommend to preprocess the fibers to achieve a better individualization and clean their surface. For non-structural applications, using frost-retted hemp fibers for the reinforcement of thermoplastic composites is a good way to value this by-product of the Nordic hemp industry.

Acknowledgments

This work was supported by the Horizon 2020 Framework Program of the European Union; H2020 WIDESPREAD-2-Teaming [grant number 739574] and investment from the Republic of Slovenia and the European Regional Development Fund.

ORCID

Laetitia Marrot http://orcid.org/0000-0002-4244-2726
Percy Festus Alao http://orcid.org/0000-0002-9720-7037

Declaration of interest statement

The authors declare that they have no known competing financial interests or personal relationships that could have appeared to influence the work reported in this paper.

References

Angelini, L. G., S. Tavarini, and M. Di Candilo. 2016. Performance of new and traditional fiber hemp (Cannabis sativa L.) cultivars for novel applications: Stem, bark, and core yield and chemical composition. *Journal of Natural Fibers* 13 (2):238–52. doi:10.1080/15440478.2015.1029193.

Baley, C.. 2002. Analysis of the flax fibres tensile behaviour and analysis of the tensile stiffness increase. *Composites. Part A, Applied Science and Manufacturing* 33 (7):939–48. doi:10.1016/S1359-835X(02)00040-4.

Barbulée, A., and M. Gomina. 2017. Variability of the mechanical properties among flax fiber bundles and strands. *Procedia Engineering* 200:487–93. doi:10.1016/j.proeng.2017.07.068.

Barbulée, A., J.-P. Jernot, J. Bréard, and M. Gomina. 2014. Damage to flax fibre slivers under monotonic uniaxial tensile loading. *Composites. Part A, Applied Science and Manufacturing* 64:107–14. doi:10.1016/j.compositesa.2014.04.024.

Bos, H. L., M. J. A. Van Den Oever, and O. C. J. J. Peters. 2002. Tensile and compressive properties of flax fibers for natural fiber reinforced composites. *Journal of Materials Science* 37 (8):1683–92. doi:10.1023/A:1014925621252.

Bourmaud, A., J. Beaugrand, D. U. Shah, V. Placet, and C. Baley. 2018. Towards the design of high-performance plant fiber composites. *Progress in Materials Science* 97:347–408.

Bourmaud, A., J. Merotte, D. Siniscalco, M. Le Gall, V. Gager, A. Le Duigou, F. Pierre, Behlouli, K., Arnould, O., Beaugrand, J. et al.. 2019. Main criteria of sustainable natural fiber for efficient unidirectional biocomposites. *Composites. Part A, Applied Science and Manufacturing* 124:105504.

Charlet, K., and A. Béakou. 2011. Mechanical properties of interfaces within a flax bundle – part I: Experimental analysis. *International Journal of Adhesion and Adhesives* 31 (8):875–81.

Coroller, G., A. Lefeuvre, A. Le Duigou, A. Bourmaud, G. Ausias, T. Gaudry, and C. Baley. 2013. Effect of flax fibers individualisation on tensile failure of flax/epoxy unidirectional composite. *Composites. Part A, Applied Science and Manufacturing* 51:62–70.

Crônier, D., B. Monties, and B. Chabbert. 2005. Structure and chemical composition of bast fibers isolated from developing hemp stem. *Journal of Agricultural and Food Chemistry* 53 (21):8279–89.

Gindl, W., M. Grabner, and R. Wimmer. 2000. The influence of temperature on latewood lignin content in treeline norway spruce compared with maximum density and ring width. *Trees* 14 (7):409–14.

Gregoire, M., E. De Luycker, M. Bar, S. Musio, S. Amaducci, and P. Ouagne. 2019. Study of solutions to optimize the extraction of hemp fibers for composite materials. *SN Applied Sciences* 1 (10):1293.

Griffith, A. A., and G. I. Taylor. 1921. VI. the phenomena of rupture and flow in solids. *Philosophical Transactions of the Royal Society of London. Series A, Containing Papers of a Mathematical or Physical Character* 221 (582–593):163–98.

Hall, J., S. P. Bhattarai, and D. J. Midmore. 2014. The effects of photoperiod on phenological development and yields of industrial hemp. *Journal of Natural Fibers* 11:87–106.

Horne, M. R. L. 2020. Bast fibres: Hemp cultivation and production. In *Handbook of Natural Fibres*, ed. R. M. Kozłowski and M. Mackiewicz – Talarczyk, Vol. 1, 2nd ed ed., 163–96. Cambridge, MA: Elsevier.

Lefeuvre, A., A. Bourmaud, C. Morvan, and C. Baley. 2014. Elementary flax fiber tensile properties: Correlation between stress–strain behaviour and fiber composition. *Industrial Crops and Products* 52:762–69.

Liu, M., A. Baum, J. Odermatt, J. Berger, L. Yu, B. Zeuner, A. Thygesen, J. Holck, and A. S. Meyer. 2017. Oxidation of lignin in hemp fibers by laccase: effects on mechanical properties of hemp fibers and unidirectional fiber/epoxy composites. *Composites. Part A, Applied Science and Manufacturing* 95:377–87.

Liu, M., D. Fernando, G. Daniel, B. Madsen, A. S. Meyer, M. T. Ale, and A. Thygesen. 2015. Effect of harvest time and field retting duration on the chemical composition, morphology and mechanical properties of hemp fibers. *Industrial Crops and Products* 69:29–39.

Madsen, B., P. Hoffmeyer, and H. Lilholt. 2007. Hemp yarn reinforced composites – II. Tensile properties. *Composites. Part A, Applied Science and Manufacturing* 38 (10):2204–15.

Marrot, L., A. Bourmaud, P. Bono, and C. Baley. 2014. Multi-scale study of the adhesion between flax fibers and biobased thermoset matrices. *Materials & Design (1980-2015)* 62:47–56.

Marrot, L., A. Lefeuvre, B. Pontoire, A. Bourmaud, and C. Baley. 2013. Analysis of the hemp fiber mechanical properties and their scattering (Fedora 17). *Industrial Crops and Products* 51:317–27.

Müssig, J., S. Amaducci, A. Bourmaud, J. Beaugrand, and D. U. Shah. 2020. Transdisciplinary top-down review of hemp fiber composites: From an advanced product design to crop variety selection. *Composites Part C: Open Access* 2:100010.

Pasila, A. 2000. The Effect of Frost on Fiber Plants and Their Processing. *Molecular Crystals and Liquid Crystals Science and Technology. Section A. Molecular Crystals and Liquid Crystals* 353 (1):11–22.

Pickering, K. L., and M. G. Aruan Efendy. 2016. Preparation and mechanical properties of novel bio-composite made of dynamically sheet formed discontinuous harakeke and hemp fiber mat reinforced PLA composites for structural applications. *Industrial Crops and Products* 84:139–50.

Ranalli, P., and G. Venturi. 2004. Hemp as a raw material for industrial applications. *Euphytica* 140 (1):1–6.

Réquilé, S., A. Le Duigou, A. Bourmaud, and C. Baley. 2018. Peeling experiments for hemp retting characterization targeting biocomposites. *Industrial Crops and Products* 123:573–80.

Romhány, G., J. Karger-Kocsis, and T. Czigány. 2003. Tensile fracture and failure behavior of technical flax fibers. *Journal of Applied Polymer Science* 90 (13):3638–45.

Appendix 2

Publication II

Alao, P.F.; Marrot, L.; Burnard, M.D.; Lavrič, G.; Saarna, M.; Kers, J. Impact of Alkali and Silane Treatment on Hemp/PLA Composites' Performance: From Micro to Macro Scale. Polymers 2021, 13, 851.

polymers

MDPI

Article

Impact of Alkali and Silane Treatment on Hemp/PLA Composites' Performance: From Micro to Macro Scale

Percy Festus Alao [1,*], Laetitia Marrot [2,3], Michael David Burnard [2,3], Gregor Lavrič [4], Mart Saarna [5] and Jaan Kers [1]

1 Department of Material and Environmental Technology, Tallinn University of Technology, Ehitajate tee 5, 19086 Tallinn, Estonia; jaan.kers@taltech.ee
2 InnoRenew CoE, Livade 6, 6310 Izola, Slovenia; laetitia.marrot@innorenew.eu (L.M.); mike.burnard@innorenew.eu (M.D.B.)
3 Andrej Marušič Institute, University of Primorska, Muzejski trg 2, 6000 Koper, Slovenia
4 Pulp and Paper Institute, Bogišićeva 8, 1000 Ljubljana, Slovenia; gregor.lavric@icp-lj.si
5 Department of Mechanical and Industrial Engineering, Tallinn University of Technology, Ehitajate tee 5, 19086 Tallinn, Estonia; mart.saarna@taltech.ee
* Correspondence: percy.alao@taltech.ee

Abstract: This study investigated the effect of hemp fiber pretreatments (water and sodium hydroxide) combined with silane treatment, first on the fiber properties (microscale) and then on polylactide (PLA) composite properties (macroscale). At the microscale, Fourier transform infrared, thermogravimetric analysis, and scanning electron microscopy investigations highlighted structural alterations in the fibers, with the removal of targeted components and rearrangement in the cell wall. These structural changes influenced unitary fiber properties. At the macroscale, both pretreatments increased the composites' tensile properties, despite their negative impact on fiber performance. Additionally, silane treatment improved composite performance thanks to higher performance of the fibers themselves and improved fiber compatibility with the PLA matrix brought on by the silane couplings. PLA composites reinforced by 30 wt.% alkali and silane treated hemp fibers exhibited the highest tensile strength (62 MPa), flexural strength (113 MPa), and Young's modulus (7.6 GPa). Overall, the paper demonstrates the applicability of locally grown, frost-retted hemp fibers for the development of bio-based composites with low density (1.13 to 1.23 g cm^{-3}).

Keywords: hemp fibers; polylactic acid; biocomposite materials; mechanical properties; surface treatments

Citation: Alao, P.F.; Marrot, L.; Burnard, M.D.; Lavrič, G.; Saarna, M.; Kers, J. Impact of Alkali and Silane Treatment on Hemp/PLA Composites' Performance: From Micro to Macro Scale. *Polymers* **2021**, *13*, 851. https://doi.org/10.3390/polym13060851

Academic Editor: Ralf Schledjewski

Received: 18 February 2021
Accepted: 5 March 2021
Published: 10 March 2021

1. Introduction

The development of structural plant fiber composite components started about 80 years ago [1] and there is considerable interest in them nowadays because of the growing environmental and ecological pressures facing industries. Characteristics and properties of biocomposites have evolved, but improvements are still needed for the effective and durable use of plant fiber reinforcement of composites. While flax has been extensively studied in this aim [1], hemp fibers also show interesting specific properties for the reinforcement of composites [2]. The rougher surface of hemp fibers compared with flax fibers could positively influence the fiber/matrix adhesion [3]. Moreover, an increase in fiber surface roughness was found to facilitate the capillary flow in fibrous porous media, which suggests a smooth composite production process [4]. Adhesion between natural fibers and thermoplastic matrices is always questioned due to the hydrophilic character of natural fibers, which induces a decrease in the interfacial contact between the natural fiber and the matrix polymer, leads to dimensional changes and lower mechanical performance from possible moisture uptake in the composite and provides favorable conditions for the development of microorganisms. In the literature, various treatments have been

investigated to improve adhesion between natural fibers and matrices, either by cleaning impurities from the surface of the fibers or by creating chemical bonding between the two components with coupling agent agents [5]. Bourmaud et al. [6] used a soft water treatment to clean flax fibers. Alkali treatments are used to remove hemicelluloses from natural fibers and can also partially remove other non-cellulosic components like lignin and pectin [7]. The removal of hemicellulose and lignin cover materials exposes more cellulose hydroxyl groups to alkali, which reduces the hydrophilic nature of natural fibers by replacing cellulose hydroxyl groups with less hydrophilic O−Na^+ groups (Fiber-H + NaOH-> Fiber-O^- Na^+ + H_2O) and improves adhesion between fibers and matrix binders [5]. Silane coupling agents are used to improve the wettability of fibers by matrix polymers through graft copolymerization. Stable covalent bonds are eventually formed between alkoxy silanes and hydroxyl groups on the fiber surface [5,8].

Fiber treatments are often conducted to improve matrix adhesion within a composite, but they may degrade the fibers' mechanical performance at the same time [9]. As highlighted by Liu et al. [5], the effect of treatment on the mechanical properties of the fibers and resulting composites should be understood to provide effective and profitable treatments. Moreover, Merotte et al. [3] showed that the improvement of interfacial shear strength brought on by a coupling agent (MAPP vs. PP) had much less influence on the mechanical properties of the composite than the nature of the fibers (flax or hemp) and their individualization. With low interfacial shear strength systems, such as plant fibers associated with polyolefin matrices like polypropylene, polyethylene, or polylactic acid (PLA), macroscale mechanical properties are governed by the fibers' mechanical properties and bonding area rather than by interfacial bond strength [3]. A composite's properties depend on multiple fiber parameters (mechanical performance, content, aspect ratio, orientation, individualization and dispersion [10], adhesion with matrix [11], and porosities), so it is difficult to unquestionably attribute an improvement or diminution of the composite mechanical properties to fiber treatment.

This study investigates step by step the effect of different surface pretreatments (water and sodium hydroxide) combined with a silane treatment of an Estonian cultivated and frost retted hemp fiber, first on the single fiber microscale properties and then on the macroscale mechanical performance of their composites with a PLA matrix. This work aims to:

i. Show an accurate inference of the fiber pretreatments and treatment on the composite's mechanical performance by linking the effects reported at the microscale, specifically the impact of the treatments on the fibers' tensile properties, to their overall impact at the macroscale. The dual scales of observation bring a complementarity to the analysis, which is not often reported in the literature. Fiber composition, tensile mechanical properties, individualization, and dispersion are thoroughly studied, while the fiber content, aspect ratio, and orientation are carefully maintained as equivalent for all the composite formulations.
ii. Provide first-hand information on the suitability of Estonian hemp fibers for composite reinforcement. Indeed, these fibers are a by-product of cannabidiol production for medicinal applications and are currently considered as a waste. PLA is selected for its renewable and compostable properties, along with its comparable performance to common petrochemically derived alternatives [12]. Figure 1 presents a schematic of the main idea and procedure of this study.

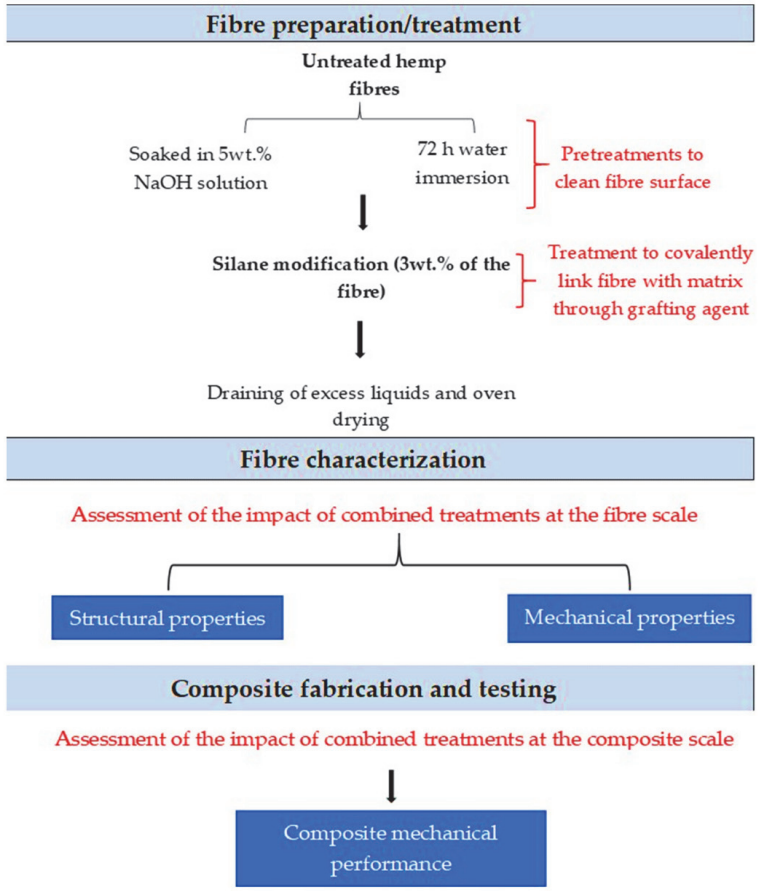

Figure 1. Schematic description of the current research aim and procedure.

2. Materials and Methods

2.1. Materials

Hemp fibers (Cannabis sativa, Tisza, Hungary) grown in Saaremaa, Estonia were used. Their properties have been characterized and described in previous work [13]. The stems were industrially decorticated by a mechanical process. PLA fibers (IngeoTM 4043D) from NatureWorks (Minnetonka, MN, USA) were used for the research. The polymer was 60 mm long, with a round cross-section, a finesse of 6.7 dtex and a density of 1.24 g cm^{-3}.

2.2. Fiber Surface Treatments

2.2.1. Water Treatment

Fibers were dried in an oven at 80 °C until constant weight to remove excess moisture and then washed by soaking in distilled water for 72 h at 23 °C according to Bourmaud et al. [6].

2.2.2. Alkali Treatment

Hemp fibers were treated with a solution of 5 wt.% sodium hydroxide (NaOH). (Sigma-Aldrich, Saint Louis, MO, USA) Sodium (Na) granules were used in preparing the NaOH solution. Hemp fibers were soaked in the solution at room temperature (23 °C) for 4 h. Fibers were then washed in tap water to remove residual alkali by measuring the wastewater's pH until it was about 7. Finally, the fibers were oven-dried at 80 °C until constant weight.

2.2.3. Silane Treatment

Hemp fibers were treated with an ethanol and water solution containing 3 wt.% silane coupling agent (3-Aminopropyl-triethoxy silane) whose structure is presented in Figure 2. The amount of silane was relative to the weight of hemp fibers. Silane was previously pre-hydrolyzed at room temperature for 2 h in an 80/20 vol % solution of ethanol/water. The pH of the solution was adjusted to 5 using acetic acid. Hemp fibers were soaked in the solution at room temperature for 2 h. Then, the hemp fibers were filtered and oven-dried at 80 °C until constant weight.

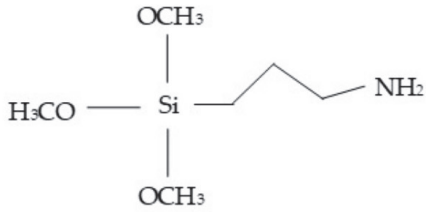

Figure 2. Structure of 3-Aminopropyl-triethoxy silane.

2.3. Fabrication of the Hemp Reinforced PLA (HPLA) Composites

Untreated (U_f) and treated (distilled water (W_f), water + silane (WS_f), alkali (A_f) and alkali + silane (AS_f)) fibers were combined with PLA by compression moulding. Two composite types were produced from 30 wt.% (160.5 g of hemp fibers) + PLA and 50 wt.% (267.5 g of hemp fibers) + PLA in a metal frame (450 mm × 450 mm × 2 mm) using a hot press. Hemp and PLA fibers were mixed using a wide classic drum carder (300 mm batt width, 72 teeth per inch (tpi) and 100 g capacity). The mixture was dried in an oven for 4 h at 80 °C before compression at 180 °C and 3 MPa for 10 min. Neat PLA boards were also fabricated as a control. Abbreviations and descriptions for the composite boards are presented in Table 1.

Table 1. Nomenclature used for polylactic acid (PLA), untreated and treated hemp fiber reinforced polylactide composites.

Abbreviation	Samples
Neat PLA	Unreinforced polylactic acid boards from 100% PLA fibers.
UH	Untreated hemp fiber (U_f) reinforced polylactide composites.
WH	Water-treated hemp fiber (W_f) reinforced polylactide composites.
WSH	Combined water- and silane- (WS_f) treated hemp fiber reinforced polylactide composites.
AH	Alkali-treated hemp fiber (A_f) reinforced polylactide composites.
ASH	Combined alkali- and silane- (AS_f) treated hemp fiber reinforced polylactide composites.

2.4. Characterization of Hemp Fibers and HPLA Composites

2.4.1. Chemical Composition by Fourier Transform Infrared (FTIR)

The spectroscopy was carried out to qualitatively identify the constituents of untreated and chemically treated hemp fibers and assess the effects of the treatments on the composition. Measurements were performed on a Nicolet™ iS50 FTIR Spectrometer (Thermo Fisher Scientific, Waltham, MA, USA) with ATR module from Thermo Scientific™. The fiber batches were conditioned in the spectrometer room for two weeks before analysis to ensure stable moisture content (MC). Analysis was performed on the fibers (not grounded) to preserve the internal organization of components. Bundles of hemp fibers were twisted by hand and placed on the ATR crystal. All FTIR spectra were collected with a spectrum resolution of 4 cm^{-1}. A background scan of clean Zn–Se diamond crystal was processed before the sample scanning procedures. Ten replicates were tested for each batch with 22 scans per sample.

2.4.2. Chemical Composition by Thermogravimetric Analysis (TGA)

Thermogravimetric analysis was performed on untreated and treated hemp fibers. The experiments were carried out using a NETZSCH STA 449F3 (NETZSCH-Gerätebau GmbH, Wittelsbacherstraße, Germany) in a nitrogen atmosphere (20 mL per min). For each sample (approximately 6 mg), three measurements were performed, beginning with an isothermal segment at 40 °C for 1 min, followed by dynamic heating from 40 °C to 600 °C at the rate of 2 °C min^{-1}. Samples were held in an aluminum pan (Al_2O_3). Specimens were kept in the testing room at a relative humidity of 43 ± 10% and a temperature of 22 ± 1 °C for one week before the test.

2.4.3. Microscopical Observations by Scanning Electron Microscopy (SEM)

SEM images of the fibers and composites were observed using a Zeiss Ultra 55 (FELMI-ZFE, Steyrergasse, Austria) at 20 kV, depth of 100nm and resolution of 50,000. For this observation, samples were carbon glued on an aluminum stub and then coated with an alloy of 2 nm thick gold (Au)/palladium (Pd) layer (80/20). For the composite samples, each specimen was mounted into Buehler EpoThin Epoxy glue before coating and observation.

2.5. Mechanical Properties of Unitary Hemp Fibers and Hemp/PLA Composites

Tensile tests were carried out on single hemp fibers for the five batches on a Zwick Roell Z010 (ZwickRoell GmbH & Co. KG, August-Nagel-Straße, Germany) tensile machine equipped with a 20 N measuring cell (Class 0.5, ISO 7500-1) at a speed of 1 mm per min. The gauge length was taken at 10 mm. For each batch, at least 50 fibers were tested. The mean diameter of each fiber was measured before testing (average of 3 points).

Tensile and flexural tests were performed on the composite samples in accordance with EVS-EN ISO 527 (Type 2) and EVS-EN ISO 14,125 (Class II) standard tests, respectively, using an Instron 8516 (Norwood, MS, USA) machine equipped with a load cell of 10 kN. The test was done at (43 ± 10)% RH, (22 ± 1) °C and test speed of 2 mm per min. Five (5) replicates per batch were used to evaluate the result, though four replicas were used for tensile strength of the UH composites due to sampling issues during testing. Specimen dimensions for the flexural test were 80 × 15 mm and thickness varied from 2–4 mm, while tensile test specimens had a dimension of 250 mm × 25 mm. An Extensometer L_o = 50 mm (model 2630-112, s/n 937) was attached to the test specimens to determine the elongation before failure. In addition, composite density was determined in accordance with EVS-EN ISO 1183-1 from five replicas, using a Mettler Toledo AX balance. Test pieces were 15 mm × 20 mm and conditioned following ISO 291.

2.6. Statistical Analysis

Statistical analysis and figures were done in R v4.0.2 (Vienna, Austria) [14] and RStudio v1.3.1073 (Boston, MA, USA) [15] using the tidyverse package [16] for data manipulation and plotting and the emmeans package [17] to compute and extract pairwise comparisons between treatments. The boot package was used to extract bootstrapped estimates and their bias-corrected accelerated (BCA) confidence intervals.

2.6.1. Statistical Analysis of Fiber Properties

Separate linear models were fit to each natural log-transformed response (Modulus, Strain and Strength) since the raw response data violated the equal variance assumption for a linear model. Models were fit with pretreatment-treatment interactions and pretreatment conditions only. Interaction models were fit without the raw pretreatment condition (degrees of freedom = 206) and resulted in conditional pairwise comparisons between treatment effects (silane or none) in each pretreatment condition (alkali, water). Pretreatment-only models excluded samples with treatments (degrees of freedom = 143) and resulted in pairwise comparisons between each of the pretreatment conditions (raw, water or alkali). Extracted pairwise comparisons between each treatment were back-transformed to the original response scale and reported as the ratio between medians of the

compared treatments. *p*-values for pretreatment comparisons were adjusted using Tukey's method for a family of 3 estimates. Significance level for all *p*-values was set to 0.05.

2.6.2. Statistical Analysis of Composite Tensile and Flexural Properties

Linear models were fit for each measured property (flexure strength, flexure modulus, tensile strength and tensile modulus). Both flexure (strength and modulus) and tensile modulus model had 7 and 42 degrees of freedom, while the tensile modulus had 7 and 41 degrees of freedom (due to some testing errors with a specimen). In each case, the response was log-transformed because the linear model's equal variance assumption was violated. Each model was fit to pretreatment and treatment main effects as well as interaction effects between the pretreatment/fiber loading and treatment/fiber loading. Due to sample sizes, linear models and resulting pairwise comparisons were bootstrapped and their BCA confidence intervals calculated. The resulting estimates were the ratios between medians of compared treatments at specified fiber loading levels (30% or 50%) on the original scale. Reported *p*-values were based on the model values (not the bootstrapped values) and adjusted for a family of 6 comparisons using Tukey's method. The significance level for all *p*-values was set to 0.05.

3. Results and Discussion

3.1. Chemical Composition by FTIR Analysis

For easier visualization, the average vertically shifted FTIR spectra are separated into two. Figure 3a displays the FTIR spectra for U_f, W_f, and A_f, while Figure 3b shows the spectra for U_f, WS_f, and AS_f. Qualitatively, U_f and W_f spectra appear similar; however, there is a higher absorbance in 3000–3600 cm^{-1} for W_f compared to U_f. The 3000–3600 cm^{-1} corresponds to OH stretching vibrations, an increase of which depicts more OH functionality and lower hydrophilic properties [18]. This implies that some non-cellulosic polysaccharide was removed from the fiber surface, as shown by Bourmaud et al. [6]. Conversely, the A_f spectrum presents peak absence/reduction at about 1735 cm^{-1} and 1235 cm^{-1}. The peak around 1735 cm^{-1} corresponds to C=O stretching vibration of conjugated carboxylic ester groups [19] of hemicellulose or wax [18], and the peak around 1235 cm^{-1} corresponds to C–O stretching of lignin acetyl groups [18,20]. Furthermore, the peak at 1635 cm^{-1} that shows C=O stretching in conjugated carbonyl of lignin or absorbed water is broader and attenuated [21]. Additionally, oscillations at 2918 cm^{-1} that correspond to C–H stretching in lignin's aromatic hydrocarbon, methoxyl, and methylene groups [9], as well as oscillations at 2850 cm^{-1} related to symmetric C–H stretching of non-aromatic compounds present in the cellulose and hemicellulose components [20], are also reduced. Higher absorbance with better peak definition from 3000–3600 cm^{-1} is achieved by alkali-treated fibers.

Ostensibly, it appears that the spectrum of WS_f and W_f is also similar, but Figure 4a clearly shows that the additional silane treatment induces a peak shift from 1635 cm^{-1} to 1624 cm^{-1} and attenuation at about 1539 cm^{-1}, 1369 cm^{-1}, and 1248 cm^{-1}. Similar peak shifts have been reported in past research after silane pretreatments of hemp fibers [9,18,21]. This suggests that the ensuing silane treatment led to the extraction of some hemicellulose, wax and lignin fiber contents. In Figure 4b, it was also discovered that the subsequent silane treatment causes higher peak intensity with new peaks that could be related to NH_2 bending vibrations in amino silane between 1500–1680 cm^{-1}, also reported by Panaitescu et al. [21]. We can infer from our results that the water treatment did not affect the lignin content of hemp fibers, but it slightly increased the functional OH due to the removal of some water-soluble polysaccharides. Alkali treatment was effective in extracting pectins, hemicellulose, and lignin content, and silane treatment showed slight removal of intercellular content, especially for water pretreated hemp fibers with some new peaks that could be due to silane molecule coatings on the fiber surface following water/alkali pretreatments.

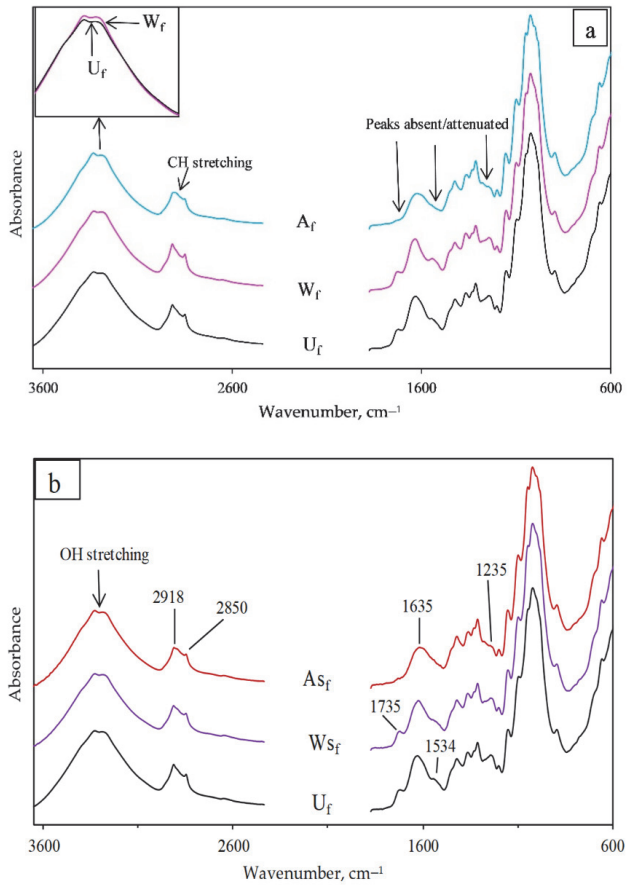

Figure 3. Vertically shifted FTIR spectra for (**a**) untreated (U_f), distilled water (W_f), and alkali-treated (A_f) hemp fibers; (**b**) U_f, water + silane (WS_f) and alkali + silane (AS_f) treated hemp fibers with the wavenumbers for differences observed.

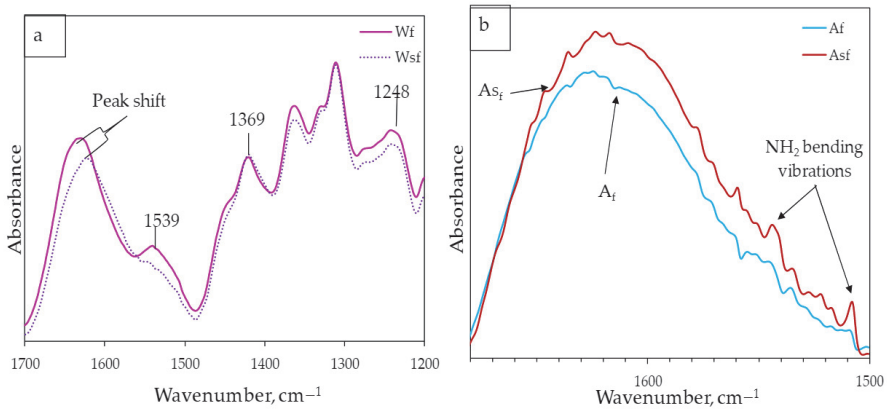

Figure 4. FTIR spectra for (**a**) degradation of a portion of lignin in WS_f; (**b**) silane coupling effect after treatment of alkali modified fibers.

3.2. Chemical Composition by Thermogravimetric Analysis (TGA)

TGA curves for all batches (Figure 5a) display two main weight losses, while for clarity, only the differential thermogravimetric analysis (dTGA) (Figure 5b) for untreated, water- and alkali-treated fibers is presented. In Figure 5a, the observed mass loss between 39–160 °C was attributed to the evaporation of water from the fibers. The estimated mass loss in this temperature range is shown in Table 2. A loss of approximately 1.4% was obtained for U_f compared to 0.3% for the batches of treated fibers. The lower moisture content observed for W_f and A_f compared to U_f is in accordance with the FTIR results for which pretreated fibers showed decreased hydrophilicity associated with the removal of non-cellulosic polysaccharides. Other studies [18,20] reported a similar decrease of mass loss in the 39–160 °C region for fibers that underwent alkali treatments.

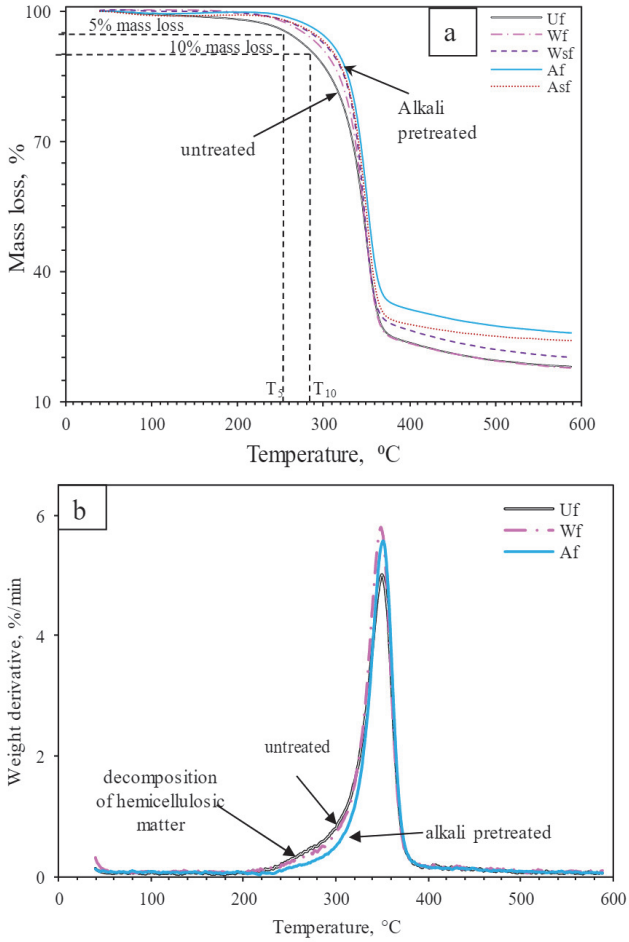

Figure 5. (**a**) TGA curves for U_f, W_f, WS_f, A_f, AS_f; (**b**) dTGA curve for U_f, W_f and A_f batches.

The second degradation appears between 160 and 600 °C with a peak of around 346 °C. Placet et al. [22] highlighted the superimposition of several degradations in this range of temperatures. The majority of hemicellulose matter degrades between 180 and 280 °C, while the remaining hemicelluloses and formed by-products decompose from 280 to 600 °C. However, cellulose decomposes roughly between 325 and 400 °C, and lignin decomposes between 150 and 450 °C. Here, the second degradation corresponds then to

the decomposition of amorphous polysaccharides (hemicelluloses and pectin) taking place between 180 and 280 °C, where a shoulder is visible on the dTGA curve, in addition to the decomposition of cellulose and lignin constituents and formed by-products. The remaining mass corresponds to the ash or non-polysaccharide contents [6]. The composition of the studied hemp fibers was investigated in previous work [13] and showed cellulose (77.4%), hemicellulose (8.3%), solubles (12.6%), and lignin (1.4%). To further investigate the fiber treatment's effectiveness, temperatures corresponding to a 5% weight loss (T_5) and a 10% weight loss (T_{10}) were considered (Table 2). It can be seen that after water and alkali pretreatment, the values shifted to higher temperatures (i.e., from 254 °C and 289 °C for U_f to 272 °C and 299 °C for W_f and 292 °C and 313 °C for A_f). This translates to the removal of hemicelluloses and pectins, which were included in the solubles content reported above.

Table 2. First TGA mass loss at 160 °C and temperatures corresponding to 5% and 10% weight loss for untreated and treated hemp fibers.

Sample	First Mass Loss (%) at 160 °C	T_5 (°C)	T_{10} (°C)
U_f	1.4	254	289
W_f	0.3	272	299
WS_f	0.3	278	305
A_f	0.3	292	313
AS_f	0.3	288	310

The reduced truncation of A_f dTGA curve (Figure 5b) compared to U_f also confirms the removal of hemicellulose matter [6], which corresponds to the FTIR observation. Likewise, Table 2 reveals an improvement in thermal stability for WS_f compared to W_f, which is mainly due to the effect of silane molecules coating the fiber surface [6]; though, there seems to also have been possible additional extraction of some non-cellulosic fiber components during silane treatment as indicated by the FTIR results. Such non-cellulosic components removal after silane treatment has also been highlighted by Panaitescu et al. [21], and a similar rise in thermal degradation temperatures was obtained for fibers treated with silane after washing in water by Dayo et al. [18]. The observed T_5 and T_{10} values for WS_f, A_f, and AS_f are comparable to values reported in the literature [18,20].

3.3. Scanning Electron Microscopical (SEM) Observations

Observation of the SEM images presented in Figure 6 shows a cleaner and clearer surface for the A_f- and AS_f-treated fibers. This cleaner appearance is associated with substantial removal of hemicellulose and lignin from the fiber surface [5,9,23,24]. However, compared to the untreated fibers, W_f does not appear to have removed non-cellulosic contents (most likely wax and lignin contents), while the fibers subsequently treated with silane (WS_f and AS_f) show a slightly smoother surface compared to those of W_f and A_f, respectively. This outcome could be due to the additional removal of pectin and hemicellulose by the ethanol/water mixture and the formation of a siloxane layer on the fiber surface due to condensation of the silane groups that are reported to be more visible with higher amounts of silane modification (5–20%) [8]. These generally agree with the FTIR and TGA analyses and show the differences in surface structure for the hemp fibers after treatments. SEM micrographs of the HPLA composites (Figure 7) visibly prove that the fiber treatments improved fiber distribution and individualization within the matrix in the highest order from ASH, AH, and WSH to WH and UH as a result of the non-cellulosic content removal, which has also been reported in past studies [25,26]. Commonly, all the composites show good fiber alignment.

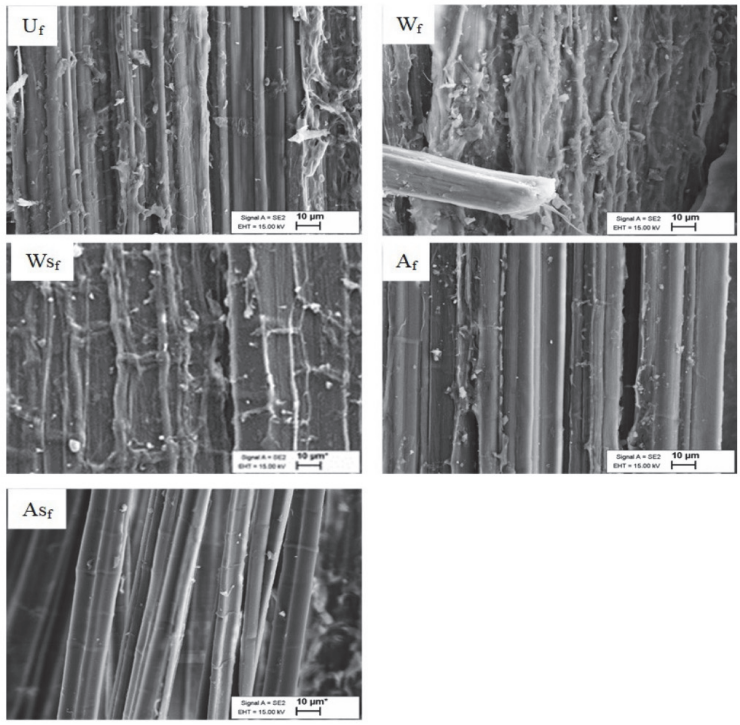

Figure 6. SEM images of (U_f) untreated, (W_f) water-treated, (WS_f) water + 3% silane-treated, (A_f) 5% alkali-treated, and (AS_f) 5% alkali + 3% silane-treated hemp fiber surfaces.

3.4. Mechanical Properties

3.4.1. Tensile Properties of the Hemp Fibers

Mechanical properties (modulus of elasticity (MoE), strength and strain) are presented in Figures 8–10, respectively. On the figures, the lower and upper hinges correspond to the first and third quartiles (the 25th and 75th percentiles). We see widely scattered values for all properties (Figures 8–10, Table 3), as is often reported in the literature for hemp and other plant fibers [2,26].

Table 3. Means and medians of tensile data for all combined treatments.

	Modulus (GPa)				Tensile Strength (MPa)				Strain%			
Combined	**Mean**	**SD ***	**Median**	**IQR ****	**Mean**	**SD**	**Median**	**IQR**	**Mean**	**SD**	**Median**	**IQR**
Raw	16.6	8.5	14.1	11.5	500	239	464	270	2.93	1.02	2.70	1.00
Water-Untreated	14.3	7.9	12.4	11.1	376	220	336	257	2.43	0.78	2.45	0.78
Alkali-Untreated	15.0	5.2	15.8	6.7	381	189	369	234	2.42	0.91	2.30	1.20
Water-Silane	17.2	8.3	15.1	12.0	490	210	459	236	2.71	1.16	2.60	1.25
Alkali-Silane	15.6	9.0	13.9	9.4	466	287	390	295	2.81	0.89	2.80	1.25

* SD = Standard Deviation; ** IQR = Interquartile Range.

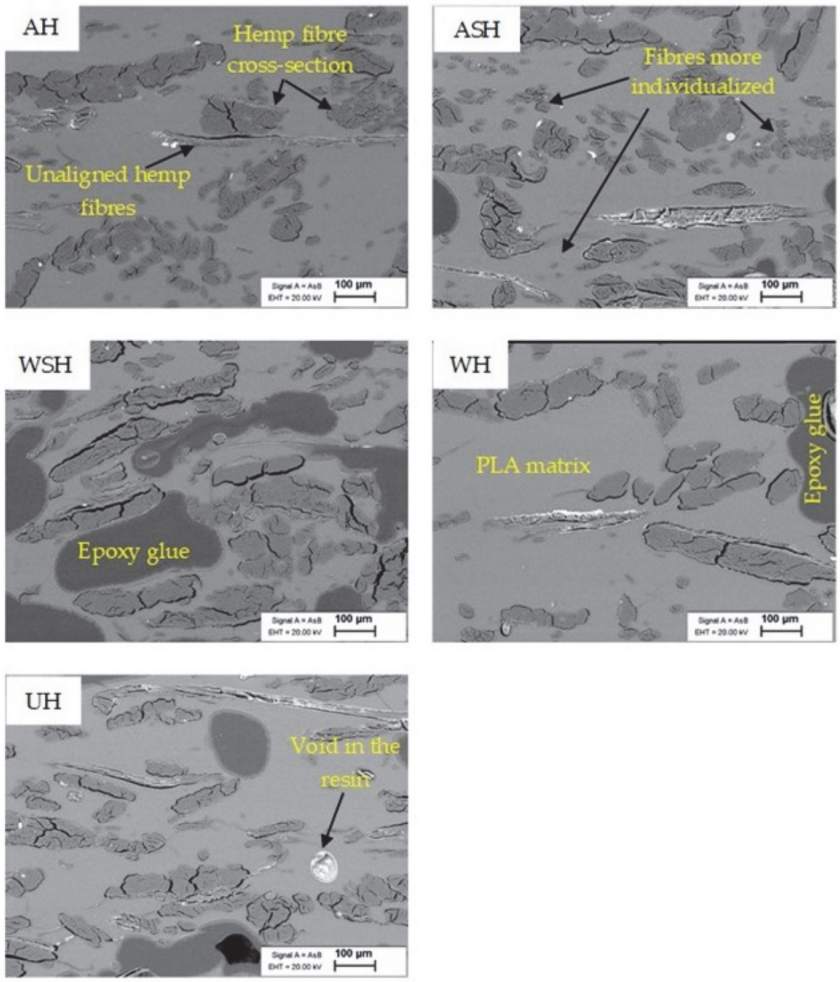

Figure 7. Cross-section SEM images of UH, WH, WSH, AH, and ASH composites from 30 wt.% hemp fibers.

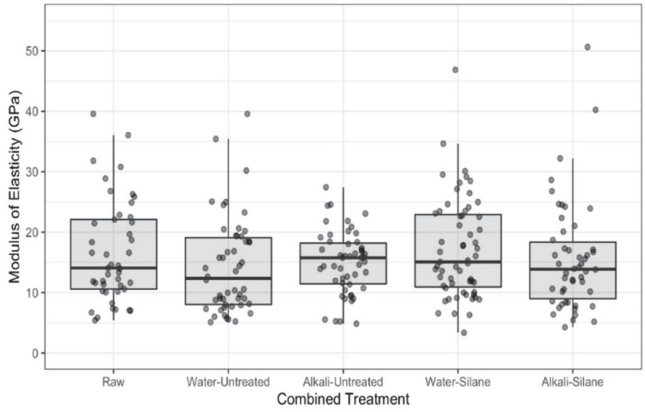

Figure 8. Modulus of elasticity for raw hemp fibers and fibers with combined treatments.

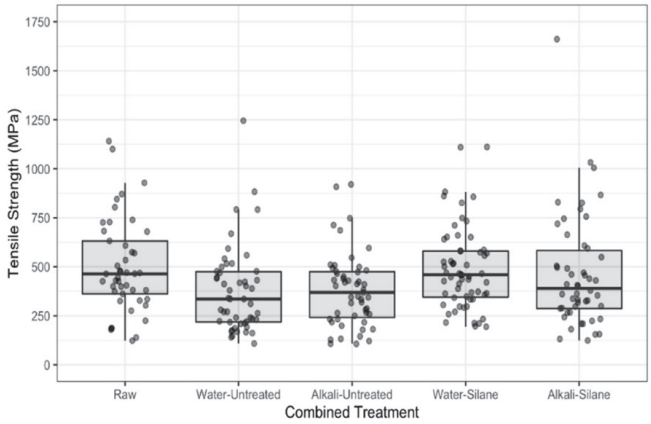

Figure 9. Tensile strength of raw hemp fibers and fibers with combined treatments.

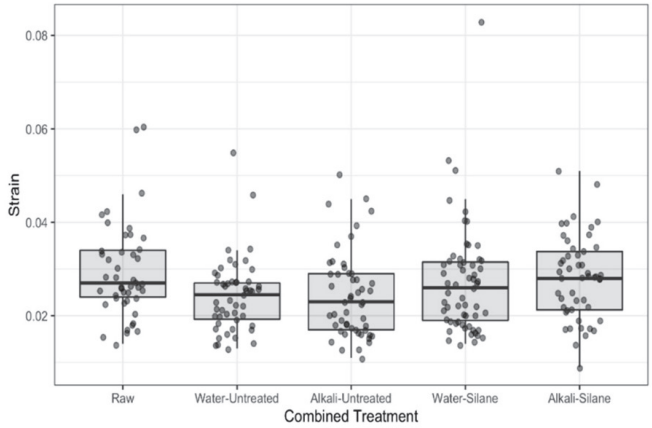

Figure 10. Strain of raw hemp fibers and fibers with combined treatments.

Table 4 presents the effect of pretreatments (none = raw fibers, water, and alkali) on the tensile properties of hemp fibers as a ratio between medians of the given treatments. We note that MoE of the hemp fibers was not affected by water or alkali pretreatments (confidence intervals for the ratios include 1). However, the tensile strength and elongation at break were both reduced after water and alkali pretreatments. The median tensile strength of raw fibers was 1.36 times greater than water pretreated fibers (95% CI: 1.06 to 1.76) and was 1.33 times greater than fibers pretreated with alkali (95% CI: 1.03 to 1.72). Median elongation at break was 1.23 times greater for raw fibers than alkali pretreated fibers (95% CI: 1.04 to 1.44) and was 1.2 times greater for raw fibers than for water pretreated fibers (95% CI: 1.02 to 1.41). There was no meaningful difference in the tensile properties between fibers pretreated with water and alkali (95% CI's include 1 in each case).

Water pretreatment generates a water uptake by the fibers, which occurs under two states in natural fibers, depending on the moisture content [22,27,28]: (i) Water bound to the different biopolymers constituting the cell walls and middle lamella, involving the formation of hydrogen bonds with hydroxyl groups OH, and (ii) free water that fills voids (micro- and macropores of cell walls and lumens) and is retained by capillary forces. Garat et al. [29] measured moisture content of 62.8 $\pm$ 0.7% for hemp fiber bundles in immersion (compared to 60.9 $\pm$ 0.7% for flax fiber bundles). Moreover, Pejic et al. [28] showed that lignin removal decreases the moisture sorption and increases the water retention ability of hemp fibers. Marrot et al. [13] highlighted that the raw hemp fibers of

this study display a particularly low lignin content, which is also confirmed by the TGA analysis. We can then assume that our fibers show high water retention ability during water pretreatment. Pectins and hemicelluloses from the surface, cell wall and middle lamella are removed during water pretreatment, confirmed by the FTIR and TGA results, and we suspect changes in the component arrangements of the S2 layer that consists of highly crystallized cellulose microfibrils embedded in an amorphous polysaccharide matrix (pectins and hemicelluloses). A decrease of the median tensile strength by 36% after water pretreatments can be explained by a component rearrangement in the S2 layer, which controls the mechanical properties of the whole fiber. Le Duigou et al. [30] also observed an alteration of the structural cohesion (cell-wall peeling process) of a flax fiber following water treatment.

Table 4. Effect of pretreatments (raw fibers, water and alkali) on the tensile properties of hemp fibers and comparison of tensile properties for hemp fibers before and after silane treatment (with water and alkali pretreatments).

	Tensile Strength			Modulus			Strain		
Comparison	**Ratio**	**95% CI**	***p*-Value**	**Ratio**	**95% CI**	***p*-Value**	**Ratio**	**95% CI**	***p*-Value**
Raw/Alkali	1.3	1.03 to 1.72	0.0255 *	1.05	0.83 to 1.33	0.8647	1.23	1.04 to 1.44	0.0092 **
Raw/Water	1.36	1.06 to 1.76	0.0131 *	1.18	0.93 to 1.5	0.2130	1.20	1.02 to 1.41	0.0261 **
Alkali/Water	1.03	0.8 to 1.32	0.9641	1.12	0.89 to 1.41	0.4459	0.98	0.83 to 1.14	0.9289
Silane/Untreated | Alkali	1.19	0.97 to 1.45	0.0938	0.97	0.8 to 1.18	0.7777	1.18	1.03 to 1.35	0.0187 *
Silane/Untreated | Water	1.38	1.13 to 1.67	0.0013 **	1.23	1.02 to 1.49	0.0294 *	1.09	0.95 to 1.24	0.2041

* $p < 0.05$, ** $p < 0.01$. *p*-values were adjusted using Tukey's method for a family of 3 estimates. Comparisons can be interpreted as the ratio between Silane and Untreated fibres that were pretreated with Alkali (Silane/Untreated | Alkali) or Water.

Regarding alkali pretreatment, the median tensile strength was found to be 33% lower than untreated fibers. The effects of alkaline treatments on the mechanical properties of hemp fibers are controversial in the literature; Kabir et al. [9], Väisänen et al. [23] and Islam et al. [31] observed a deterioration of tensile properties (strength and modulus) that they attributed to lignin removal and other non-cellulosic components that reinforce the fibers and to potential degradation of cellulose chains [32]. On the contrary, Sawpan et al. [24] and Sair et al. [33] observed an increase of tensile properties for hemp fibers after alkali treatments that they attributed to a relaxation and reorganization of the microfibrils along the principal axis of the fiber, resulting in a more rigid structure thanks to the elimination of lignin and hemicellulose components. Besides a reduction of lignin and hemicellulose amounts [29,30], authors report a transformation of cellulose II to cellulose I [33] and an augmentation of the cellulose crystallinity [31] after application of an alkaline pretreatment to the fibers.

Furthermore, the effect of silane treatment on the tensile properties of hemp fibers pretreated with water and alkali is also shown in Table 4. In the case of alkali pretreatment, silane did not affect MoE, but fiber elongation and tensile strength were greater (strain: 1.18 times, 95% CI: 1.03 to 1.35; tensile strength: 1.19 times, 95% CI: 0.97 to 1.45). When pretreated with water, both MoE and tensile strength were greater when treated additionally with silane (MoE: 1.38 times, 95% CI: 1.13 to 1.67; tensile strength: 1.23 times, 95% CI: 1.02 to 1.49). There was a moderate increase in fiber elongation in this case as well. Silane couplings with cellulose microfibrils formed a layer of chemicals on the fiber surface, acting like a coating, which agrees with the FTIR and TGA results. During the tensile test, an additional shear resistance was brought by the layer of chemicals that attached to the microfibrils. Shear resistance creates higher elongation of the microfibrils, resulting in increased deformation of the fiber as highlighted by Kabir et al. [9].

3.4.2. Tensile Properties of HPLA Composites

From the TS results presented in Figure 11, UH shows a lower outcome of 48 ± 2.4 MPa (30 wt.%) and 37 ± 7 MPa (50 wt.%), compared to the neat PLA, 51 ± 0.45 MPa. This indicates an ineffective reinforcement of PLA with untreated hemp fibers. There was a slight increase of about 6% for WH compared to UH (30 wt.%), but no meaningful improvement

was achieved for WSH compared to WH. On the other hand, alkali pretreatment of the hemp fibers significantly boosted the composite TS by about 14%; subsequent treatment with silane added another 10% compared to AH. At the fiber level, both water and alkali pretreatments decreased TS of the fibers by about 30%. The increase in TS for WH and AH compared to the untreated hemp fiber reinforced PLA composites, despite the treatment's negative impact on fiber performance, can be attributed to: (1) The better level of fiber individualization as observed by SEM technique, which induces a higher aspect ratio, and (2) the enhanced PLA-fiber bonding after removal of water-soluble polysaccharides in water pretreatment and removal of pectin, wax and intercellular components in alkali pretreatment. Removal of these components exposes more hydroxyl groups and increases access to cellulose sites for interlocking with the PLA matrix, which corroborates previous studies [23,34,35]. At the fiber scale, silane treatment increased the TS of hemp fibers pretreated with water and alkali. Additional improvement to TS observed on composites at the macroscale after silane treatment was attributable to higher fiber performance and improved fiber compatibility with the polymer matrix brought on by the silane couplings.

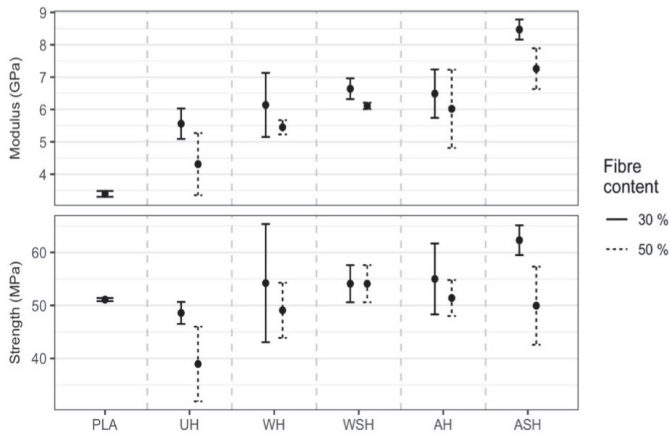

Figure 11. Medians (●) for YM and TS at 30 and 50 wt.% hemp fiber content for untreated (UH) and treated (WH, WSH, AH, and ASH) compared to neat PLA (bars show the one interquartile range on either side of the median).

Regarding the 50 wt.% HPLA composites, there was generally a decrease in TS compared to 30 wt.%, which was ascribed to insufficient wetting of the fibers by the PLA matrix [24,26] and, consequently, an inefficient load transfer between fibers and matrix. Sawpan et al. [23] also showed that there was no linear improvement in TS with an increase in fiber loading from 10–30 wt.%; moreover, previous studies show that 30 wt.% was the maximum fiber volume fraction at which optimum composite mechanical performance was achieved [20,36]. From the result of the specimens' Young's modulus (YM), a significant rise of about 37% and 23.5% was obtained with reinforcements of 30 and 50 wt.% U_f compared to neat PLA due to much higher elastic modulus of the hemp fibers (Figure 8) compared to PLA (approx. 3.8 GPa based on technical data). At the fiber scale, hemp fibers' MoE was not affected by water or alkali pretreatments and showed only a slight increase for WSf. However, on the composite scale, water pretreatment increased YM by 19 and 23% at 30 and 50 wt.%, respectively, while alkali treatment offered an even more superior outcome of 29 and 44%. Following the additional silane treatment of W_f (i.e., WSH), a further improvement of 6 and 15% was achieved at 30 and 50 wt.%, respectively. This mirrors the outcome at the fiber scale; though not meaningful at 30 wt.%, it was very significant at 50 wt.%, indicating better entrapment of the PLA by the fiber interpenetrating network that is due to silane molecules coating the fiber surface, as described by Xie et al. [37].

Likewise, for TS, YM declined at 50 wt.%, implying inadequate fiber wetting by the PLA matrix as earlier mentioned. We clearly observed that UH exhibited the most meaningful reduction (18%) in this regard, which is probably due to the increasingly less favorable matrix/fiber interface with higher fiber content. Overall, ASH (30 wt.%) exhibited the best outcome of 8.51 ± 0.2 GPa, representing a notable increase of 1.5 times (95% CI: 1.40 to 1.64) that of UH.

3.4.3. Flexural Properties of HPLA Composites

Median flexural strength (FS) and modulus (FM) for the specimens are presented in Figure 12. Neat PLA performed better in FS than UH, WH, and WSH composites, which gave lower outcomes. The reduction in FS compared to neat PLA, after reinforcement, was WSH < WH < UH at both 30 and 50 wt.%, implying improvement in the bonding between PLA and hemp fibers following water and a combination of water and silane fiber treatments. Alkali- and silane-treated hemp fiber reinforced composites (ASH) exhibited the most significant boost in FS (34% at 30 wt.% and 30% at 50 wt.%), compared to neat PLA, and was, significantly, 1.5 times (95% CI: 1.29 to 1.74) and 2 times (95% CI: 1.92 to 2.38) greater than 30 and 50 wt.% UH, respectively. AH also showed a meaningful 13% improvement at lower fiber content compared to neat PLA. As observed, there was a similar reduction in FS with an increase in the composite fiber content from 30 to 50 wt.%. The most notable reduction was by WH (33%), UH (26%) and AH (12%), while there was no meaningful decrease in performance for either ASH or WSH even though both exhibited about 3% lower FS at 50 wt.%. Compared to AH, there was an insignificant increase at 30 wt.% by ASH, but at 50 wt.%, there was a reasonably better outcome (1.4 times AH; 95% CI: 1.29 to 1.50), showing the positive influence of additional silane treatment on the hemp fibers. The higher outcomes for AH and ASH compared to UH was consistent with earlier presented results from FTIR, TGA, and SEM and also agrees with past studies [18,24,35].

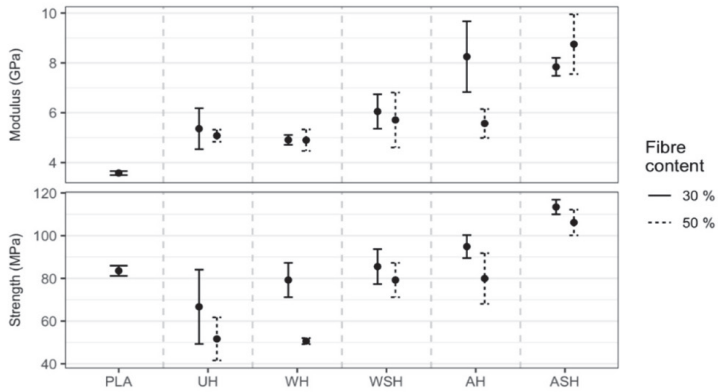

Figure 12. Medians (●) for FM and FS at 30 and 50 wt.% hemp fiber content for untreated (UH) and treated (WH, WSH, AH, and ASH) compared to neat PLA.

Similar to YM, composite FM also increased by about 49% after the PLA was reinforced with untreated hemp fibers (30 wt.%) and, ultimately, by over 120% when treated hemp fibers (alkali + silane) were used. The outcome for UH compared to neat PLA was also inferred to be due to the superior elastic modulus of the hemp fibers, and the further consequential boost by ASH was the result of enhanced PLA/hemp fiber bonding after alkali and silane treatments. When we compared all composites, the increase in FM was UH = WH < WSH < AH < ASH. Generally, composite FM also decreased with an increase in fiber content, though we noticed a 6% rise for ASH at 50 wt.%, which was not significant and implied that there was no further improvement in performance.

Consistent with past studies, our research reported better composite flexural performance after alkali and silane fiber pretreatments [18,24,33,34], and the 8.58 GPa FM obtained in the current study for this particular treatment approach represents one of the best outcomes achieved using the hot press method and a fiber content of 50 wt.%. Hu and Lim [34] employed a similar fabrication and treatment method (i.e., hot pressing and alkali treatment, respectively), though with short fibers, and obtained slightly lower average FS results of 87.5 MPa for alkali-treated hemp fiber reinforced PLA composites at 30 wt.%. Sawpan et al. [24] obtained FS and FM of about 95 MPa and 6.59 GPa for alkali-treated, long-aligned 35 wt.% hemp fiber reinforced PLA composites that declined by about 29% and 15%, respectively, at 40 wt.%.

In addition to the mechanical properties discussed above, average density, specific tensile and flexural strength values for the HPLA composites are given in Table 5. Density of the neat PLA board is 1.24 g cm^{-3}, which is the same value stipulated by the manufacturer and confirms the effectiveness of the fabrication approach. Densities for the composites are 1.13 to 1.23 g cm^{-3}. There appears to be no significant difference in densities for composites of similar fiber content, but the 50 wt.% composites exhibit a slightly lower density compared to the 30 wt.% composites. Overall, the alkali pretreated and alkali + silane-treated hemp fiber reinforced composites show slightly higher density compared to the other composite variants, which could be due to consistency in hemp fiber content following the removal of most non-cellulosic elements. Lower density of the 50 wt.% composites could be the result of more voids, which decrease resin flow through the fibers at higher contents, and differences across all samples may also arise from fabrication irregularities, which may occur from the manual composite manufacturing processes. Pappu et al. [35] achieved specific TS and FS of (27.9 ± 2.5) σ/ρ and (64.9 ± 1.13) σ/ρ for neat PLA, which increased by 27% after incorporation of hybrid fibers of hemp and flax (composite density of 1.19 ± 0.02 g cm^{-3}). Hu and Lim [34] obtained specific TS of 34.5 σ/ρ and 35.8 σ/ρ for untreated and alkali-treated hemp fiber reinforced PLA composites, respectively, at 50 wt.%. Compared to these past studies, the current study showed slightly higher outcomes. The use of such low-density composites could offer a suitable alternative to composites from synthetic fibers, reduce carbon dioxide emissions and increase energy savings in transportation applications.

Table 5. Average density and specific mechanical properties of the neat PLA and HPLA composites.

	Specimen	Density (g/cm^{-3})	Specific TS σ/ρ	Specific FS σ/ρ		Density (g/cm^{-3})	Specific TS σ/ρ	Specific FS σ/ρ
100%	PLA	1.24 ± 0.01	41.29 ± 0.36	68.19 ± 2.03				
30 wt.%	UH	1.19 ± 0.11	40.19 ± 2.19	60.92 ± 10.51	50 wt.%	1.13 ± 0.05	33.06 ± 6.60	47.24 ± 5.68
	WH	1.20 ± 0.13	42.46 ± 6.05	67.05 ± 4.54		1.13 ± 0.10	42.85 ± 4.39	47.51 ± 5.97
	WSH	1.18 ± 0.05	43.94 ± 3.15	70.47 ± 4.01		1.13 ± 0.10	45.90 ± 3.29	71.63 ± 4.50
	AH	1.23 ± 0.02	45.20 ± 4.67	77.22 ± 2.61		1.16 ± 0.06	45.27 ± 1.98	72.59 ± 8.03
	ASH	1.21 ± 0.05	51.00 ± 2.64	93.64 ± 2.69		1.16 ± 0.03	46.67 ± 6.33	94.22 ± 6.68

4. Conclusions

This study was an in-depth investigation into the effect of different hemp fiber surface pretreatments (water and sodium hydroxide) combined with silane treatment. At the microscale, FTIR, TGA, and SEM investigations highlighted structural alterations in the fibers, with the removal of targeted components and rearrangement in the cell wall. These structural changes influenced unitary fiber properties. At the fiber microscale, preliminary treatment tended to reduce tensile strength and elongation at break but did not affect the modulus of elasticity. Silane treatment improved tensile strength for both pretreatments and modulus of elasticity after water pretreatment. At the macroscale, both pretreatments increased the composites' tensile properties, despite their negative impact on fiber performance. This improvement was the result of a better level of fiber individualization after pretreatment and enhanced PLA-fiber bonding induced by the removal of water-soluble polysaccharides during water pretreatment and removal of pectin, wax and intercellular

components during alkali pretreatment. Additionally, silane treatment improved composite performance thanks to the higher performance of the fibers themselves and improved fiber compatibility with the polymer matrix brought on by the silane couplings. This study showed successful development of low-density composites suitable for transportation applications, which will allow for a reduction of weight and carbon dioxide emissions. Future study will examine the influence of these chemical treatments on composite moisture/humidity sensitivity and fire performance.

Author Contributions: Validation, P.F.A. and M.D.B.; Formal Analysis, P.F.A. and M.D.B.; Visualization, P.F.A. and L.M.; Writing—original draft, P.F.A. and L.M.; Writing—review and editing, P.F.A.; L.M. and M.D.B.; Funding Acquisition, P.F.A.; J.K. and L.M.; Investigation, P.F.A., L.M., M.S. and G.L.; Conceptualization, L.M. and J.K.; Resources, J.K. and L.M.; Supervision, J.K. All authors have read and agreed to the published version of the manuscript.

Funding: This project has received funding from the European Regional Development Fund, European Union's Horizon 2020 research and innovation programme under the Marie Sklodowska-Curie Actions (grant number 898179), European Union's Horizon 2020 research and innovation programme under H2020 WIDESPREAD-2-Teaming (grant number 739574) and investment from the Republic of Slovenia and ARRS (Slovenian Research Agency) Bilateral Project Slovenia—Estonia (grant agreement number BI-EE/20-22-007).

Institutional Review Board Statement: Not applicable.

Informed Consent Statement: Not applicable.

Data Availability Statement: Not applicable.

Conflicts of Interest: Authors declare no conflict of interest.

References

1. Baley, C.; Bourmaud, A.; Davies, P. Eighty years of composites reinforced by flax fibers: A historical review. *Compos. Part A Appl. Sci. Manuf.* **2021**, *144*, 106333. [CrossRef]
2. Marrot, L.; Lefeuvre, A.; Pontoire, B.; Bourmaud, A.; Baley, C. Analysis of the hemp fiber mechanical properties and their scattering (Fedora 17). *Ind. Crop. Prod.* **2013**, *51*, 317–327. [CrossRef]
3. Merotte, J.; Le Duigou, A.; Kervoelen, A.; Bournmaud, A.; Behlouli, K.; Sire, O.; Baley, C. Flax and hemp nonwoven composites: The contribution of interfacial bonding to improving tensile properties. *Polym. Test.* **2018**, *66*, 303–311. [CrossRef]
4. Xiao, B.; Huang, Q.; Chen, H.; Chen, X.; Long, G. A fractal model for capillary flow through a single tortuous capillary with roughened surfaces in fibrous porous media. *Fractals* **2021**, *29*, 2150017. [CrossRef]
5. Liu, M.; Thygesen, A.; Summerscales, J.; Meyer, A.S. Targeted pre-treatment of hemp bast fibers for optimal performance in biocomposite materials: A review. *Ind. Crop. Prod.* **2017**, *108*, 660–683. [CrossRef]
6. Bourmaud, A.; Morvan, C.; Baley, C. Importance of fiber preparation to optimize the surface and mechanical properties of unitary flax fiber. *Ind. Crop. Prod.* **2010**, *32*, 662–667. [CrossRef]
7. Liu, M.; Meyer, A.; Fernando, D.; Silva, D.A.S.; Daniel, G.; Thygesen, A. Effect of pectin and hemicellulose removal from hemp fibers on the mechanical properties of unidirectional hemp/epoxy composites. *Compos. Part A Appl. Sci. Manuf.* **2016**, *90*, 724–735. [CrossRef]
8. Sepe, R.; Bollino, F.; Boccarusso, L.; Caputo, F. Influence of chemical treatments on mechanical properties of hemp fiber reinforced composites. *Compos. Part B Eng.* **2018**, *133*, 210–217. [CrossRef]
9. Kabir, M.M.; Wang, H.; Lau, K.T.; Cardona, F. Tensile properties of chemically treated hemp fibers as reinforcement for composites. *Compos. Part B Eng.* **2013**, *53*, 362–368. [CrossRef]
10. Coroller, G.; Lefeuvre, A.; Le Duigou, A.; Bourmaud, A.; Ausias, G.; Gaudry, T.; Baley, C. Effect of flax fibers individualisation on tensile failure of flax/epoxy unidirectional composite. *Compos. Part A Appl. Sci. Manuf.* **2013**, *51*, 62–70. [CrossRef]
11. Marrot, L.; Bourmaud, A.; Bono, P.; Baley, C. Multi-scale study of the adhesion between flax fibers and biobased thermoset matrices. *Mater. Des.* **2014**, *62*, 47–56. [CrossRef]
12. Brounstein, Z.; Yeager, C.M.; Labouriau, A. Development of Antimicrobial PLA Composites for Fused Filament Fabrication. *Polymers* **2021**, *13*, 580. [CrossRef]
13. Marrot, L.; Alao, P.F.; Mikli, V.; Kers, J. Properties of frost-retted hemp fibers for the reinforcement of composites. *J. Nat. Fibers* **2021**, in press.
14. R Core Team. *R: A Language and Environment for Statistical Computing*; R Foundation for Statistical Computing: Vienna, Austria, 2019. Available online: http://www.r-project.org/index.html (accessed on 16 February 2021).
15. RStudio Team. *RStudio: Integrated Development for R*; RStudio, PBC: Boston, MA, USA, 2020. Available online: http://www.rstudio.com/ (accessed on 16 February 2021).

16. Wickham, H.; Averick, M.; Bryan, J.; Chang, W.; McGowan, L.; François, R.; Grolemund, G.; Hayes, A.; Henry, L.; Hester, J.; et al. Welcome to the Tidyverse. *J. Open Source Softw.* **2019**, *4*, 1686. [CrossRef]
17. Lenth, R.; Buerkner, P.; Herve, M.; Love, J.; Riebl, H.; Singmann, H. Emmeans: Estimated Marginal Means, Aka Least-Squares Means 2020. Available online: https://cran.r-project.org/web/packages/emmeans/emmeans.pdf (accessed on 16 February 2021).
18. Dayo, A.Q.; Zegaoui, A.; Nizamani, A.A.; Kiran, S.; Wang, J.; Derradji, M.; Cai, W.-A.; Liu, W.-B. The influence of different chemical treatments on the hemp fiber/polybenzoxazine based green composites: Mechanical, thermal and water absorption properties. *Mater. Chem. Phys.* **2018**, *217*, 270–277. [CrossRef]
19. Rasheed, M.; Jawaid, M.; Parveez, B.; Hussain Bhat, A.; Alamery, S. Morphology, Structural, Thermal, and Tensile Properties of Bamboo Microcrystalline Cellulose/Poly(Lactic Acid)/Poly(Butylene Succinate) Composites. *Polymers* **2021**, *13*, 465. [CrossRef] [PubMed]
20. Viscusi, G.; Barra, G.; Verdolotti, L.; Galzerano, B.; Viscardi, M.; Gorrasi, G. Natural fiber reinforced inorganic foam composites from short hemp bast fibers obtained by mechanical decortation of unretted stems from the wastes of hemp cultivations. *Mater. Today Proc.* **2020**, *34*, 176–179. [CrossRef]
21. Panaitescu, D.M.; Fierascu, R.C.; Gabor, A.R.; Nicolae, C.A. Effect of hemp fiber length on the mechanical and thermal properties of polypropylene/SEBS/hemp fiber composites. *J. Mater. Res. Technol.* **2020**, *9*, 10768–10781. [CrossRef]
22. Placet, V.; Day, A.; Beaugrand, J. The influence of unintended field retting on the physicochemical and mechanical properties of industrial hemp bast fibers. *J. Mater. Sci.* **2017**, *52*, 5759–5777. [CrossRef]
23. Väisänen, T.; Batello, P.; Lappalainen, R.; Tomppo, L. Modification of hemp fibers (*Cannabis Sativa* L.) for composite applications. *Ind. Crop. Prod.* **2018**, *111*, 422–429. [CrossRef]
24. Sawpan, M.A.; Pickering, K.L.; Fernyhough, A. Effect of various chemical treatments on the fiber structure and tensile properties of industrial hemp fibers. *Compos. Part A Appl. Sci. Manuf.* **2011**, *42*, 888–895. [CrossRef]
25. Sood, M.; Dwivedi, G. Effect of fiber treatment on flexural properties of natural fiber reinforced composites: A review. *Egypt. J. Pet.* **2018**, *27*, 775–783. [CrossRef]
26. Bourmaud, A.; Beaugrand, J.; Shah, D.U.; Placet, V.; Baley, C. Towards the design of high-performance plant fiber composites. *Prog. Mater. Sci.* **2018**, *97*, 347–408. [CrossRef]
27. Engelund, E.T.; Thygesen, L.G.; Svensson, S.; Hill, C.A.S. A critical discussion of the physics of wood–water interactions. *Wood Sci. Technol.* **2013**, *47*, 141–161. [CrossRef]
28. Pejic, B.M.; Kostic, M.M.; Skundric, P.D.; Praskalo, J.Z. The effects of hemicelluloses and lignin removal on water uptake behavior of hemp fibers. *Bioresour. Technol.* **2008**, *99*, 7152–7159. [CrossRef]
29. Garat, W.; Le Moigne, N.; Corn, S.; Beaugrand, J.; Bergeret, A. Swelling of natural fiber bundles under hygro- and hydrothermal conditions: Determination of hydric expansion coefficients by automated laser scanning. *Compos. Part A Appl. Sci. Manuf.* **2020**, *131*, 105803. [CrossRef]
30. Le Duigou, A.; Bourmaud, A.; Balnois, E.; Davies, P.; Baley, C. Improving the interfacial properties between flax fibers and PLLA by a water fiber treatment and drying cycle. *Ind. Crop. Prod.* **2012**, *39*, 31–39. [CrossRef]
31. Islam, M.S.; Pickering, K.L.; Foreman, N.J. Influence of alkali treatment on the interfacial and physico-mechanical properties of industrial hemp fiber reinforced polylactic acid composites. *Compos. Part A Appl. Sci. Manuf.* **2010**, *41*, 596–603. [CrossRef]
32. Beckermann, G.W.; Pickering, K.L. Engineering and evaluation of hemp fiber reinforced polypropylene composites: Fiber treatment and matrix modification. *Compos. Part A Appl. Sci. Manuf.* **2008**, *39*, 979–988. [CrossRef]
33. Sair, S.; Oushabi, A.; Kammouni, A.; Tanane, O.; Abboud, Y.; Hassani, F.O.; Laachachi, A.; El Bouari, A. Effect of surface modification on morphological, mechanical and thermal conductivity of hemp fiber: Characterization of the interface of hemp -Polyurethane composite. *Case Stud. Therm. Eng.* **2017**, *10*, 550–559. [CrossRef]
34. Hu, R.; Lim, J.-K. Fabrication and Mechanical Properties of Completely Biodegradable Hemp Fiber Reinforced Polylactic Acid Composites. *J. Compos. Mater.* **2007**, *41*, 1655–1669. [CrossRef]
35. Pappu, A.; Pickering, K.L.; Thakur, V.K. Manufacturing and characterization of sustainable hybrid composites using sisal and hemp fibers as reinforcement of poly (lactic acid) via injection moulding. *Ind. Crop. Prod.* **2019**, *137*, 260–269. [CrossRef]
36. Mazian, B.; Bergeret, A.; Benezet, J.C.; Malhautier, L. Influence of field retting duration on the biochemical, microstructural, thermal and mechanical properties of hemp fibers harvested at the beginning of flowering. *Ind. Crop. Prod.* **2018**, *116*, 170–181. [CrossRef]
37. Xie, Y.; Hill, C.A.S.; Xiao, Z.; Militz, H.; Mai, C. Silane coupling agents used for natural fiber/polymer composites: A review. *Compos. Part A Appl. Sci. Manuf.* **2010**, *41*, 806–819. [CrossRef]

Appendix 3

Publication III

Alao, P.F.; Marrot, L.; Kallakas, H.; Just, A.; Poltimäe, T.; Kers, J. Effect of Hemp Fiber Surface Treatment on the Moisture/Water Resistance and Reaction to Fire of Reinforced PLA Composites. Materials 2021, 14, 4332.

materials

MDPI

Article

Effect of Hemp Fiber Surface Treatment on the Moisture/Water Resistance and Reaction to Fire of Reinforced PLA Composites

Percy Festus Alao [1,*], Laetitia Marrot [2], Heikko Kallakas [1], Alar Just [3], Triinu Poltimäe [1] and Jaan Kers [1]

[1] Department of Material and Environmental Technology, Tallinn University of Technology, Ehitajate tee 5, 19086 Tallinn, Estonia; heikko.kallakas@taltech.ee (H.K.); triinu.poltimae@taltech.ee (T.P.); jaan.kers@taltech.ee (J.K.)
[2] InnoRenew CoE, Livade 6, 6310 Izola, Slovenia; laetitia.marrot@innorenew.eu
[3] Department of Civil Engineering and Architecture, Tallinn University of Technology, Ehitajate tee 5, 19086 Tallinn, Estonia; alar.just@taltech.ee
* Correspondence: percy.alao@taltech.ee

Abstract: The effects of surface pretreatment (water and alkali) and modification with silane on moisture sorption, water resistance, and reaction to fire of hemp fiber reinforced polylactic acid (PLA) composites at two fiber loading contents (30 and 50 wt.%) are investigated in this work. Moisture adsorption was evaluated at 30, 50, 75 and 95% relative humidity, and water resistance was determined after a 28-day immersion period. The cone calorimetry technique was used to investigate response to fire. The fiber surface treatment resulted in the removal of cell wall components, which increased fiber individualization and homogeneity as shown in scanning microscopic pictures of the composite cross-section. Although the improved fiber/matrix bonding increased the composite's water resistance, the different fiber treatments generated equal moisture adsorption results for the 30 wt.% reinforced composites. Overall, increasing the fiber amount from 30 to 50 wt.% increased the composite sensitivity to moisture/water, mainly due to the availability of more hydroxyl groups and to the development of a higher pore volume, but fire protection improved due to a reduction in the rate of thermal degradation induced by the reduced PLA content. The new Oswin's model predicted the composite adsorption isotherm well. The 30 wt.% alkali and silane treated hemp fiber composite had the lowest overall adsorption (9%) while the 50 wt.% variant produced the highest ignition temperature (181 ± 18 °C).

Keywords: hemp fiber composites; water absorption; hygroscopic properties; thermal properties; fire resistance

Citation: Alao, P.F.; Marrot, L.; Kallakas, H.; Just, A.; Poltimäe, T.; Kers, J. Effect of Hemp Fiber Surface Treatment on the Moisture/Water Resistance and Reaction to Fire of Reinforced PLA Composites. *Materials* **2021**, *14*, 4332. https://doi.org/10.3390/ma14154332

Academic Editor: Costantino Menna

Received: 22 June 2021
Accepted: 30 July 2021
Published: 3 August 2021

1. Introduction

The EU Green deal policy aims to achieve a carbon neutral economy by 2050, which requires redesigning different industrial sectors, their processes and their products. As a result, there is a growing challenge toward the use of healthy, sustainable, non-hazardous, biodegradable and renewable resources while maintaining reliability in product performances [1]. Due to low embodied production energy, plant fibers have gained a lot of attention in this regard [2,3]. Flax, jute, hemp, sisal and ramie figure amongst the widely accessible source of plant fibers [4]. Specifically, studies [5–8] have shown that hemp fiber can be a suitable natural reinforcing material for composite application due to its vast availability, price stability and good mechanical properties.

Furthermore, to obtain fully compostable composites and to enhance positive environmental impact, bio-thermoplastic matrices such as polylactic acid (PLA) are being preferred to replace traditional synthetic polymers with the same performances (polyester, polypropylene and polyurethane). PLA is produced from annual bioresources, mainly through the fermentation of corn, and display a cost-effective production compared to other polymers developed from renewable resources such as soya oil-based epoxy, lignin and

starch [9]. Hemp PLA composites have shown promising results [10] and can be regarded as appropriate materials for a vast range of applications and minimize the environmental threats associated with petroleum-based products.

Despite their proven competitive properties when compared to composites reinforced with synthetic fibers, there is a crucial need to improve performance and durability during service of natural fiber composites. The performance of natural fibers as a reinforcing material is influenced by essential parameters such as fiber treatment and content, matrix/binder type, interfacial strength and the manufacturing process [11]. Natural fibers are composed of cellulose and amorphous cell wall biopolymers (hemicellulose, pectins and lignin), highly rich in hydroxyl groups responsible for the hydrophilic nature of the fiber and conferring a high affinity for moisture. When these fibers are blended with the hydrophobic matrix, weak interfacial bonds are formed, spawning a deterioration in service due to voids and debonding within the composite [5]. The hemicellulose and lignin covering components reduce the ability of cellulose, which is liable for the specific mechanical properties and structural stability, to effectively adhere to the polymer matrix. The hygroscopic properties of such plant-based composite materials are thus affected by the high moisture sensitivity resulting from the presence of these hydroxyl groups [2]. The chemical modification of the fibers appears to successfully remove the covering materials (hemicellulose, lignin & extractives) responsible for the moisture absorption [12,13]. According to Pejic et al. [14] the alkali treatment of hemp fibers results in the gradual removal of hemicellulose and lignin that causes the rearrangement of fibrils and the formation of new capillary spaces between completely or partially separated fibers, which increases the roughness of the hemp fiber surface and enhances wetting with the polymer matrix. Additionally, the modification of the hemp fiber surface by alkali treatment brought improvements of the composite tensile and flexural properties [10]. Due to their elemental composition (carbon, hydrogen and oxygen) associated with cellulose, hemicelluloses and lignin main components, lignocellulosic fibers are flammable and can easily decompose in the event of a fire hazard [15]. The fire resistance characterization of hemp fiber reinforced polyesters was assessed by Naughton et al. [16]. It was reported that the increase in the composite hemp fiber volume contributed to the formation of an effective thermally insulating char layer. However, based on current knowledge, there is no recent study about the fire behavior of hemp fiber reinforced PLA composites and the effect of surface treatments on the composite fire reaction. The characterization of the fire resistance would increase the consideration of natural fiber reinforced composites in construction and demanding transportation (automobile/aeronautical) applications.

This study focused on inspecting the contribution of surface pretreatment (water and alkali pretreatment) and modification (silane treatment) on the moisture adsorption, water absorption and reaction to fire of hemp fiber reinforced PLA (HPLA) composites. The objectives of this work are as follows:

i To produce composites with two fiber loadings (30 and 50 wt.%) using frost-retted hemp fibers from Estonia and polylactic acid (PLA). These locally obtained hemp fibers are commonly considered as waste. Using them as PLA reinforcement is a way to value these by-products from the cannabidiol industry [17] and to enhance the contribution to a carbon-neutral environment;

ii To study the influence of a combination of fiber surface pretreatments and modification of hemp fibers on the hemp PLA properties of interest (moisture/water resistance and fire behaviour) to promote the development of biocomposites as building materials.

Figure 1 presents a scheme of the main objective of this research.

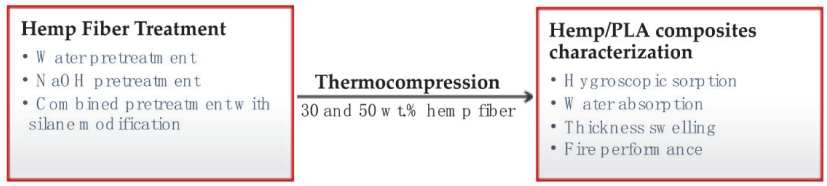

Figure 1. Schematic representation of the research objective.

2. Materials and Methods

2.1. Materials

The hemp fibers used for this study were grown, frost-retted and harvested between 10th of June 2016 and 4th of May 2017, in Saaremaa, Estonia. The chemical composition of these hemp fibers has been described previously in our paper [17] and is reported in Table 1. The fibers were manually cleaned to remove hurds, carded twice with a wide classic drum carder (300 mm batt width and 72 teeth per inch) and dried in the oven at 80 °C to achieve uniform weight before use. Staple polylactic acid (PLA) from NatureWorks LLC was used as a matrix. The density of the PLA was 1.24 g.cm^{-3}.

Table 1. The percentage biochemical composition of the untreated frost-retted hemp fibres used in this study [17].

Cellulose	Hemicellulose	Lignin	* Solubles	Inorganic Matter
77.4 ± 0.3	8.3 ± 0.3	1.4 ± 0.0	12.6 ± 0.4	0.3 ± 0.0

* Soluble content is characterized by pectin + wax + water extractives.

2.2. Methods

2.2.1. Hemp Fibers Treatments

The hemp fiber pretreatments (water, alkali) and modification with silane were carried out according to Alao et al. [10] (Figure 2). In all cases, the hemp fibers were oven-dried at 80 °C before and after treatment. The pretreatment with 5 wt.% NaOH was performed for 4 h at room temperature (23 °C). Regarding the silane treatments, the hemp fibers (water/alkali pretreated) were soaked in a solution of 3-Aminopropyl-triethoxy silane (3 wt.% of hemp fibers) with 99% concentration and ethanol (97% concentration, 80 vol.%) with distilled water (20 vol.%) for 2 h. Before the treatment process, the solution was activated with acetic acid and constantly stirred for 2 h to control the pH to 5 and to pre-hydrolyze the silane.

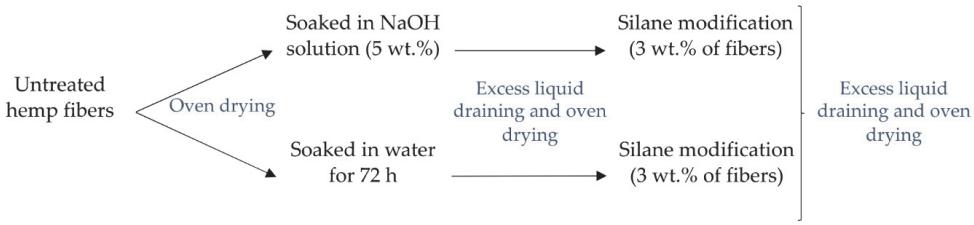

Figure 2. The surface pretreatments and treatment of hemp fibers.

Hemp fibers are pretreated to eliminate non-cellulosic compounds (hemicellulose, lignin and pectins). The elimination of these components results in a loss of fiber weight.

The fiber weight reduction (F_W) associated to each treatment was measured on three batches of 10 g hemp fibers and was estimated using the following Equation (1):

$$F_w\ (\%) = \frac{F_0 - F}{F_0} \times 100 \quad (1)$$

where F_0 is the weight of the fiber before any treatment, and F is the weight of the fiber after pretreatment/treatment.

2.2.2. Fabrication of the Hemp Reinforced Polylactide (HPLA) Composite

The dried untreated and treated hemp fibers were combined with PLA fibers by hot pressing. Ten composite variants were produced based on hemp fiber composition (30 wt.%; 50 wt.%) and treatment type (UH: untreated; WH: water treated; WSH: water + silane; AH: alkali treated; ASH: alkali + silane). Hemp and PLA fibers were weighed using a ±0.1 mg precision balance (Mettler Toledo ME4002E, Greifensee, Switzerland) and carded. The mix was transferred to a metal frame (450 mm × 450 mm × 2 mm), then pre-heated for 5 min at a temperature of 180 °C before applying a pressure of 3 MPa for 10 min. The final product was allowed to cure at room temperature for 30 min underweight before removal from the frame. A silicon-based release agent was used to prevent sticking of the fabricated composite to the mould. Figure 3 shows the hemp reinforced PLA composite from untreated hemp fiber at Figure 3a 30 wt.% and Figure 3b 50 wt.%.

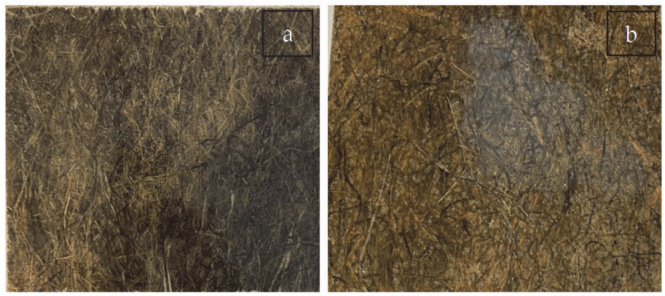

Figure 3. Specimens (**a**) 30 wt.% hemp reinforced PLA composite and (**b**) 50 wt.% hemp reinforced PLA composite.

The composite void fraction (V_p %) was calculated using Equation (2) according to Marrot et al. [17] from the density of the fibrous reinforcement (ρ_f) (taken as 1.38 gcm^{-3}), density of the PLA matrix (ρ_m) (1.24 gcm^{-3}) and density of the composites (ρ_c).

$$V_P(\%) = 1 - \frac{\frac{W_f}{\rho_f} + \frac{W_m}{\rho_m}}{\frac{W_c}{\rho_c}} \times 100 \quad (2)$$

where W_f, W_m and W_c represent the weight of the hemp fiber, PLA and the composite, respectively.

2.2.3. Scanning Electron Microscopy (SEM)

The morphology of the composite cross section was studied using a Zeiss Ultra v.55 (FELMIZFE, Graz, Austria) SEM at 20 kV, depth of 100 µm and 50,000 resolution. The samples were mounted into epoxy glue and coated with 2 nm thick gold-palladium layer (80% Au + 20% Pd) before imaging.

2.2.4. Moisture Adsorption Properties

The moisture sorption was performed following the EN ISO 12571:2013 standard at relative humidity (RH) levels of 30, 50, 75 and 95% and constant temperature (23 ± 0.5 °C) in a climatic chamber. Four replicas of each composite variant measuring 100 mm × 100 mm were dried in the oven as stipulated by EN ISO 12570:2000 standard and weighed until the mass change was ≤0.1% of the preceding 24 h. The data for the equilibrium moisture content (*EMC*) was obtained by weighing the samples at the specified RH until the weight was ≤0.1% of the previous 24 h. The *EMC* on dry bases (d.b) was then calculated using the following Equation (3). The obtained *EMC*s were statistically analyzed with ANOVA single factor and an alpha of 0.05.

$$EMC_{\mathrm{d.b}}(\%) = \frac{M - M_0}{M_0} \times 100 \tag{3}$$

where M_0 is the mass of the oven dried samples; M is the mass of the specimens at any given RH.

The modified Oswin model shown in Equation (4), identified by Palumbo et al. [18] as a good fitting model, was used to predict the moisture adsorption. This model has also been adopted for frost-retted hemp fibers by Nilsson et al. [19].

$$M_D = \frac{(A + \mathrm{BT})}{(H_R - 1)^{\frac{1}{C}}} \tag{4}$$

where M_D is equilibrium moisture content, d.b%; H_R is the relative humidity in decimal; T is the temperature, °C; A, B and C are the modified Oswin model constants.

The parameters in the equation were determined using nonlinear regression analysis. In this regard, constants A, B and C were assumed values and then used to calculate the model (M_D) at the experimental temperature and the specific relative humidity. For each specimen, the differences between the measured equilibrium moisture contents ($EMC_{\mathrm{d.b}}$) and the estimated equilibrium moisture contents (M_D) were taken for each RH to obtain the sum of squares. This sum of squares was then reapplied in a non-linear regression to re-obtain the value of the constants A, B and C, which were then used in the model fitting.

2.2.5. Long-Term Water Absorption (WA) and Thickness Swelling (TS)

The long-term WA was determined by measuring the mass change of the specimen after an immersion in water for 28 days in accordance with EN ISO 16535 standard from five replicas that were first conditioned at 23 ± 2 °C and RH of 50 ± 5% for 24 h. The TS was determined based on the EN 317 standard after 28 days of water immersion. The initial thickness of the specimens was measured following the EN 325 standard using a digital micrometer screw gauge (Hans Schmidt & Co. GmbH, Waldkraiburg, Germany) with a precision of ± 0.01 mm. All specimens were conditioned in the climatic chamber at a temperature of 20 ± 2 °C and RH of 65 ± 5% before the test. For the test, specimens were placed uprightly in water covering up to 25 ± 5 mm of the top edges. The *WA* (Equation (5)) and *TS* (Equation (6)) were calculated and analyzed with ANOVA single way using an alpha of 0.05.

$$WA\ (\%) = \frac{W - W_0}{W_0} \times 100 \tag{5}$$

where W_0 is the mass of the conditioned specimens (g) prior to water immersion; W is the mass of the specimens at the end of 28 days of immersion.

$$TS\ (\%) = \frac{T - T_0}{T_0} \times 100 \tag{6}$$

where T_0 is thickness of the conditioned specimens (mm) prior to water immersion; T is the thickness of the specimens at the end of 28 days of immersion.

2.2.6. Reaction to Fire of the Composites

The cone calorimeter was used to investigate the fire test in accordance with the EN 5660-1:2015 standard. This approach was chosen because it is useful for estimating the fire safety of materials in European classification [20]. Composite samples (100 × 100 mm^2 in size) were exposed to a heat flux of 50 kWm^{-2} using a cone heater. The specimens were conditioned for seven (7) days prior to the test at a temperature of 23 °C and RH of 50%. Figure 4 depicts a 2D drawing of the specimen setup on a timber (pine) block. Timber was used as base material because it is an important construction material susceptible to fire hazards. The hemp PLA composite is assessed as a protection against the thermal degradation of the timber, though the research disregarded the decomposition of the timber. To ensure uniformity of results, all timber specimens were cut from the same pine lumber and conditioned with the same parameters as the hemp PLA composite prior to the experiment, as stipulated in the standard. A 0.25 mm diameter type K thermocouple (Pentronic AB, Vastervik, Sweden) was placed at the midpoint (50 mm) on the top of the specimen, to record the surface temperature, and between the composite and timber block. The edge of the entire piece was covered with self-bonding aluminium tape that reached 0.5 mm on the sample surface. The specimen was mounted in a retainer frame with the exposed surface held at a distance of 60 mm from the base of the cone heater. The result of the fire test is shown as a temperature-time curve at 5 s intervals. To correctly predict the composites' fire reaction, the mass and thickness of the composites were measured. The composite fire performance was characterized in terms of (i) Ignition time, (ii) Ignition temperature, (iii) Temperature response through depth (i.e., temperature determined between the surface of the composite and the timber block), (iv) Weight loss, (v) Basic protection time of the composite (t_{prot}) and (vi) Start time of charring of timber (t_{ch}), which is a function of t_{prot} of the composites. Temperature values of 270 °C and 300 °C were used to obtain the t_{prot} and t_{ch}, respectively, as recommended in the literature [21].

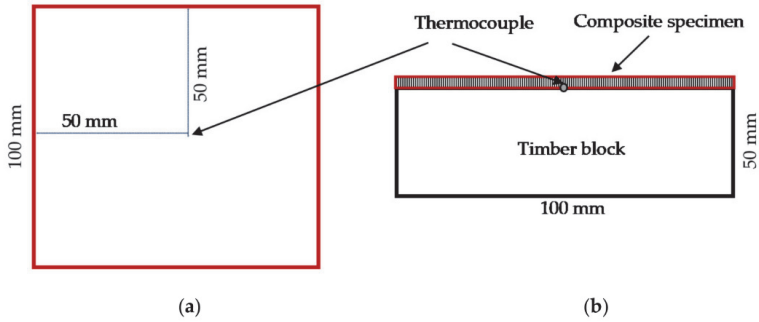

Figure 4. The set-up of test specimen: (**a**) top view of timber surface; (**b**) cross-sectional view of specimen on timber block.

3. Results and Discussion

3.1. Impact of Fiber Treatment on the Fiber Mass

Table 2 presents the hemp fiber mass change following the pretreatments/treatment. For both pretreatments, hemp fibers showed a reduction in weight. The 4% weight reduction measured on the water pretreated hemp fibers is the result of the removal of water-soluble, fiber cell wall contents, as it was qualitatively characterized by Fourier transform infrared (FTIR) in a previous work [10] and also observed by Bourmoud et al. [22]. The higher 14% drop in fiber mass due to alkali pretreatment is attributable to the extraction of significant non-cellulosic components (hemicelluloses, lignin, and some quantities of solubles (wax)) [10]. Indeed, in a previous study, FTIR peaks attributed to conjugated carboxylic esters in hemicelluloses and wax, acetyl groups in lignin and conjugated carbonyl groups in lignin disappeared after alkali pretreatment [10]. The overall quantity of

non-cellulosic content in the hemp fiber used in this study is 22.6 ± 0.7%, including 8.3% hemicellulose and 12.6% solubles (shown in Table 1), suggesting that the hemp fiber still contains some non-cellulosic components after pretreatments. Hu et al. [23] reported 25.9% weight reduction of hemp fibers after treatment with 6% NaOH solution at 40 °C for 24 h. The extended treatment duration and the volume of NaOH solution used by Hu et al. [23] possibly explain the discrepancy in results. However, no information was presented about fiber biochemical composition in the cited study.

Table 2. The mass change of the hemp fiber following pretreatment/treatment.

Treatment	Weight Change %
Water	−4.0 ± 0.3
Alkali treatments	−14.2 ± 0.8
Silane modification of water pre-treated fibers	−3.0 ± 0.6
Silane modification of alkali pre-treated fibers	+0.9 ± 0.0

The outcome for the water pretreated fibers following silane treatment show that when significant amounts of non-cellulosic fiber content are present, portions of the hemicellulose can be removed in addition to the deposition of silane molecules on the hemp fiber surface. These non-cellulosic fiber components may have been extracted during the hemp fiber immersion in the ethanol/water solution. Regarding the combined alkali and silane treatment, the hemp fibers showed a 0.9% weight gain, which can be attributed to the surface deposition of silane molecules.

3.2. Cross-Sectional SEM Observations of the Hemp Reinforced PLA Composites

The cross-sectional SEM images of the hemp fiber reinforced PLA composites are shown in Figure 5 for the untreated (UH_{30}; UH_{50}), water pretreated (WH_{30}; WH_{50}), alkali pretreated (AH_{30}; AH_{50}), water-silane treated (WSH_{30}; WSH_{50}) and alkali-silane treated (ASH_{30}; ASH_{50}) hemp fiber reinforced composites at 30 and 50 wt.%. The darker spots observed in the SEM images and identified on WH_{50} is related to the epoxy glue used to embed all the composites before the imaging. Some voids can be observed in most of the specimens, which suggest air entrapment within the composites during the fabrication process. The volume of porosities V_p of the composites are presented in Table 3. For both fiber contents, the volume of porosities was the highest for UH samples, due to the high amount of non-cellulosic components at the surface of the hemp fibers which prevents the wetting of the fibers by the PLA matrix, in addition to the weak interfacial bonds formed between fibers and the hydrophobic matrix. The removal of non-cellulosic components and the coupling brought by the silane agent tended to decrease the volume of porosities. Composites with 50 wt.% fibers displayed higher volumes of porosities overall when compared to 30 wt.% fibers, due to the additional difficulties in wetting and matrix flow during processing linked to the increased fiber amount.

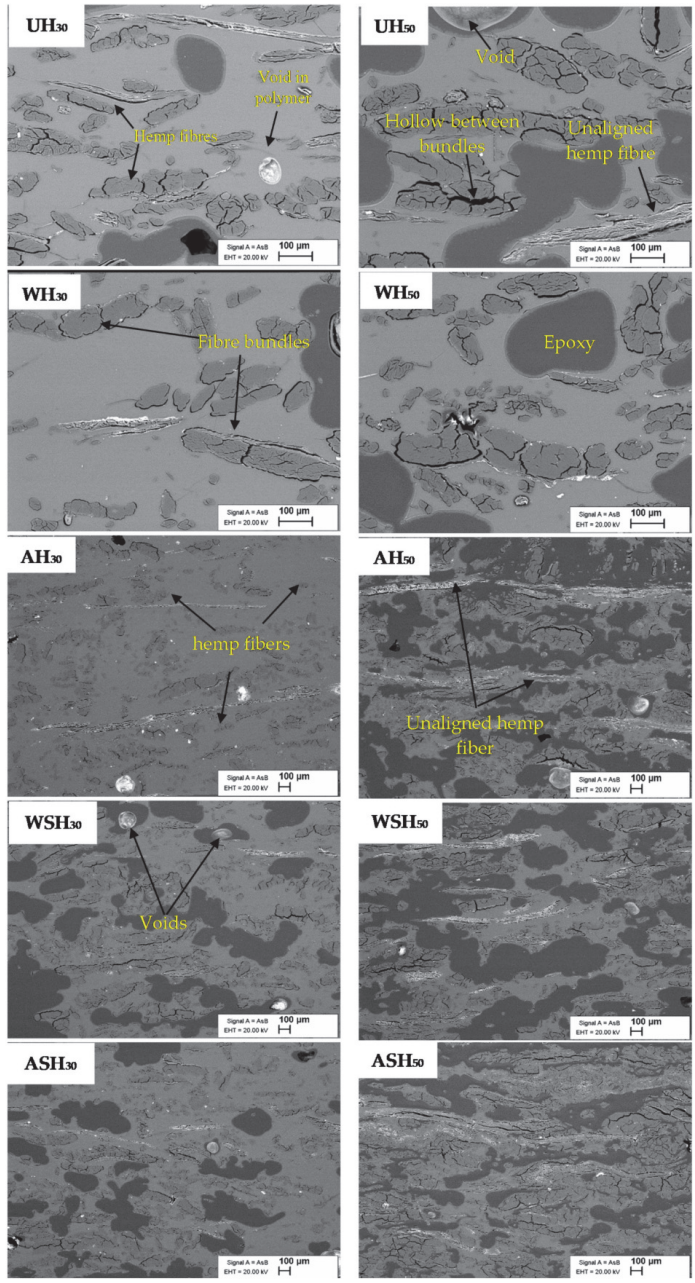

Figure 5. The cross-sectional images of reinforced PLA composites (UH, WH, AH, WSH and ASH) at 30 and 50% hemp fiber loading.

Table 3. Volume of porosities of the composites.

Composites	30 wt.% V_P (%)	50 wt.% V_P (%)
UH	10	13
WH	6	13
WSH	7	9
AH	4	7
ASH	4	8

UH composites are characterized by poorly dispersed, aggregated fiber bundles having inherent defibrillations. WH composites show a similar outcome, though fiber aggregates are more homogeneous and fewer bundles are visible, especially for 50 wt.% fiber content. The removal of water-soluble, fiber cell wall contents induced by the water pretreatment contributed to the better fiber individualization and homogeneity within the composite network without discernible effect on the surface morphology. The AH composites cross-sections appear homogenous, with individualized and uniformly dispersed fibers within the PLA matrix. Ray et al. [24] found that alkali fiber pretreatment causes gaps in the fiber structure owing to the extraction of fiber binding components, splitting the strands into single fibers and improving dispersion.

When WSH is compared to WH composites, the silane treatment resulted in clearer improvements in fiber separation, homogeneity and dispersion, which may be partly attributed to the elimination of a portion of the cell wall component, as seen in Table 2. Though ASH composites show similar observation as AH composites at 30% fiber loading, at 50 wt.% the composites present more homogenous fibers and fewer voids. As previously reported [10], there is a poor fiber wetting by the PLA matrix at 50 wt.% fiber content. Hence, the effective condensation of the siloxane layer on the fiber surface following silane modification improved the fiber/matrix adhesion more visibly at the higher fiber content.

3.3. Moisture Adsorption Properties

Figure 6a presents the measured and predicted adsorption isotherms for the neat PLA and the 30 wt.% reinforced composites while Figure 6b presents the outcome at 50% fiber loading. All samples displayed similar patterns in the form of sigmoidal shapes, classified as a type II isotherm, synonymous with cellulose-based materials [25]. Generally, the neat PLA remained significantly unaffected by the changing humidity conditions while the moisture adsorption decreases with fiber treatment and increased with the fiber contents. The highest EMC of 11.76% (at 95% RH) was displayed by UH (50 wt.%), which was significantly decreased by 18% following alkali pre-treatment and 16% with combined alkali and silane treatments. For 30 wt.% composites, there was no notable difference in the outcome for AH and ASH, though at 50 wt.%, a 13% meaningful reduction in EMC was achieved for ASH composites.

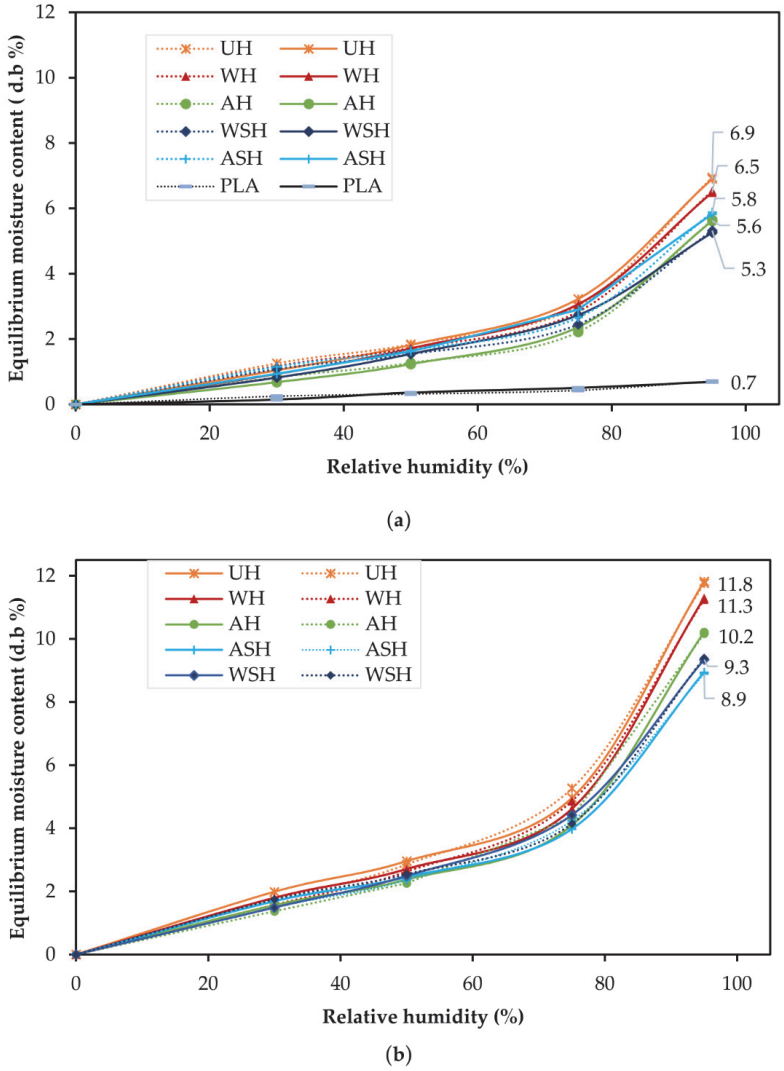

Figure 6. Adsorption isotherms (predicted (- -) and observed (—) for (**a**) the neat PLA, the 30wt.% composites and (**b**) the 50 wt.% composites (untreated (UH ж), water pretreated (WH ▲), alkali pretreated (AH ●) and combined treatment with silane (water (WSH ♦); alkali (ASH +)).

To complete Figure 6, Table 4 shows the difference of the results at 95% RH and the level of significance according to the ANOVA analysis. The most essential outcomes are by the chemically treated hemp fiber-reinforced composites, showing low *P*-values.

Table 4. The differences between the *EMC* of the HPLA composites (30 and 50 wt.%) at 95% RH and the obtained *P*-value from an alpha of 0.05 (ANOVA single factor analysis).

	30 wt.% HF		50 wt.% HF	
Composite Comparison	**Difference at 95% RH**	***P*-Value**	**Difference at 95% RH**	***P*-Value**
WH < UH	6	0.144	5	0.5
AH < UH	18	0.012	14	0.012
WSH < UH	24	0.001 **	21	0.002
ASH < UH	16	0.001	25	0.001 **
WSH < WH	19	0.006	17	0.002
AH < ASH/AH > ASH	4	0.603	13	0.002
WSH < AH	7	0.369	4	0.034
WSH < ASH	10	0.051	5	0.144

** lesser than 0.001.

The significant composite moisture adsorption at 50 wt.% fiber loading (1.5 to 1.8 times the moisture absorption of the 30% fiber loading at 95% RH) is ascribable to two combined factors: (1) the presence of higher fibrous ratio with more hydrophilic groups than the PLA matrix, (2) the higher volume of porosities for the 50 wt.% fibers highlighted in the Section 3.2 (Table 3). According to Pejic et al. [14], the amount of free amorphous and crystalline OH available in hemp fiber determines moisture sorption up to a RH of 65%, whereas the biochemical compositions (lignin, pectin, hemicellulose, and celluloses) and their locations are the main factors influencing the moisture absorption by capillary condensation above the RH of 65%. Thus, the decreased EMC for the AH composite can be attributed to (i) less free OH groups, and (ii) a change in the fiber microstructure described by Alao et al. [10] and (iii) enhanced bonding between the fiber and PLA as demonstrated in Figure 5. The negligible effect of water fiber pretreatment on composite moisture adsorption compared to untreated fiber composites might be due to the moderate removal of the fiber hemicellulose content [10], as indicated by the low mass loss associated to this pretreatment (Table 2).

The values of the *A*, *B*, *C* parameters from the modified Oswin model with the calculated standard error of estimate (E_S) and the mean relative percentage deviation (Pd.), for all the composite specimens' adsorption are presented in Table 5. To access the accuracy of this model, the Es and Pd. values are used. A model is reasonably accepted if the estimated Pd. is below 10% [26]. The calculated Pd. for all the composites did not exceed 10% while the Es were also low (<1), which confirms the suitability of this model in predicting the moisture adsorption of hemp fiber reinforced PLA composites. No study has been found using such model fitting to describe the isotherms of HPLA composites. However, Nilsson et al. [19] reported an Es and Pd. value of 0.68 and 4.19% respectively, for frost retted hemp fibers.

Table 5. Adsorption parameters and goodness of fit for Oswin model determined from sorption isotherms of untreated (UH), and treated (WH, WSH, AH and ASH) composites at 30 and 50 wt.% of hemp fiber content.

	Constants			ROOT Mean Square (R^2)	Standard Error of Estimate (Es)	Pd., %
	A	*B*	*C*			
				30 wt.% HF		
UH	1.48	0.02	2.22	0.997	0.17	7.2
WH	1.37	0.02	2.21	0.996	0.19	8.9
WSH	0.10	0.00	2.37	0.991	0.22	8.7
AH	0.95	0.01	1.97	0.998	0.12	8.0
ASH	1.30	0.02	2.33	0.995	0.19	8.8
				50 wt.% HF		
UM	2.54	0.02	2.13	0.998	0.24	6.2
WH	2.29	0.02	2.06	0.987	0.57	5.7
WSH	2.13	0.02	2.25	0.997	0.22	6.6
AH	1.97	0.02	2.02	0.998	0.19	6.3
ASH	2.04	0.02	2.28	0.997	0.20	6.1

3.4. Water Absorption and Thickness Swelling Results

Figure 7 presents the water absorption (*WA*) and thickness swelling (*TS*) of the HPLA composites. The neat PLA showed no noticeable changes in mass or thickness (0%) after the 28 days of total immersion, so the associated values are not reported in the Figure 7. With the composites, the moisture affinity is the highest for the 50 wt.% fiber reinforced composite. The UH composite exhibited the most change in *WA* and *TS* of 23 and 48%, respectively. Compared to the UH, WH composites showed a slight reduction in WA, of 9% (30 wt.% fibers) and 11% (50 wt.% fibers), but the *TS* appeared unchanged. Nonetheless, compared to UH, the WSH composite *TS* for 50 wt.% fiber showed a significant decrease, and a notable reduction in WA for both fiber ratios. Compared to UH, AH composites showed a 27% drop in *WA* at 30 wt.% fiber content, and 16% drop at 50 wt.%, while the *WA* of ASH composites further decreased by 13 and 3% at 30 wt.% and 50 wt.% fibers, respectively. However, the difference between the outcomes for ASH and AH was statistically insignificant.

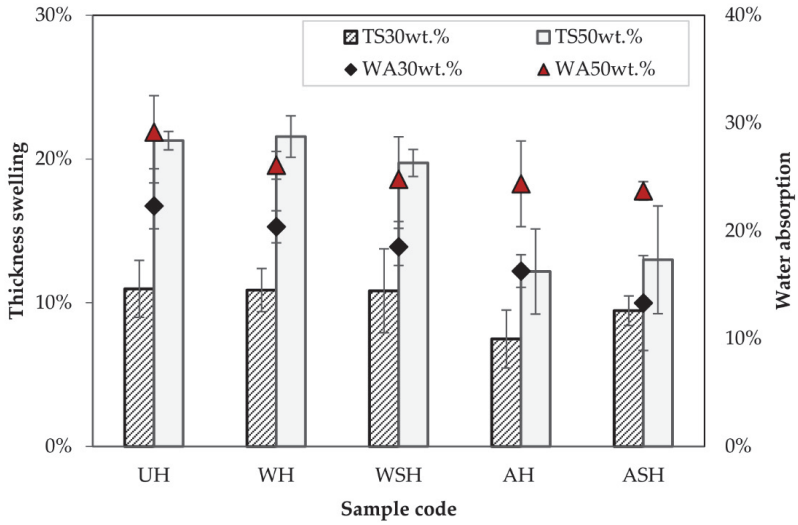

Figure 7. Water absorption and thickness swelling of the HPLA composites.

The low *WA* for AH and ASH composites can be ascribed to (i) the changes that have occurred to the porous structure of the hemp fibers in the case of the alkali pretreatment, (ii) the better interfacial polymer/fiber adhesion induced by the silane coupling and, (iii) the reduced hydrophilic properties arising from the less available OH needed for bonding with water molecules. Moreover, AH and ASH are the composites which contain the less porosities, at both 30 and 50 wt.%, thanks to the efficient removal of non-cellulosic components by the alkali treatment, and to the silane coupling that enhance the fiber-matrix interface. The reduced level of porosity also partially contributes to the low WA of these composites. When a strong bond exists between the polymer matrix and the fiber, better packing occurs in the composite, leading to a decrease in the distance travelled by the diffusion water molecules and a reduction in the composite's water uptake [27]. Alkali pretreatment of hemp fibers changes the surface topology, inducing a higher roughness that leads to better fiber/matrix anchorage, and removed non-cellulosic impurities from the fiber surface, allowing and improving bonding with the matrix due to a better accessibility of hydroxyl groups of cellulose. Väisänen et al. [28] and Baghaei et al. [29] obtained results similar to that of this current study. Väisänen et al. [28] reported 30% WA after 28 days of immersion for the untreated hemp-epoxy composites that decreased to 12.5% *WA* following alkali treatment, while Baghaei et al. [29] showed a *WA* of about 21% for untreated, nonwoven HPLA composites after 10 days of water immersion. Conversely, Sgriccia et al. [30] showed that for 25 wt.% hemp/epoxy composites, the NaOH treatment prompted higher moisture absorption than the untreated fiber composites, which was related to the presence of voids induced by the rougher fiber surface following the treatment.

3.5. Reaction to Fire of Composite Materials

3.5.1. Temperature Response through Depth

The average surface temperatures and temperature response (i.e., temperature determined between the surface of the composite and the timber block) of neat PLA and the 30 wt.% composites are presented in Figure 8a, while Figure 8b shows the temperature response for the 50 wt.% composites. The average surface temperature rose from 27 to 693 °C, while the temperature response through depth measured between the surface of the composite and the timber was at a maximum, 598 °C and 550 °C for UH_{30} and UH_{50}, respectively. The exposure to the heat flux was performed for 480 s. However, the neat PLA boards completely decomposed after about 180 s. Composites with 30 wt.% fibers displayed higher temperatures measured between the interface of the composite and the timber than composites with 50 wt.% fibers. For instance, for a surface temperature range of 300 to 400 °C (regarded as the temperature range for the pyrolysis of cellulose), UH_{30} produced an average of 61 °C temperature response through depth compared to UH_{50} (57 °C). The reaction to fire of the neat PLA was shown as a reference. Compared to the composites, the PLA has a rapid ignition (as measured from the temperature response through depth) and decomposition (180 s). It is thus observed that the 30 wt.% composites with higher PLA content, when compared to composites of 50 wt.% fibers, showed a slightly higher temperature response through depth and also higher rate of decomposition.

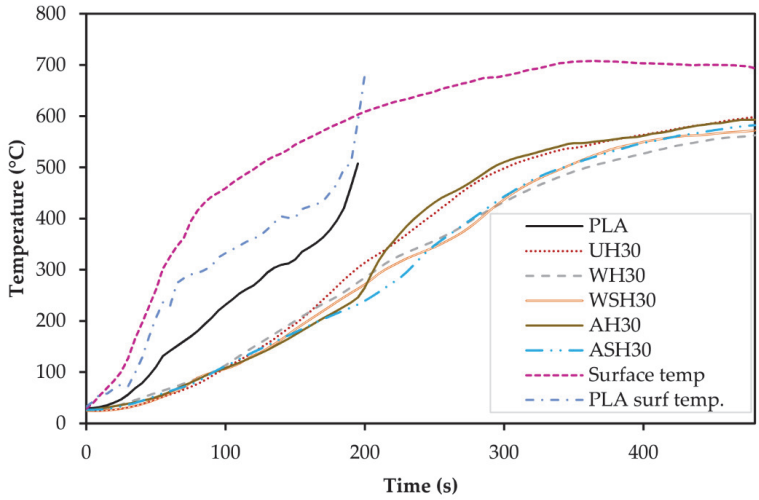

(**a**)

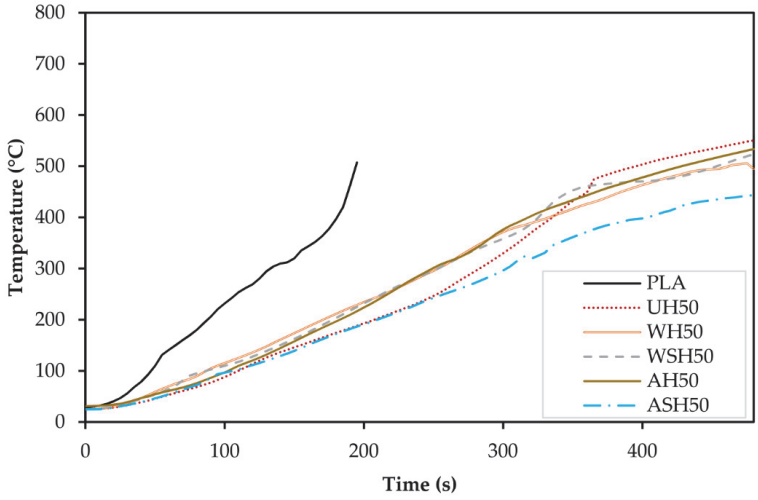

(**b**)

Figure 8. Surface temperature and temperature response behind the neat PLA and composites at (**a**) 30%;(**b**) 50% hemp fiber content.

The Basic protection time (t_{prot}) of the specimens and start of char of the timber base (t_{ch}) did not present meaningful difference between the composites.

3.5.2. Other Reaction to Fire Test Results

Table 6 displays the specimen thickness, density, mass prior to testing, mass loss after fire exposure, ignition time and ignition temperature. The average weight and thickness of the composites were greater for fiber reinforced PLA composites with 50% loading. The discrepancy in weight and thickness could be attributed to the bulky nature of hemp fiber and the density difference between PLA and fiber. In terms of ignition temperature and mass loss, there does not appear to be any significant improvement with the increase in fiber content, but the average mass loss was about 4% lower compared to the 30%

fiber content, which is due to higher ash content at the higher fiber amount. The average temperature for AH and combined treatments (WSH and ASH) were significantly improved at 50 wt.% compared to 30 wt.%, but the changes for UH and WH were statistically insignificant. Ahmed et al. [31] also demonstrated that fiber modification by grafting of silane coupling agents can improve the thermal stability of the composites. Moreover, the ignition temperatures of UH and WH composites at both fiber compositions were identical, which might be attributed to the lack of a major difference in the fiber cell wall content. Although it is possible that the increased ignition temperature for WSH is due to the silane coupling agent, SEM pictures (Figure 5) and fiber mass change (Table 2) revealed inconsistencies in cell wall structure and composition after combine modification that implies that the better performance is the result of the extraction of portion of the fiber cell wall components and the silane molecules attached to the fiber surface.

Table 6. Specimen properties, mass loss and ignition time and temperature.

Fiber Content	Samples	Weight of Board before Test (g)	Thickness (mm)	Density (gcm^{-3})	Average Ignition Time (s)	Ignition Temperature (°C)	Mass Loss (%)
30%	UH	28 ± 1.8	2.8 ± 0.4	1.01 ± 0.1	29 ± 10	112 ± 23	93 ± 2.0
	WH	27 ± 1.4	2.5 ± 0.2	1.10 ± 0.0	31 ± 10	117 ± 18	95 ± 0.1
	WSH	28 ± 1.2	2.6 ± 0.3	1.04 ± 0.1	30 ± 04	131 ± 28	94 ± 0.4
	AH	26 ± 0.6	2.5 ± 0.2	1.07 ± 0.1	44 ± 02	118 ± 08	94 ± 1.0
	ASH	28 ± 1.6	2.7 ± 0.2	1.07 ± 0.0	33 ± 03	159 ± 18	94 ± 2.0
50%	UH	29 ± 0.8	3.2 ± 0.2	0.91 ± 0.1	32 ± 07	129 ± 15	90 ± 1.0
	WH	29 ± 1.8	3.3 ± 0.2	0.90 ± 0.1	49 ± 06	134 ± 17	91 ± 2.0
	WSH	30 ± 1.0	3.1 ± 0.1	0.97 ± 0.0	46 ± 10	179 ± 29	90 ± 1.0
	AH	30 ± 0.3	3.2 ± 0.1	0.92 ± 0.0	51 ± 10	178 ± 18	90 ± 4.0
	ASH	30 ± 0.6	3.2 ± 0.1	0.98 ± 0.0	47 ± 09	181 ± 18	89 ± 1.0
0%	Neat PLA	26 ± 1.2	2.2 ± 0.2	1.2 ± 0.1	37 ± 02	104 ± 04	100 ± 0.0

When compared to the neat PLA, the ignition temperature of all the composites increased. The deviation observed in the ignition properties within series are attributable to the fabrication of the replica from separate boards rather than the machining of a single board. Furthermore, even though the cone heater was pre-calibrated before each test, the ambient conditions slightly influenced ignition properties since the experiments were performed over several days. The delayed composite ignition with increase in fiber volume is reportedly attributed to the higher density of the composite [16]. However, the current study's findings demonstrate that, while ignition time rises with fiber content, there appears to be no association with composite densities. At 30%, there was no significant variation in the densities of the composites. When the density of the composites at the same fiber content was compared to the ignition time, it was discovered that though the 30 wt.% WH had the highest density, the ignition time difference (28%) was insignificant compared to AH, which had 3% less density. In addition, at 50 wt.%, despite the decreased density of WH compared to UH, the ignition time was dramatically delayed by 35%. The results of thermogravimetric analysis earlier published [10] found that hemp fiber surface pretreatments and treatments improved the fiber's thermal stability because of the removal of non-cellulosic contents that have lower degradation temperature. This improvement of thermal stability at the microscale after treatment could be the main reason influencing the fire resistance of the hemp reinforced PLA composites. It may be summarized that the reaction to fire of hemp fiber reinforced PLA composites depends largely on the PLA/fiber content and fiber surface pretreatment, though a more detailed study may be required.

4. Conclusions

In this research, the moisture, water resistance and response to fire performance of hemp fiber reinforced polylactide composites were investigated in regard to a combination of fiber surface treatments. Moisture behaviour and reaction to fire of hemp fiber reinforced

PLA composites were found to largely depend on the PLA/fiber content and fiber surface (pre)treatment, though a more detailed study of the fire behaviour of the composite may be required. Besides improving the fiber dispersion and homogeneity within the composites, alkali pretreatment and silane modification were found to decrease the composite's hydrophilic characteristics. Water pretreatment showed little effect on the composite studied characteristics; however, the further silane modification produced significantly higher moisture resistance and better reaction to fire, which may be attributed to the extra removal of the amorphous cell wall content and silane coupling at the hemp fiber surface. The Oswin model accurately predicted the adsorption isotherm for all composites.

Although composites containing higher hemp fiber content were more sensitive to moisture/water, a greater fire resistance was discovered, resulting in a slower rate of thermal breakdown owing to the low PLA ratio. The combined surface treatments of the fibers primarily improved the composite fire protection qualities. Overall, the alkali pretreatment of hemp fibers and surface modification with silane led to the most promising results for the use of hemp reinforced PLA composites. However, considering the expense of silane agents, a simple alkali treatment may be sufficient to efficiently increase the considered properties. This study showed that adequate hemp fiber surface treatment allows the improvement of the composite durability during service, which opens opportunities for the use of sustainable composites in the transportation and construction sectors.

Future study will examine the impact of fire-retardant treatment as a means to improve hemp fiber reinforced composite fire performance, the effect of the fiber surface pretreatment on the effectiveness of the fire-retardant modification and the overall impact of the combined fiber surface and fire-retardant treatment on the mechanical and physical properties of the composites.

Author Contributions: Conceptualization, P.F.A., H.K. and J.K.; formal analysis, P.F.A.; investigation, P.F.A. and A.J.; methodology, P.F.A. and A.J.; resources, T.P. and H.K.; writing original draft, P.F.A. and L.M.; writing-review & editing, P.F.A., L.M., H.K., A.J. and J.K.; supervision, T.P. and J.K.; funding acquisition, P.F.A., L.M. and J.K. All authors have read and agreed to the published version of the manuscript.

Funding: This work was supported by the European Regional Development fund, ASTRA "TUT Institutional Development Programme for 2016–2022" Graduate school of Functional Materials and Technologies (2014–2020.4.01.16-0032)" and investment from the Republic of Slovenia and ARRS (Slovenian Research Agency) Bilateral Project Slovenia—Estonia (grant agreement number BI-EE/20-22-007).

Institutional Review Board Statement: Not applicable.

Informed Consent Statement: Not applicable.

Data Availability Statement: Data sharing not applicable.

Acknowledgments: Valdek Mikli and Margus Kangur for their technical support during the research.

Conflicts of Interest: The authors declare no conflict of interest.

References

1. Hroudová, J.; Zach, J. The Possibilities of Modification of Crop-based Insulation Materials Applicable in Civil Engineering in Low-energy and Passive Houses. *Procedia Eng.* **2017**, *180*, 1186–1194. [CrossRef]
2. Hussain, A.; Calabria-Holley, J.; Lawrence, M.; Jiang, Y. Hygrothermal and mechanical characterisation of novel hemp shiv based thermal insulation composites. *Constr. Build. Mater.* **2019**, *212*, 561–568. [CrossRef]
3. Stevulova, N.; Estokova, A.; Cigasova, J.; Schwarzova, I.; Kacik, F.; Geffert, A. Thermal degradation of natural and treated hemp hurds under air and nitrogen atmosphere. *J. Therm. Anal. Calorim.* **2017**, *128*, 1649–1660. [CrossRef]
4. Xie, Y.; Hill, C.A.S.; Xiao, Z.; Militz, H.; Mai, C. Silane coupling agents used for natural fiber/polymer composites: A review. *Compos. Part A Appl. Sci. Manuf.* **2010**, *41*, 806–819. [CrossRef]
5. Sawpan, M.A.; Pickering, K.L.; Fernyhough, A. Improvement of mechanical performance of industrial hemp fibre reinforced polylactide biocomposites. *Compos. Part A Appl. Sci. Manuf.* **2011**, *42*, 310–319. [CrossRef]

6. Lu, N.; Swan, R.H.; Ferguson, I. Composition, structure, and mechanical properties of hemp fiber reinforced composite with recycled high-density polyethylene matrix. *J. Compos. Mater.* **2012**, *46*, 1915–1924. [CrossRef]
7. Oksman, K.; Skrifvars, M.; Selin, J.F. Natural fibres as reinforcement in polylactic acid (PLA) composites. *Compos. Sci. Technol.* **2003**, *63*, 1317–1324. [CrossRef]
8. Islam, M.S.; Pickering, K.L.; Foreman, N.J. Influence of alkali treatment on the interfacial and physico-mechanical properties of industrial hemp fibre reinforced polylactic acid composites. *Compos. Part A Appl. Sci. Manuf.* **2010**, *41*, 596–603. [CrossRef]
9. Pappu, A.; Pickering, K.L.; Thakur, V.K. Manufacturing and characterization of sustainable hybrid composites using sisal and hemp fibres as reinforcement of poly (lactic acid) via injection moulding. *Ind. Crop. Prod.* **2019**, *137*, 260–269. [CrossRef]
10. Alao, P.F.; Marrot, L.; Burnard, M.D.; Lavrič, G.; Saarna, M.; Kers, J. Impact of Alkali and Silane Treatment on Hemp/PLA Composites' Performance: From Micro to Macro Scale. *Polymers* **2021**, *13*, 851. [CrossRef]
11. Pickering, K.L.; Efendy, M.G.A.; Le, T.M. A review of recent developments in natural fibre composites and their mechanical performance. *Compos. Part A Appl. Sci. Manuf.* **2016**, *83*, 98–112. [CrossRef]
12. Kabir, M.M.; Wang, H.; Lau, K.T.; Cardona, F. Effects of chemical treatments on hemp fibre structure. *Appl. Surf. Sci.* **2013**, *276*, 13–23. [CrossRef]
13. Pickering, K.L.; Beckermann, G.W.; Alam, S.N.; Foreman, N.J. Optimising industrial hemp fibre for composites. *Compos. Part A Appl. Sci. Manuf.* **2007**, *38*, 461–468. [CrossRef]
14. Pejic, B.M.; Kostic, M.M.; Skundric, P.D.; Praskalo, J.Z. The effects of hemicelluloses and lignin removal on water uptake behavior of hemp fibers. *Bioresour. Technol.* **2008**, *99*, 7152–7159. [CrossRef] [PubMed]
15. Kozlowski, R.M.; Muzyczek, M.; Walentowska, J. Chapter 23—Flame Retardancy and Protection against Biodeterioration of Natural Fibers: State-of-Art and Future Prospects. *Polym. Green Flame Retard.* **2014**, 801–836. [CrossRef]
16. Naughton, A.; Fan, M.; Bregulla, J. Fire resistance characterisation of hemp fibre reinforced polyester composites for use in the construction industry. *Compos. Part B Eng.* **2014**, *60*, 546–554. [CrossRef]
17. Marrot, L.; Alao, P.F.; Mikli, V.; Kers, J. Properties of Frost-Retted Hemp Fibers for the Reinforcement of Composites. *J. Nat. Fibers* **2021**, 1–12. [CrossRef]
18. Palumbo, M.; Lacasta, A.M.; Holcroft, N.; Shea, A.; Walker, P. Determination of hygrothermal parameters of experimental and commercial bio-based insulation materials. *Constr. Build. Mater.* **2016**, *124*, 269–275. [CrossRef]
19. Nilsson, D.; Svennerstedt, B.; Wretfors, C. Adsorption equilibrium moisture contents of flax straw, hemp stalks and reed canary grass. *Biosyst. Eng.* **2005**, *91*, 35–43. [CrossRef]
20. Tsantaridis, L.D.; Östman, B.A.L.; Köning, J. Short communication: Fire protected wood by different gypsum plasterboards. *Fire Mater.* **1999**, *23*, 45–48. [CrossRef]
21. Kallakas, H.; Liblik, J.; Alao, P.F.; Poltimaë, T.; Just, A.; Kers, J. Fire and Mechanical Properties of Hemp and Clay Boards for Timber Structures. In *IOP Conference Series: Earth and Environmental Science*; IOP Publishing: Prague, Czech Republic, 2019; Volume 290, p. 012019. Available online: https://iopscience.iop.org/article/10.1088/1755-1315/290/1/012019/pdf (accessed on 14 May 2021).
22. Bourmaud, A.; Morvan, C.; Baley, C. Importance of fiber preparation to optimize the surface and mechanical properties of unitary flax fiber. *Ind. Crop. Prod.* **2010**, *32*, 662–667. [CrossRef]
23. Hu, R.; Lim, J.-K. Fabrication and Mechanical Properties of Completely Biodegradable Hemp Fiber Reinforced Polylactic Acid Composites. *J. Compos. Mater.* **2007**, *41*, 1655–1669. [CrossRef]
24. Ray, D.; Sarkar, B.K.; Rana, A.K.; Bose, N.R. Mechanical properties of vinylester resin matrix composites reinforced with alkali-treated jute fibres. *Compos. Part A Appl. Sci. Manuf.* **2001**, *32*, 119–127. [CrossRef]
25. Alix, S.; Philippe, E.; Bessadok, A.; Lebrun, L.; Morvan, C.; Marais, S. Effect of chemical treatments on water sorption and mechanical properties of flax fibres. *Bioresour. Technol.* **2009**, *100*, 4742–4749. [CrossRef]
26. Arslan, N.; Toğrul, H. The fitting of various models to water sorption isotherms of tea stored in a chamber under controlled temperature and humidity. *J. Stored Prod. Resour.* **2006**, *42*, 112–135. [CrossRef]
27. Sreekumar, P.A.; Thomas, S.P.; Saiter, J.M.; Joseph, K.; Unnikrishnan, G.; Thomas, S. Effect of fiber surface modification on the mechanical and water absorption characteristics of sisal/polyester composites fabricated by resin transfer molding. *Compos. Part A Appl. Sci. Manuf.* **2009**, *40*, 1777–1784. [CrossRef]
28. Väisänen, T.; Batello, P.; Lappalainen, R.; Tomppo, L. Modification of hemp fibers (*Cannabis sativa* L.) for composite applications. *Ind. Crop. Prod.* **2018**, *111*, 422–429. [CrossRef]
29. Baghaei, B.; Skrifvars, M.; Salehi, M.; Bashir, T.; Rissanen, M.; Nousiainen, P. Novel aligned hemp fibre reinforcement for structural biocomposites: Porosity, water absorption, mechanical performances and viscoelastic behaviour. *Compos. Part A Appl. Sci. Manuf.* **2014**, *61*, 1–12. [CrossRef]
30. Sgriccia, N.; Hawley, M.C.; Misra, M. Characterization of natural fiber surfaces and natural fiber composites. *Compos. Part A Appl. Sci. Manuf.* **2008**, *39*, 1632–1637. [CrossRef]
31. Ahmed, S.N.; Prabhakar, M.N.; Siddaramaiah, J.; Song, I.L. Influence of silane-modified Vinyl ester on the properties of Abaca fiber reinforced composites. *Adv. Polym. Technol.* **2018**, *37*, 1970–1978. [CrossRef]

Curriculum vitae

Personal data

Name:	Percy Festus Alao
Date of birth:	30.04.1987
Place of birth:	Kaduna, Nigeria
Citizenship:	Nigerian

Contact data

E-mail:	percy.alao@taltech.ee

Education

2018–2022	Tallinn University of Technology, Chemical and Materials Technology, Doctor of Philosophy
2016–2018	Tallinn University of Technology, Technology of Wood and Plastics, Master of Science, *cum laude*
2005–2011	University of Ibadan, Nigeria, Wood Products Engineering, Bachelor of Science, Honours
2001–2004	Government College Ibadan, Oyo State, Nigeria, Senior School Education
1998–2001	Gindiri Boys High School, Plateau State, Nigeria, Junior School Education

Language competence

English	Fluent
Yoruba	Fluent
Estonian	Basic

Professional employment

25.10.2018–…	Tallinn University of Technology, School of Engineering, Department of Materials and Environmental Technology, Early-Stage Researcher (1,00)
01.09.2018–…	Tallinn University of Technology, School of Engineering, Department of Materials and Environmental Technology, Engineer (0,5)
0.2.10.2013–30.06.2016	Digital Communications Konsult Nig Ltd, Lagos, Nigeria, Operations/Performance Management Executive (1,00)

Defended thesis

Master thesis “Effect of Hemp fibre length on the properties of polypropylene composites”, Tallinn University of Technology, Faculty of Chemical and Materials Technology, Department of Materials and Environmental Technology, Chair of Woodworking.

Supervisor: Doctor Heikko Kallakas

Elulookirjeldus

Isikuandmed

Nimi:	Percy Festus Alao
Sünniaeg:	30.04.1987
Sünnikoht:	Kaduna, Nigeeria
Kodakondsus:	Nigeeria

Kontaktandmed

E-post:	percy.alao@taltech.ee

Hariduskäik

2018–2022	Tallinna Tehnikaülikool, Keemia ja materjalitehnoloogia eriala, doktorantuur
2016–2018	Tallinna Tehnikaülikool, materjalitehnoloogia õppekeva, puidutöötlemine, loodusteaduste magistrikraad, *cum laude*
2005–2011	Ibadani ülikool, Nigeeria, Puittoodete ehitus, tehnikateaduse bakalaureuse, autasud
2001–2004	Ibadani valitsuskolledž, Oyo osariik, Nigeeria, Kõrgemate koolide haridus
1998–2001	Gindiri poiste keskkool, Plateau osariik, Nigeeria, Noorem kooliharidus

Keelteoskus

Inglise keel	Kõrgtase
joruba keel	Kõrgtase
Eesti keel	Algtase

Teenistuskäik

25.10.2018–…	Tallinna Tehnikaülikool, Inseneriteaduskond, materjali- ja keskkonnatehnoloogia instituut, doktorant-nooremteadur (1,00)
01.09.2018–…	Tallinna Tehnikaülikool, Inseneriteaduskond, materjali- ja keskkonnatehnoloogia instituut, Insener (0,5)
0.2.10.2013–30.06.2016	Digitaalne kommunikatsioon Konsult Nig. Ltd, Lagos, Nigeeria, Operatsioonide / tulemuslikkuse juhtimise juht (1,00)

Defended thesis

Magistritöö “Kanepikiu pikkuse mõju polüpropüleenist komposiitide omadustele”, Tallinna Tehnikaülikool, Keemia ja materjalitehnoloogia teaduskond, materjali- ja keskkonnatehnoloogia instituut, Puidutöötlemise õppetool.
Juhendaja: doktorant Heikko Kallakas

ISSN 2585-6901 (PDF)
ISBN 978-9949-83-830-1 (PDF)